

EDITORIAL BOARD

Editor-in-Chief

B.E. Paton

Scientists of PWI, Kiev

S.I. Kuchuk-Yatsenko (*vice-chief ed.*),

V.N. Lipodaev (*vice-chief ed.*),

Yu.S. Borisov, G.M. Grigorenko,

A.T. Zelnichenko, V.V. Knysh,

I.V. Krivtsun, Yu.N. Lankin,

L.M. Lobanov, V.D. Poznyakov,

I.A. Ryabtsev, K.A. Yushchenko

Scientists of Ukrainian Universities

V.V. Dmitrik, NTU «KhPI», Kharkov

V.V. Kvasnitsky, NTUU «KPI», Kiev

V.D. Kuznetsov, NTUU «KPI», Kiev

Foreign Scientists

N.P. Alyoshin

N.E. Bauman MSTU, Moscow, Russia

Guan Qiao

Beijing Aeronautical Institute, China

A.S. Zubchenko

DB «Gidropress», Podolsk, Russia

M. Zinigrad

Ariel University, Israel

V.I. Lysak

Volgograd STU, Russia

Ya. Pilarczyk

Welding Institute, Gliwice, Poland

U. Reisgen

Welding and Joining Institute, Aachen, Germany

G.A. Turichin

St. Petersburg SPU, Russia

Founders

E.O. Paton Electric Welding Institute, NASU

International Association «Welding»

Publisher

International Association «Welding»

Translators

A.A. Fomin, O.S. Kurochko, I.N. Kutianova

Editor

N.G. Khomenko

Electron galley

D.I. Sereda, T.Yu. Snegiryova

Address

E.O. Paton Electric Welding Institute,

International Association «Welding»

11 Kazimir Malevich Str. (former Bozhenko Str.),

03680, Kiev, Ukraine

Tel.: (38044) 200 60 16, 200 82 77

Fax: (38044) 200 82 77, 200 81 45

E-mail: journal@paton.kiev.ua

www.patonpublishinghouse.com

State Registration Certificate

KV 4790 of 09.01.2001

ISSN 0957-798X

Subscriptions

\$348, 12 issues per year,

air postage and packaging included.

Back issues available.

All rights reserved.

This publication and each of the articles contained
herein are protected by copyright.

Permission to reproduce material contained in this
journal must be obtained in writing from the Publisher.

CONTENTS

SCIENTIFIC AND TECHNICAL

- Yushchenko K.A., Yarovitsyn A.V. and Chervyakov N.O.* Effect of energy parameters of microplasma powder surfacing modes on susceptibility of nickel alloy ZhS32 to crack formation 2
- Akhonin S.V. and Belous V.Yu.* Argon-arc welding of titanium and its alloys using fluxes (Review) 7
- Maksymova S.V., Voronov V.V., Kovalchuk P.V. and Larionov A.V.* Producing dissimilar joints of molybdenum–stainless steel using vacuum brazing 13
- Efimenko N.G., Artemova S.V. and Bartash S.N.* Effect of welding modes on mechanical properties, structure and brittle fracture susceptibility of welded joints of steel 15Kh1M1FL made without preheating 19
- Somonov V.V.* Influence of parameters of ultrasonic mechanical oscillations on the structure and mechanical properties of weld metal in laser welding of ferritic steels 23
- Falchenko Yu.V., Khokhlov M.A., Khokhlova Yu.A. and Sinyuk V.S.* Formation of diffusion zone in welded joints of porous aluminium alloy with monolithic magnesium alloy at chemical activation by gallium 28

INDUSTRIAL

- Zhuk G.V., Moroz I.V., Barvinko A.Yu., Barvinko Yu.P. and Posypajko Yu.N.* Peculiarities of construction and service of tank RVS-200 for storage of diesel fuel in Antarctica at the station «Akademik Vernadsky» 33
- Degtyarev V.A.* Effect of vibrotreatment on fatigue resistance and damping capacity of structural elements with residual stresses 38
- Levchenko O.G. and Kharlamov A.Yu.* Mobile protective screen for nonstationary workplaces for manual arc welding 45

NEWS

- Seminar «Welding Materials» 50

EFFECT OF ENERGY PARAMETERS OF MICROPLASMA POWDER SURFACING MODES ON SUSCEPTIBILITY OF NICKEL ALLOY ZhS32 TO CRACK FORMATION

K.A. YUSHCHENKO, A.V. YAROVITSYN and N.O. CHERVYAKOV

E.O. Paton Electric Welding Institute, NASU

11 Kazimir Malevich Str., 03680, Kiev, Ukraine. E-mail: office@paton.kiev.ua

Presented is a technological experience of the E.O. Paton Electric Welding Institute in area of development of surfacing technologies for serial repair of blade flanges of aircraft GTE of nickel heat-resistant alloys ZhS26 and ZhS32 with oriented crystallization based on microplasma powder surfacing. It is shown that heat input value in a single-layer or multilayer surfacing using up to 40 A welding current can uniquely determine susceptibility to crack formation in «base–deposited metal» joints. A range of values of total heat input was determined. They can be used to predict absence or presence of cracks (hot or reheating cracks) with high probability. 18 Ref., 7 Figures.

Keywords: *nickel heat-resistant alloys, microplasma powder surfacing, weldability, crack formation susceptibility, effective heat power of arc, heat input, total heat input*

Nickel heat-resistant alloys ZhS26 and ZhS32 with oriented and single-crystal structure, containing 60 vol.% and more of strengthening γ' -phase are used in a series of current aircraft engines as a material of cast blades of high- and middle-pressure turbines (HPT and MPT) [1, 2]. Their sealing and antivibration elements working under more than 900 °C temperature wear and damage in process of operation most of all. Due to significant cost of the blades development of technology of their flange repair has been very relevant for long period of time [3–9] at extension of aircraft engine life.

Earlier these nickel heat-resistant alloys due to high content of strengthening γ' -phase were considered unweldable because of high susceptibility to hot crack formation in application of filler material similar on composition to base metal and level of high-temperature strength.

Appearance of hot cracks in the deposited metal and HAZ of the base metal with austenite structure is caused by exceeding a level of deformations, developing in a welded joint at cooling or under outside effect, and metal ductility in its specific zone [10]. Young's elasticity modulus in alloy ZhS32 at $T = 20\text{--}1100$ °C reduces from 140 to 90 GPa and thermal coefficient of linear expansion α rises in $(1.1\text{--}2.4) \cdot 10^{-5}$ 1/°C interval [11]. Due to known proportionality of solid body deformation in process of heating to $E\alpha T$ product [12] it can be assumed that the high values of rate of tensile deformations growth in cooling of welded joint

including ZhS32 alloy are caused by respective combination of indicated physical-mechanical properties of this material at high temperature. It is considered that one of the most efficient techniques for prevention of crack appearance in fusion welding of nickel heat-resistant alloys is reduction of heat input in the product [13] that in most cases is reached by limitation of welding current intensity.

E.O. Paton Electric Welding Institute has developed a process of microplasma powder surfacing of ZhS32 alloy, which is currently used for serial repair of the blades of alloys ZhS26 and ZhS32 [5–9].

Peculiarity of this process is on-line control of welding current in 2–35 A range, surfacing rate in 0.2–3.0 m/h range and amount of filler powder in 0.5–5.0 g/min range depending on thickness of deposited blade flange and required bead section [5–9]. Necessary section of the deposited bead is determined by depth of wear or damage of blade flange (Figure 1) and can be provided per one [5–7] or several [8, 9] layers of repair surfacing.

In earlier published works [5–6] the main attention was paid on registration of separate modes of microplasma surfacing, at which in alloys ZhS26 and ZhS32 their susceptibility to crack formation in fusion welding and further heat treatment didn't appear.

Mastering of multilayer surfacing of alloy ZhS32 is very relevant in recent time due to expansion of a range of repaired parts and increase of zone of service

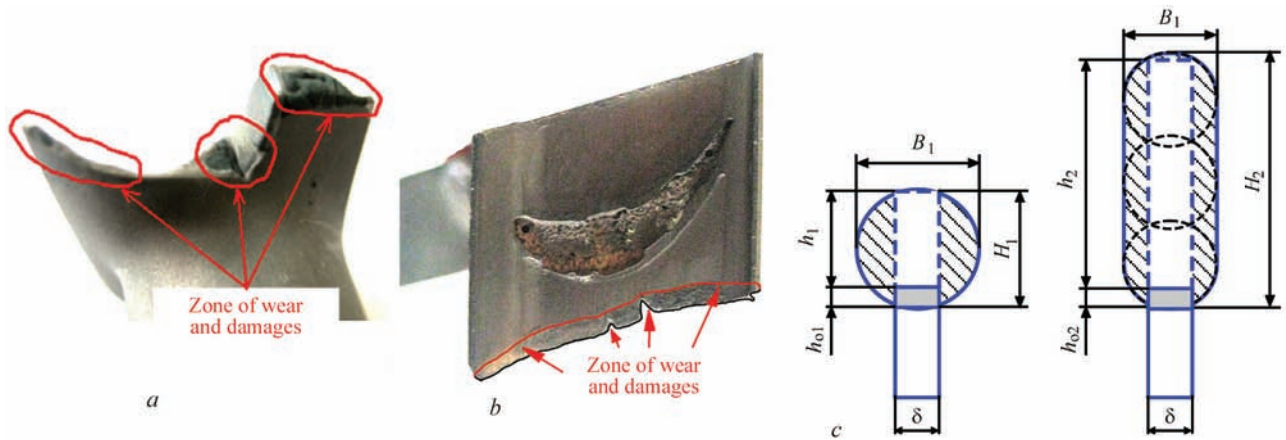


Figure 1. Appearance of wear removed zone and damages on blade flanges of aircraft GTE (a, b) and scheme of distribution of base and deposited metal in cross-sections of bead at their single-layer ($h_1 \leq 4$ mm) and multilayer ($h_1 > 4$ mm) repair surfacing (c) (δ is the thickness of blade flanges; h_{o1} , h_{o2} are the depth of base metal penetration; H_1 , H_2 are the height of deposited bead; h_1 , h_2 are efficient height of deposited bead; B_1 , B_2 are the width of deposited bead

damages [8, 9]. In this connection, aim of the present paper is evaluation of process ranges of modes of microplasma powder surfacing from point of view of crack formation resistance in «base–deposited metal» welded joint of ZhS26–ZhS32 and ZhS32–ZhS32-systems. The cracks can be hot as a result of fusion welding as well as appearing at their further heat treatment.

Series of leading foreign researchers characterize the welding processes on location of areas susceptible and unsusceptible to crack formation in corresponding welded joints of nickel heat-resistant alloys depending on value of heat input and welding rate [14]. The attempts of such an analysis for investigated alloys and process of microplasma powder surfacing have not been made yet.

In our case the following was taken as analyzed total indices of its modes:

- effective heat power of arc $q_{\text{heat s.}}$ characterizing specific power of heat flow of the microplasma arc in anode per unit of time, and first of all, depending on value of welding current intensity [5, 15];

- heat inputs in the product, characterizing average amount of heat introduced per 1 mm of length of deposited bead and, in particular, caused by duration of weld pool existence in molten state [16, 17].

In single-layer surfacing they correspond to heat input $q_{\text{heat s.}}/v$ (taking into account effective efficiency of the product); and in multilayer surfacing they are determined by sum of heat inputs in deposition of each layer $\Sigma Q_z/L$.

The results were received in process of adjustment and mastering of commercial technologies for of microplasma powder surfacing repair of the flanges of blades of ZhS26 and ZhS32 alloys with up to 3–6 thou. h of running, in particular, in aircraft engine D18T [6, 7]. At that in this case of multilayer surfac-

ing no intermediate heat treatments were used for welding stresses relaxation after deposition of each layer or due to technological requirements they were limited by 1050 °C mode (2.5 h) [6, 7]. At that, solubility of γ' -phase in ZhS32 alloy does not exceed 50% [18] at such modes of heat treatment. Therefore, it is assumed that they do not have significant relaxation effect on accumulated welding stresses and deformations in contrast to $\gamma + \gamma' \rightarrow \gamma \rightarrow \gamma + \gamma'$ -transformation in process of homogenization of nickel heat-resistant alloys ZhS26 and ZhS32.

Statistical data on the modes of microplasma powder surfacing were collected in course of registration of its electric parameters and their further treatment using procedure of work [16]. Averaged energy indices of surfacing modes [15, 16], namely effective heat power of arc $q_{\text{heat s.}}$ and heat input $q_{\text{heat s.}}/v$, were determined in 5–40 A range. Used procedure through $q_{\text{heat s.}}$ (I) dependence allowed taking into account pulse modes of welding current with different pulse shape and time of pulse duration as well as level of constriction of microplasma arc, caused by diameters of plasma and focusing nozzle channels of the microplasmatron and composition of shielding gas in Ar + (0–10) % H_2 system. At that, the analysis was made for the process of surfacing (Figure 2) of directly pilot and pilot-commercial batches of GTE aircraft blades (Figure 3) or the process of deposition of the samples in form of narrow substrate [15] of up to 5 mm width, simulating real modes of repair of blade flanges (Figure 4). In some cases (see Figure 4, a) such samples were later on used for evaluation of level of heat resistance of «base–deposited metal» welded joint of alloy ZhS32 [6].

Analyzed values of heat inputs in the product in the studied welded joints were correlated with process strength on criterion of crack formation susceptibility

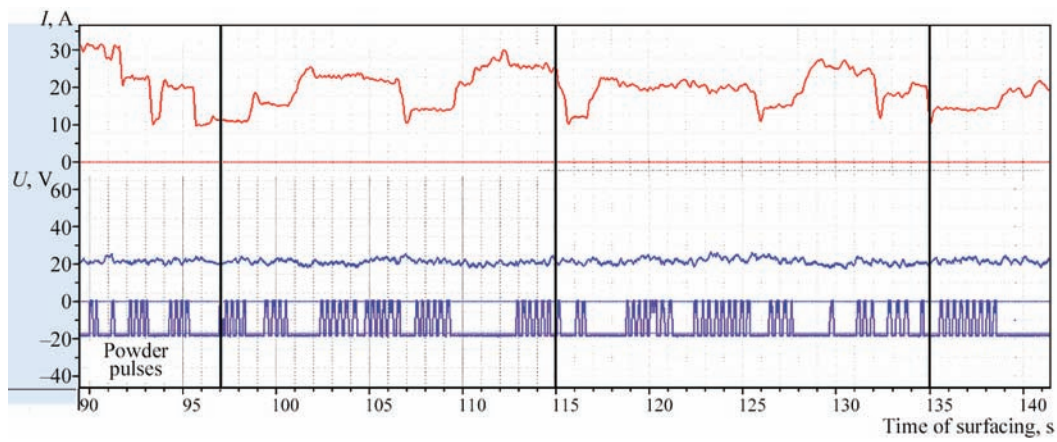


Figure 2. Fragments of registration of parameters of surfacing mode in flange surface of upper platform of MPT blade of ZhS26 alloy



Figure 3. Appearance of aircraft GTE blades, repaired with microplasma powder surfacing of ZhS32 alloy: *a* — HPT blade, alloy ZhS32, engine D18T [6]; *b* — MPT blade, alloy ZhS26, engine D18T [7]; *c* — shroudless HPT blade with inner gas-cooled cavity [8] in «base–deposited metal» joint of nickel heat-resistant ZhS26–ZhS32 and ZhS32–ZhS32 alloy systems. Failures of the process strength of respective joint did not appear in process of fusion welding and their further heat treatment (Figure 5) or under some conditions appeared with high probability in form of macro- and microcracks in fusion welding and/or further heat treat-

ment of the deposited parts (Figure 6). Macrocracks were detected visually or using penetrant testing, microcracks were found applying metallographic analysis of longitudinal cross-sections of «base–deposited metal» joint at $\times 50$ – 200 magnification.

Statistical analysis showed that in microplasma powder surfacing the value of effective heat power of arc in a range less than 650 W and, respectively, the value of welding current up to 30–40 A inclusively can not be uniquely considered as a process parameter completely determining crack formation susceptibili-

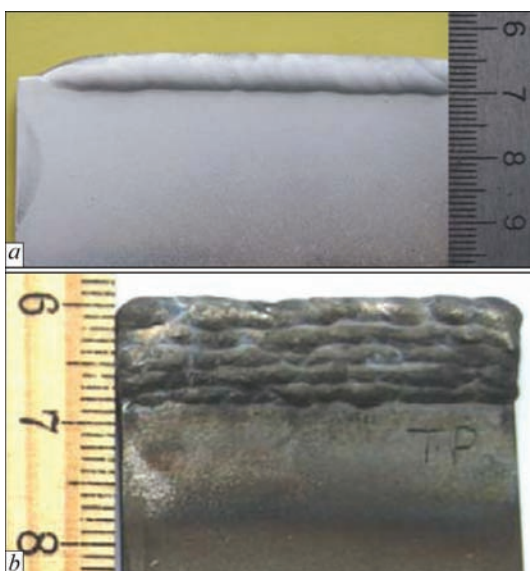


Figure 4. Appearance of samples of ZhS32 alloy simulating repair surfacing of blade flanges of aircraft GTE: *a* — single-layer surfacing on 3.5 mm narrow substrate width; *b* — five-layer surfacing on 2.5 mm narrow substrate width

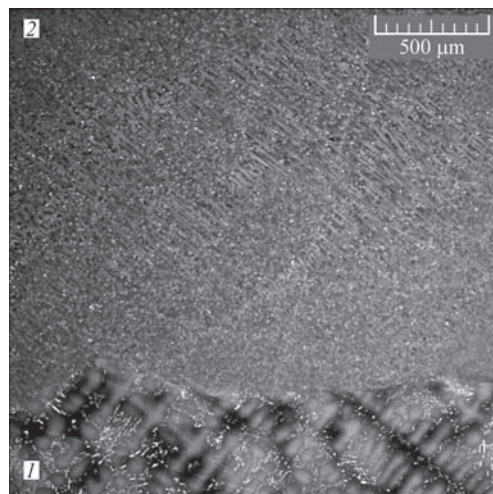


Figure 5. Example of sound microstructure of «base (1) — deposited (2) metal» joint of ZhS32-ZhS32 system, area of fusion line, REM

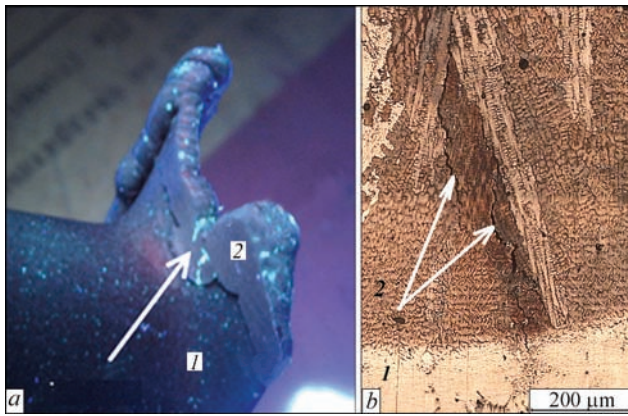


Figure 6. Examples of appearance of macro- and microcracks (indicated by arrows) in «base (1) — deposited (2) metal» joint, detected in process of adjustment of technology of microplasma powder surfacing of MPT blade of aircraft engine D18T (alloy ZhS26): *a* — at penetrant testing; *b* — at metallographic testing (optical microscopy)

ty in «base–deposited metal» joints, made on narrow substrate of 1–5 mm width. Failures of the process strength in $q_{\text{heat s.}} = 150\text{--}450$ W value range as well as obtaining of respective welded joints without crack formation at $q_{\text{heat s.}} \approx 600$ W are possible.

At the same time, the value of total heat inputs $\Sigma Q_{\Sigma}/L$ (Figure 7) can sufficiently uniquely characterize the possibility of crack formation in studied «base–deposited metal» joints of ZhS26–ZhS32 and ZhS32–ZhS32 system. Boundary between the zones, in which the process strength of corresponding joints is provided with high probability or does not provided, lies depending on narrow substrate width $\delta = 1\text{--}5$ mm at $\Sigma Q_{\Sigma}/L = 3200\text{--}4200$ J/mm. In future work, a level of maximum allowable heat inputs for serial repair shall be additionally specified depending on a level of effect of serial of the process factors, namely state of the base metal; height of deposited bead and number of its layers; initial temperature of the joint before deposition of the next layer and others.

It was experimentally determined that in cooling the rate of tensile deformations growth in heat-affected zone of the deposited bead, as a rule, does not exceed the critical values of maximum allowable deformation for alloys ZhS26 and ZhS32. The bead is deposited using single-layer and multilayer microplasma powder surfacing on narrow substrate of 1–5 mm width in a process range of parameters characterized by $I \leq 40$ A, $q_{\text{heat s.}} \leq 650$ W and $\Sigma Q_{\Sigma}/L \leq 3000\text{--}4000$ J/mm.

Thus, it is shown that the effective heat power of arc and value of welding current in up to 40 A range play smaller role, than it was supposed earlier, from point of view of demonstration of susceptibility of the studied nickel heat-resistant alloys with oriented

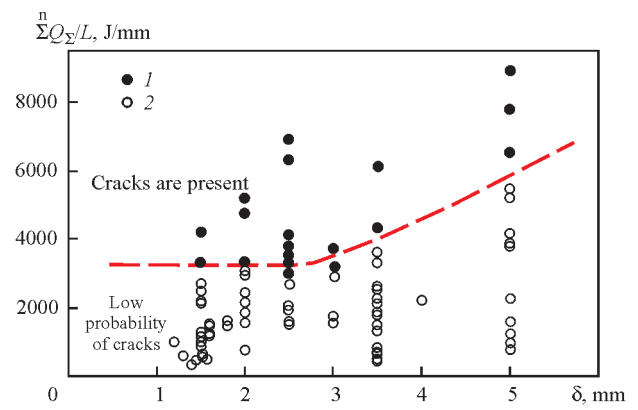


Figure 7. Dependence of obviousness (1) and non-obviousness (2) of susceptibility to crack formation in «base-deposited metal» joint of ZhS26–ZhS32 and ZhS32–ZhS32 systems on value of total heat inputs $\Sigma Q_{\Sigma}/L$ and width of narrow substrate δ

crystallization to crack formation in fusion welding. In particular, this fact is proved by the possibility of performance of sound deposits at variation of welding current intensity in 2–3 times in course of sufficiently long period of time (see Figure 2). It is more reasonable to assume that effect of current intensity and effective heat power of arc develop indirectly via the value of total heat inputs together with surfacing rate and amount of deposited metal layers.

Conclusions

1. A process range of energy parameters of surfacing modes, used for repair of blade flanges of aircraft GTE and providing absence of hot cracks or reheating cracks, was analyzed for conditions of microplasma powder surfacing on narrow 1–5 mm substrate of nickel heat-resistant alloy ZhS32 of limited weldability.
2. For the first time, a boundary was set between process ranges of surfacing modes, where absence or presence of cracks, including hot ones in process of fusion welding, is observed. Its position depending on width of narrow substrate is characterized by value of total heat input 3200–4200 J/mm.

1. Boguslaev, V.A. et al. (2003) *Technological support of service characteristics of GTE parts. Turbine blades. Pt 2.* Zaporozhie: OJSC Motor Sich.
2. Melekhov, R.K., Pokhmursky, V.I. (2003) *Structural materials of power equipment. Properties. Degradation.* Kiev: Naukova Dumka.
3. Pejchev, G.I. et al. (2000) Development and implementation of high-temperature wear-resistant alloy for strengthening of blade flange platforms of GTE. *Tekhnologicheskie Sistemy*, **3**, 40–42.
4. Petrik, I.A., Peremilovsky, I.A. (2001) Further development of strengthening technology of flange platforms of turbine blades heat-resistant alloys. *Ibid.*, **3**, 90–92.
5. Yarovitsyn, O.V. (2009) *Microplasma powder surfacing of nickel heat-resistant alloys containing 45–65 % of γ' -phase.* Syn. of Thesis for Cand. of Techn. Sci. Degree. Kiev: PWI.
6. Yushchenko, K.A., Savchenko, V.S., Yarovitsyn, A.V. et al. (2010) Development of the technology for repair microplas-

- ma powder cladding of flange platform faces of aircraft engine high-pressure turbine blades. *The Paton Welding J.*, **8**, 21–24.
7. Yushchenko, K.A., Yarovitsyn, A.V. (2012) Improvement of technology for reconditioning upper flange platform of aircraft GTE blades. In: Integrated program of NANU: Problems of life and service safety of structures, constructions and machines. Transact. on results of 2010–2012. Kiev: PWI.
 8. Yushchenko, K.A. et al. (2016) Development of technology of microplasma powder surfacing of ZhS32 alloy for reconditioning of gas-cooled blades of aircraft high-pressure turbine. *Ibid.*, 696–701.
 9. Zhemanyuk, P.D., Petrik, I.A., Chigilejchik, S.L. (2015) Experience of introduction of the technology of reconditioning microplasma powder surfacing at repair of high-pressure turbine blades in batch production. *The Paton Welding J.*, **8**, 39–42.
 10. *ISO 17641-1:2004*: Destructive tests on welds in metallic materials. Hot cracking tests for weldments. Arc welding process. Pt 1: General.
 11. Budinovsky, S.A., Kablov, E.N., Muboyadzhan, S.A. (2011) Application of analytical model for determination of elastic stresses in multilayer system in solution of problems on development of high-temperature heat-resistant coatings for aircraft turbine blades. *Vestnik NGTU im. N.E. Baumana. Ser. Mashinostroenie. Spec. issue: Advanced structural materials and technology*, 26–37.
 12. Boley, B., Weiner, J. (1964) *Theory of thermal stresses*. Ed. by E.I. Grigolyuk. Moscow: Mir.
 13. (2004) *Welding. Cutting. Control*: Refer. Book. Ed. by N.P. Alyoshin, G.G. Chernyshov. Moscow: Mashinostroenie.
 14. DuPont, J.N., Lippold, J.C., Kisser, S.D. (2009) *Welding metallurgy and weldability of nickel-base alloys*. J. Willey&Sons, Inc., Hoboken, New Jersey.
 15. Gladky, P.V., Pereplyotchikov, E.F., Ryabtsev, I.A. (2007) *Plasma surfacing*. Kiev: Ekotekhnologiya.
 16. Yarovitsyn, A.V. (2015) Energy approach in analysis of microplasma powder surfacing modes. *The Paton Welding J.*, **5/6**, 14–21.
 17. Yushchenko, K.A., Yarovitsyn, A.V., Chervyakov, N.O. (2016) Dependencies of discrete-additive formation of microvolumes of metal being solidified in multilayer microplasma powder surfacing of nickel alloys. *Ibid.*, **5/6**, 143–149.
 18. (2006) *Cast heat-resistant alloys*. S.T. Kishkin effect. Ed. by E. Kablov. Moscow: Nauka.

Received 01.08.2016

ARGON-ARC WELDING OF TITANIUM AND ITS ALLOYS USING FLUXES (REVIEW)

S.V. AKHONIN and V.Yu. BELOUS

E.O. Paton Electric Welding Institute, NASU

11 Kazimir Malevich Str., 03680, Kiev, Ukraine. E-mail: office@paton.kiev.ua

In 1950–1980 PWI laid the scientific foundations of development of fluxes for welding and melting titanium and its alloys. Technology of automatic consumable electrode welding of titanium with application of oxygen-free fluxes was developed. Processes of tungsten electrode argon-arc welding over a layer of flux (TIG-F) and tungsten electrode welding with application of titanium flux-cored wire (TIG-FW) were developed. These methods expand the technological capabilities of tungsten electrode arc welding, provide high quality of titanium welded joints and guarantee absence of pores in welds. 17 Ref., 4 Tables, 9 Figures.

Keywords: *automatic arc welding, argon-arc welding, titanium alloys, consumable electrode, nonconsumable electrode, oxygen-free fluxes, flux-cored wire*

Complexity of technological processes of titanium welding is due, primarily, to its high reactivity. In welding, titanium actively absorbs gases from the environment leading to an essential lowering of ductile characteristics of the weld. In addition, pores can form in the weld that abruptly lowers fatigue characteristics of welded joints.

One of the founders of studies conducted at PWI to solve the problems of welding titanium, as well as reactive, refractory and non-ferrous metals, was Prof. S.M. Gurevich. Many years of work of the research team led by him, allowed solving for our country the problem of producing sound welds of titanium and its alloys. Owing to detailed investigations, performed under the leadership of Prof. S.M. Gurevich, scientific fundamentals for development of oxygen-free fluxes were laid, and fluxes for titanium welding were developed. As a result, application of practically all the known methods of fusion welding became possible at present to produce titanium welded joints, including consumable electrode submerged-arc welding, tungsten electrode welding, electroslag and electron beam welding, as well as solid-phase welding.

Automatic consumable electrode welding of titanium with application of oxygen-free fluxes. Consumable electrode submerged-arc welding taking one of the leading positions in modern industry by the scope and scale of commercial application, has a number of significant features, compared to other processes. First of all, this is the presence of a shell of molten flux, covering the welding zone and protecting it from harmful effect of atmospheric gases. Here interaction of metal and flux-slag takes places, and metallurgical reactions are running which may lead to weld enrichment in impurities.

It is known that fluxes applied for welding steels, have different oxidizing properties with respect to

iron. Investigations conducted in 1950s in our country and abroad showed that in welding titanium even with low-silicon fluxes, conditionally called basic, which are characterized by the lowest oxidation ability, the metal is intensively saturated with oxygen, leading to a brittle joint [1].

As a result, in the initial period of industrial application of titanium as a structural material, some foreign researchers even denied the principal possibility of submerged-arc welding application for titanium, as at that time metallurgists failed to select a material that would not react with it or contaminate it with oxygen [2].

Theoretical studies, confirmed by experimental work conducted at PWI under the leadership of Prof. S.M. Gurevich, allowed refuting this erroneous opinion. Possibility of welding titanium using special refractory fluxes was proved, principles of construction were established and new systems of halogene oxygen-free fluxes were created [3].

Analysis of metallurgical and technological features of welding titanium allowed defining special requirements, which should be met by the developed flux systems. The main of them is complete absence of oxides. It was established that presence of even such stable oxides as Al_2O_3 , ZrO_2 and TiO_2 in the flux does not prevent weld metal oxidation (Figure 1). Only complete removal of oxides from the flux ensures oxygen content below 0.1 % in the deposited metal.

Investigations, led by Prof. S.M. Gurevich, showed that oxygen-free fluxes for welding titanium and its alloys, meeting the above requirements, can be created by applying fluorides and chlorides of alkali and alkali-earth metals as their components [4]. Interaction of weld pool metal with the flux should be considered primarily as one of the most important metallurgical features of submerged-arc welding of titanium. Thermodynamic calculations, as well as results of some direct studies showed that two types of reactions can run: titanium reaction

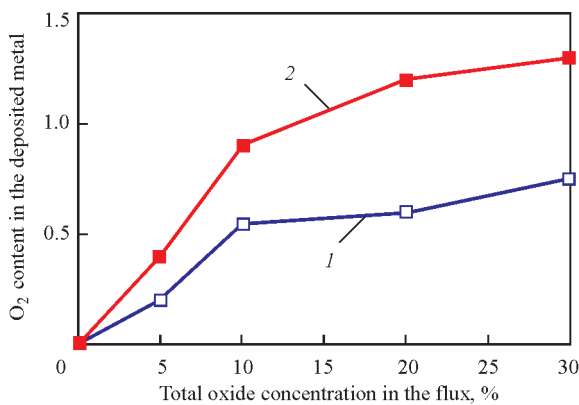


Figure 1. Oxygen content in the deposited layer, depending on concentration of some oxides in the flux: 1 — Al₂O₃; 2 — SiO₂ with flux components and titanium oxide reaction with the flux. Thermodynamic calculations, studies of the slag crust and deposited metal allowed formulating requirements to fluxes for welding titanium alloys:

- for a more complete interaction of flux with titanium and its oxides it is desirable for the flux composition to contain maximum amount of fluorides and minimum amount of chlorides;
- the most suitable components for the flux are fluorides, characterized by the greatest ability to react with titanium oxides.

The best results were obtained when CaF₂ was used as the flux base. An important property of this refractory fluoride is its ability to intensively interact with water vapour with formation of hydrogen fluoride, presence of which in the arc zone was established experimentally. Thermodynamic calculations show the possibility of running of a reaction between CaF₂ and water vapour at temperatures above 2000 °C. Ability to remove absorbed moisture from the welding zone and owing to that, protection of weld metal from saturation with hydrogen and oxygen, is an important feature of welding titanium using CaF₂-based flux, that is one of the causes of complete absence of porosity in welds made with consumable electrode using fluoride fluxes.

Selection of optimum composition of CaF₂ based fluxes is a complex task in connection with the fact that numerous eutectics form with lower-melting fluorides, while regions of melt concentrations characterized by sufficiently high melting temperature, are extremely limited. PWI studies were the basis to develop oxygen-free halogenide fluxes of ANT series, such as ANT-1, ANT-3, and ANT-7, designed for consumable electrode welding of titanium and its alloys [3, 5]. During welding, the developed fluxes reliably isolate the molten metal pool and cooling sections of

the weld and HAZ from harmful contact with atmospheric gases, that is indicated by the results of analysis of gas content in the metal of commercial titanium weld (Table 1). To ensure impurity content in the weld metal on the level of their concentration in BM, it is necessary to apply flux with moisture content of not more than 0.05 %. Particle size distribution in the flux is from 0.3 up to 1.5 mm. Investigations showed that welds made with flux application, have no pores, slag inclusions, cracks or other defects.

Technological properties of fluxes of ANT series, designed for automatic consumable electrode welding of titanium (process stability, good weld formation, etc.), largely depend on CaF₂ purity. It is established that the cause for flux properties deterioration is CaO content in the flux, the amount of which should not be higher than 0.5 %. To ensure maximum purity of the fluxes, primarily, for oxide content, chemically pure reagents are used in their manufacture, application of minerals and components of commercial purity is not allowed.

Development of welding consumables for submerged-arc welding of titanium was also the basis for development of fluxes and technology for electrosag welding and melting of titanium [6].

Technology of automatic consumable electrode welding of titanium using oxygen-free fluxes was developed at PWI under the leadership of Prof. S.M. Gurevich [7]. This method allows making all the main types of welds on titanium, namely butt, fillet, tee and overlap welds at 3 to 40 mm thickness of the elements being joined.

A quite essential feature of automatic submerged-arc welding of titanium is the need to perform the process at minimum admissible distance between the surface of metal being welded and lower point of the nozzle — dry extension of electrode wire. This is due to the fact that titanium has very high specific electric resistance and increase of dry extension leads to excess heating of electrode wire, its saturation by harmful gas impurities, violation of welding process stability, and, consequently, deterioration of mechanical properties and quality of weld formation. Welding is performed at reverse polarity direct current. Welding at straight polarity and alternating current markedly impairs weld formation. Welding wires of 2.5; 3.0; 4.0 and 5.0 mm can be applied. Application of larger diameter wires is difficult, because of their higher rigidity. Welding wire of VT1-00sv grades is used for welding commercial titanium VT 1-00 and VT 1-0 and low alloys OT4, OT4-0, OT4-1, VT-5, VT5-1, and 4200. Wires of SPT2, VT20sv and other

Table 1. Content of main impurities in the metal of welds in VT1-00 titanium welded joints made with ANT-1 flux

Metal thickness <i>b</i> , mm	Content, % (BM/weld metal)			
	N ₂	O ₂	H ₂	C
2.0	0.029/0.025	0.085/0.085	0.008/0.007	0.07/0.05
4.5	0.037/0.030	0.078/0.077	0.004/0.005	0.06/0.04

grades are applied for welding medium and high alloys. It is recommended to perform welding of PT-3V, PT-7M type alloys with 2V wire.

It is recommended to perform welding of longitudinal welds on thin metal (3–6 mm), as well as multilayer welds on metal of medium thickness at small current using ANT-1 flux. ANT-3 flux is applied for making circumferential welds on titanium of small thickness and all single-pass welds on titanium of medium thickness. ANT-5 and ANT-7 fluxes are designed for joining thick metal in welding at currents exceeding 700 A.

Comparison of the results of testing the metal of welds made by automatic submerged-arc welding and nonconsumable tungsten electrode welding in a chamber with argon atmosphere showed that the strength and ductility characteristics are almost equal in both the cases. However, toughness of welds made by submerged-arc welding, even though it is at a sufficiently high level, is inferior to the respective indices of welds, made with tungsten electrode in argon. Thus, impact toughness KCU of the metal of weld on VT5-1 alloy made by automatic submerged-arc welding, is equal to 48 J/cm², here impact toughness of the metal of weld made by tungsten electrode in argon, has the value of $KCU = 62$ J/cm².

A combined flux-gas method of weld pool shielding during automatic consumable electrode welding was developed for welding special-duty structures [8]. Its essence consists in that flux blowing with argon is performed in a hopper of special design during flux feeding into the welding zone. Nitrogen and oxygen penetration into the weld pool is completely eliminated as a result of argon ousting the air present between the flux granules. Mechanical properties of the metal of weld, produced with consumable electrode flux-gas shielding, and of the weld, made with tungsten electrode in a chamber with inert atmosphere of argon, were similar (Table 2). Flow rate of argon required for blowing the flux in the hopper, is equal to 3–4 l/min.

Butt joints up to 10 mm thick can be welded with success from one side. It is rational to perform butt joints of 10–16 mm thickness by welding from two sides on a copper water-cooled backing with inert gas shielding of the butt reverse side. For better penetration of the butt and quality of weld formation, it is rational to apply X-shaped groove preparation of the edges to be welded. Here, groove preparation with 90 deg bevel offers the greatest advantages from the technological point of view. This provides a high stability of the welding process, good separability of the slag crust, and improves the penetration depth. Experimental data enables establishing the dependence of welding current on electrode wire feed rate (Figure 2).

Automatic submerged-arc welding of titanium items of more than 16–18 mm thickness was performed with edge preparation by deposition of sever-

Table 2. Mechanical properties of welded joints (VT1-0) made with flux-gas shielding and with shielding in a chamber with controlled atmosphere

Weld pool shielding method	$\sigma_{0.2}$, MPa	σ_r , MPa	δ , %	ψ , %	a_k , J/cm ²
Flux-gas	315	407	28.6	61.3	83
Inert gas	310	402	30.2	62.8	81

al layers. The surface of the previous weld should be thoroughly scraped before welding of each next layer. Number of weld scraping operations can be reduced by application of welding by two arcs, positioned one behind the other and shifted to a certain distance across the weld axis. This method allows producing welds with greater coefficient of groove filling, smooth transition from BM to weld reinforcement and high values of strength and ductility (Table 3). This method is also effective in welding fillet, tee and overlap joints [1].

Tungsten electrode argon-arc welding of titanium with application of oxygen-free fluxes. As shown by experience of application of automatic consumable electrode welding with oxygen-free fluoride-chloride fluxes, the produced welds are characterized by high density and absence of porosity. This was noted by the authors of works [9, 10], who studied the measures to prevent porosity, forming in nonconsumable electrode argon-arc welding of titanium. They showed experimentally that positive influence of fluorides on weld density is also preserved in welding in inert atmosphere. So, a radical method of prevention of weld porosity by metallurgical measures, namely welding with activating CaF₂ reagent, was proposed for the first time for argon-arc welding of titanium. Later on, more effective and adaptable-to-fabrication fluxes for tungsten electrode welding of titanium and its alloys were developed. More over, it turned out that halogenides of alkali and alkali-earth metals, when penetrating into the arc zone, constrict the arc and change the nature of metal penetration and weld formation. At arc movement along the butt at the moment of its transition from the surface of metal not coated by flux,

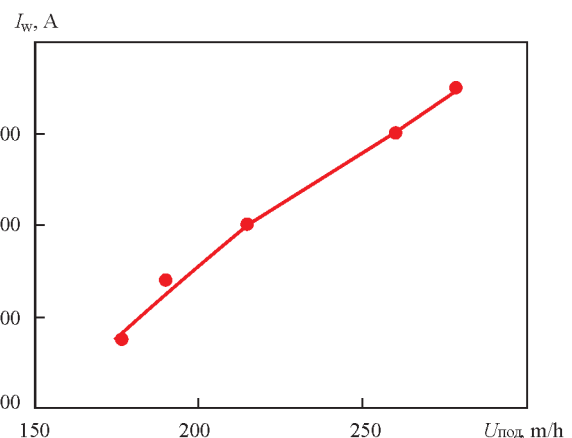


Figure 2. Dependence of welding current value on electrode wire feed rate in submerged-arc welding of titanium

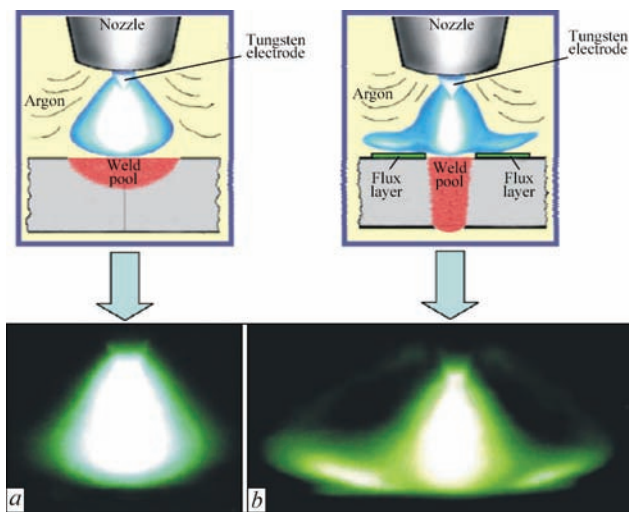


Figure 3. Schematic and photo of an arc without flux (a) and with flux (b)

to a layer of halogenide, arc constriction and change of its colour is visually observed, the arc moves deeper into the metal and the weld becomes narrower.

PWI studied the influence of fluorides of alkali and alkali-earth metals on the process of tungsten electrode welding, such as, for instance, LiF, CaF₂, SrF₂, BaF₂, KF, RbF, CsF, NaF, MgF₂, etc., investigated binary and ternary fluoride systems and as a result, developed ANT-17, ANT-32 and ANT-25 fluxes, designed for automatic tungsten electrode argon-arc welding of titanium. A method of argon-arc welding by tungsten electrode over a layer of flux (TIG-F) [1, 11] and with titanium flux-cored filler wire (TIG-FW) was developed [11, 12]. In both cases, the shielding role of the flux is secondary. Its main function is enhancement of technological capabilities of the arc. Deep penetration of metal, narrow welds, short extent of the HAZ, relatively low heat-input, and, consequently, reduction of residual welding deformations are some of the advantages of TIG-F welding process (Figure 3).

Flux addition to the arcing zone in argon-arc welding leads to a change of spatial characteristics and electric parameters of the arc, in particular, to compression of the arc column and increase of anode current density (Figure 4), and consequently, it allows controlling the parameters of welds, and, primarily, increasing penetration depth [12, 13].

The observed physical phenomena in the arc, dependent, primarily, on flux composition, determine also the technological advantages of TIG-F and TIG-FW welding, compared to TIG process. At unchanged value of welding current and welding speed flux application significantly increases penetration depth,

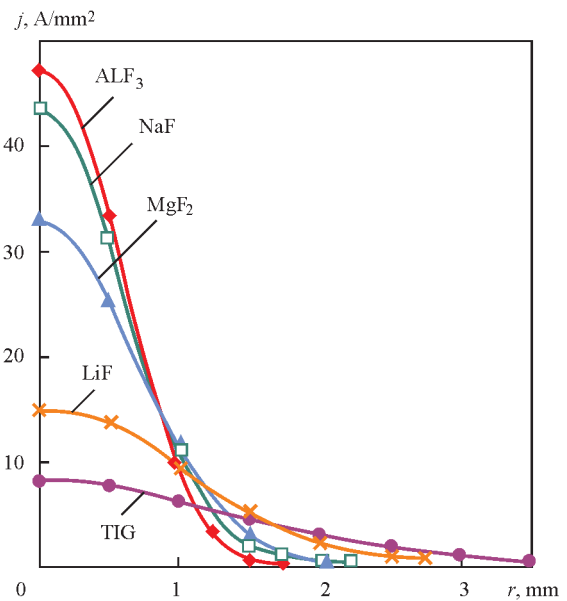


Figure 4. Radial distribution of current density in the anode spot in welding of titanium with different fluorides ($I_w = 100$ A; $v_w = 10$ m/h)

reduces weld width, as well as lowers heat input (Figure 5). However, at current increase above 200 A, the applied quantity of flux is no longer sufficient and flux effectiveness drops markedly. Considering such a feature of TIG-F welding, this welding process is recommended to perform welds on metal of 0.8 to 6.0 mm thickness [14, 15]. ANT-23 flux is designed for welding sheets of 0.8–3.0 mm thickness, and ANT-25 flux is used for square edge welding of 3 to 6 mm thick sheets in a single pass. A small volume of the weld pool allows application of single-pass automatic welding over a layer of ANT-25 flux to join metal up to 6 mm thick on vertical plane.

Argon-arc tungsten electrode welding of titanium with application of flux-cored wires. As was already mentioned, at current increase above 200 A, the quantity of flux preapplied on the edges being welded is no longer sufficient and flux effectiveness decreases. The quantity of flux, added to the arc, i.e. the applied layer thickness, has the strongest effect on penetration depth, as greater penetration depth corresponds to greater thickness of the flux layer. Therefore, a welding consumable, principally new for titanium applications, namely flux-cored filler wire (Figure 6), and technology of tungsten electrode welding of titanium with application of flux-cored wire (TIG-FW), were developed for welding titanium of more than 6 mm thickness. Flux-cored wire basically is a titanium foil sheath, containing flux filler [14, 15]. Two types of

Table 3. Mechanical properties of welded joints made by automatic two-arc welding with ANT-7 flux*

Alloy grade	b , mm	$\sigma_{0.2}$, MPa	σ_t , MPa	δ , %	ψ , %	a_T , J/cm ²
PT-3V	25	676/617	727/677	20.2/19.5	39.6/36.2	68/62
OT4	32	694/661	769/739	23.2/22.3	38.1/35.3	96/88

*VT1-0 electrode wire.

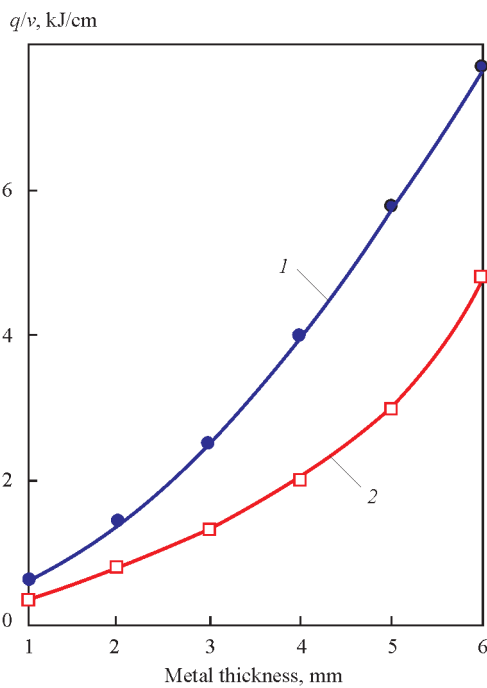


Figure 5. Dependence of heat input on metal thickness in welding without flux (1) and over a layer of flux (2) (ANT-23 and ANT-25A fluxes)

flux-cored wire were developed, namely PPT-1 and PPT-2, differing both by chemical composition of the filler, and by their design. Wire of PPT-1 grade is used in those cases, when no weld reinforcement is required by service conditions. Wire of PPT-2 grade with solid titanium wire inside it, allows producing welds with reinforcement.

Application of flux-cored filler wire allows increasing the quantity of flux in the welding zone. Due to that TIG-FW method (Figure 7) allows welding titanium alloys 6.0–16.0 mm thick in a single pass without edge reparation. Flux-cored wire can be applied with success for making not only butt, but also tee joints. As an illustration, Figure 8 gives the macrosections of welded joints of different types, made by TIG-F and TIG-FW processes.

After welding, a layer of solidified slag remains on the surface, which provides additional shielding of solidifying metal. Its removal is performed as after welding over a layer of flux. In addition to technological advantages, application of fluxes and flux-cored wires in argon-arc welding of titanium has an essen-

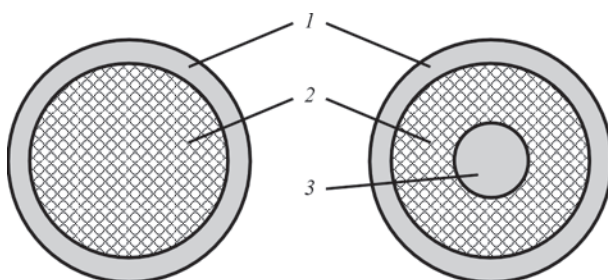


Figure 6. Flux-cored wire cross-section: 1 — sheath; 2 — flux filler; 3 — core

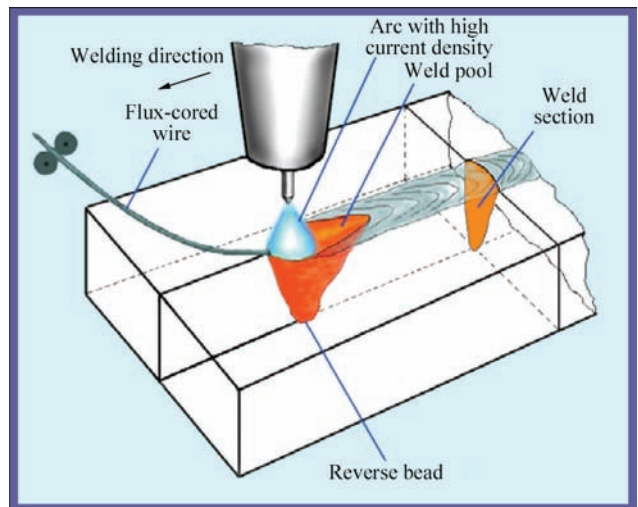


Figure 7. Schematic of TIG welding with flux-cored wire

tial influence on metallurgical processes in the weld pool, in particular, it prevents formation of pores in welds. Porosity is known to be the main type of metallurgical defects in titanium alloy welded joints, made both by arc and beam welding processes. Presence of pores in welds only slightly affects the properties of welded joints at static loads, but significantly lowers their performance under dynamic loads, markedly decreasing the fatigue limit.

Defects developing in the weld in the form of pores significantly lower welded joint fatigue resistance. Now, application of halogenide fluxes and flux-cored wires, allows prevention of pore formation in welds (Table 4).

As is seen from the above data, volume fraction of pores in the metal of welds made on commercial titanium by different fusion welding processes differs essentially by its value. Maximum number of pores is found in EBW welds and minimum number of pores is present in welds made by ESW and TIG with application of flux that is attributable to active metallurgical interaction of flux with molten metal of the weld pool [16].

Investigations showed that application of fluxes and flux-cored wires in welding leads to hydrogen binding by fluorine in the weld pool into hydrofluorides of $TiF_{x-}H_y$ type, which remain in weld metal as microscopic slag inclusions, that, as shown by testing, have no es-

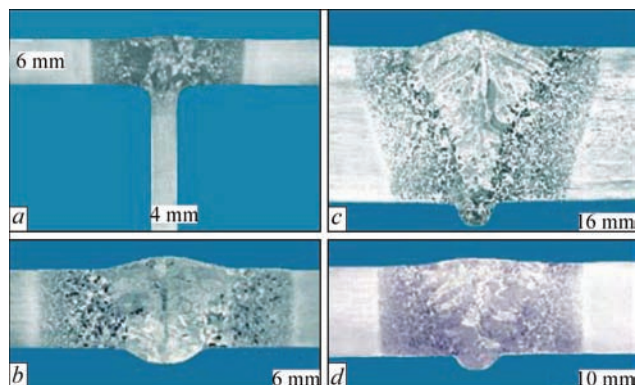


Figure 8. Macrosections of welded joints made over a layer of flux ANT-25A (a, b); PPT-2 (c); PPT-1 (d)

Table 4. Volume fraction of pores in titanium joints made by different welding processes

Welding process	Metal	Volume fraction of pores $m_2, \%$
Argon-arc welding (TIG)	Base metal	0
	Weld made with through penetration of the plate	0.82
	Weld made over a layer of ANT-17A flux	0.65
	Weld made over a layer of ANT-25A flux	0.43
Electron beam welding (EBW)	Base metal	0
	Weld made with through penetration of the plate	1.40
	Butt weld	1.34
Electroslag welding (ESW)	Base metal	0
	Weld	0.46

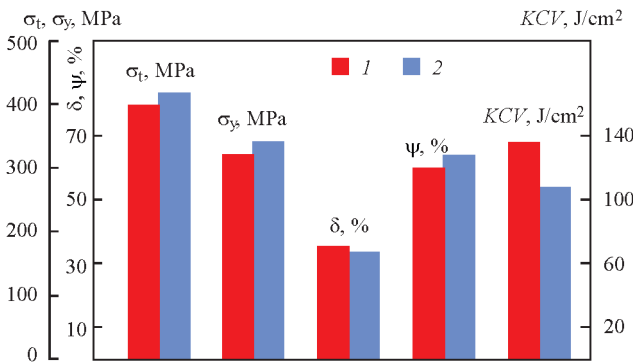


Figure 9. Mechanical characteristics of welded joint of unalloyed titanium of Grade 2 (6 mm thickness): 1 — base metal; 2 — weld metal

stantial influence on mechanical properties of welded joints (Figure 9), made with flux application.

Application of welding over a layer of flux allows a significant improvement of technico-economic indices of welding [17]. So, for instance, in welding 5 mm titanium sheet welding time, wire consumption and argon flow rate are reduced by more than 60 %, and power consumption decreases by more than 50 %. Here, the cost of 1 m of weld (including additional cost of flux), decreases almost two times.

Conclusions

1. PWI developed a series of oxygen-free fluxes and technology of consumable electrode welding of titanium with application of the developed fluxes for welding titanium and alloys on its base.

2. Developed fluxes and method of tungsten electrode welding of titanium over a layer of flux (TIG-F) widen the technological capabilities of tungsten electrode welding of titanium, provide greater penetrability of the arc, absence of pores in welds, and high quality of the produced joints.

3. Application of flux-cored wire and TIG-FW method of tungsten electrode welding of titanium allows performing single-pass welding of up to 16 mm thick metal with complete penetration and guarantees absence of pores in welds and high quality of the produced joints.

- Gurevich, S.M. et al. (1986) *Metallurgy and technology of welding of titanium and its alloys*. Kiev: Naukova Dumka.
- Hoefler, H.W. (1958) Fusion welding of titanium in jet engine applications. *Hawker-Siddeley Techn. J.*, 1(1), 61–64.
- Gurevich, S.M. (1961) Fluxes for automatic welding of titanium alloys. *Aviats. Promyshlennost*, 5, 55–59.
- Gurevich, S.M. (1960) Problems of metallurgy of welding of titanium. *Titan i jego Splavy*, Issue 3, 127–132.
- Gurevich, S.M. (1957) Submerged-arc welding of titanium. *Aviats. Promyshlennost*, 4, 13–16.
- Gurevich, S.M., Didkovsky, V.P. (1960) Technology of electroslag welding of titanium alloy forgings. In: *New welding processes*. Moscow: Mashinostroenie.
- Gurevich, S.M. (1958) Technology of welding of parts from titanium and its alloys. In: *Transact. on Advanced Sci.-Techn. and Production Experience*. Kiev: AN SSSR.
- Gurevich, S.M. (1957) Some peculiarities of submerged-arc welding of titanium. *Avtomatich. Svarka*, 5, 38–48.
- Timoshenko, A.N., Pidzhary, A.F., Bessonov, A.S. (1966) *Method of argon-arc welding of titanium alloys*. USSR author’s cert. 183303. Publ. 1966.
- Maslyukov, O.A. (1965) Prevention of porosity in argon-arc welding of titanium and other metals and alloys. In: *Abstr. of Pap. of All-Union Meeting of Fusion Welding of Thin Metals*. Kiev: PWI, 49–53.
- Zamkov, V.N., Akhonin, S.V. (2001) New methods for welding titanium and manufacture of unique large-sized titanium semi-finished products. *The Paton Welding J.*, 9, 33–39.
- Paton, B.E., Zamkov, V.N., Prilutsky, V.P. et al. (2000) Contraction of the welding arc caused by the flux in tungsten-electrode argon-arc welding. *Ibid.*, 1, 5–11.
- Prilutsky, V.P., Yeroshenko, L.E., Zamkov, V.N. (1997) Distribution of vapours of metals and welding consumables in arc during TIG welding. In: *Proc. of the ASM Int. Europ. Conf. on Welding and Joining Science and Technology* (10–12 March 1977, Madrid, Spain).
- Zamkov, V.N., Prilutsky, V.P., Topolsky, V.F. (2000) Consumables and methods of welding titanium for aerospace engineering application. *J. of Advanced Materials*, 32(3), 57–61.
- Paton, B.E., Zamkov, V.N., Prilutsky, V.P. (1998) Le soudage A-TIG du titane et de ses alliages. *Soudage et Techniques Connexes*, 52, 11–12.
- Prilutsky, V.P., Akhonin, S.V. (2007) Tungsten electrode argon-arc welding of titanium alloys using fluxes. In: *Proc. of Int. Conf. on Titanium-2007 in CIS* (Yalta, 15–18 April, 2007), 441–448.
- Prilutsky, V.P., Akhonin, S.V. (2014) TIG welding of titanium alloys using fluxes. *Welding in the World*, 58, 245–251.

Received 23.01.2016

PRODUCING DISSIMILAR JOINTS OF MOLYBDENUM–STAINLESS STEEL USING VACUUM BRAZING

S.V. MAKSYMOVA, V.V. VORONOV, P.V. KOVALCHUK and A.V. LARIONOV

E.O. Paton Electric Welding Institute, NASU

11 Kazimir Malevich Str., 03680, Kiev, Ukraine. E-mail: office@paton.kiev.ua

In this work the possibility of using brazing alloys with the structure of a solid solution based on Cu–Mn–Ni system for brazing dissimilar joints of molybdenum-stainless steel was shown, the results of micro X-ray spectrum examinations and strength characteristics of brazed joints were presented. The micro X-ray spectrum examinations revealed that in producing dissimilar joints of molybdenum-stainless steel using brazing alloys based on Cu–Mn–Ni system the central zone of a brazed weld is composed of a solid solution on copper base. The diffusion zone of weld (on the side of molybdenum) is formed by the phase based on molybdenum, which is precipitated in the form of a continuous band along the brazed weld. The application of brazing alloy based on Cu–Mn–Ni system with the structure of a solid solution provides formation of dense brazed welds without cracks. The shear strength is at the level of 200–210 MPa during fracture in the brazed weld and at 300 MPa during fracture in the base metal (molybdenum). 9 Ref., 3 Tables, 10 Figures.

Keywords: *dissimilar joints, vacuum brazing, brazing alloy, structure, solid solution, weld, mechanical properties*

The optimum service properties of a number of structures can be provided by applying the composite combined units of dissimilar metals. In this case, the advantages of each of them are most completely realized and the expensive metals are saved [1]. The joints of dissimilar materials produced using brazing, are in demand in different branches of industry [2, 3].

In particular, the joints of molybdenum-stainless steel are used in manufacturing parts operating for a long time at a high temperature in the nozzles of rockets and electric vacuum devices, in nuclear power industry in manufacture of nuclear reactors, in production of round anodes of X-ray tubes, heat exchangers, for manufacture of equipment operating in aggressive environments and a number of other products [4, 5]. It was managed to reach the higher manufacturability of many modern structures mainly due to the use of the latest achievements in the field of brazing. The selection and use of dissimilar metals as structural materials are determined by the service requirements specified for the structure and by economic indicators.

It is naturally, that the joining of dissimilar metals represents a more complicated problem than joining of similar joints. This is due to the difference in chemical composition and physical and mechanical properties of materials being joined. Thus in brazing dissimilar metals a big problem is to provide wetting of both materials and overcoming the difference in the coefficients of thermal expansion, which may lead to formation of brittle intermetal-

lic interlayers at the interface, occurrence of inner stresses, appearance of cracks.

Each pair of the dissimilar materials being joined requires an individual approach in choosing brazing alloys and parameters of technological brazing process [6]. The applied brazing alloys should provide good wetting of both metals, the melting temperature of brazing alloy should not exceed the solidus temperature of a more low-melting base metal. The final aim of the technological process of brazing is the formation of serviceable joints with the specified service characteristics.

In brazing of refractory, chemically active metals (molybdenum, etc.) with corrosion-resistant steels it is necessary to apply brazing alloys with the structure of a solid solution or plastic brazing alloys based on the copper-silver system, which will contribute to relaxation of stresses in the brazed joint and serve as a damper between two metals being joined. However, brazing alloys based on silver are characterized by a low melting temperature and a low resistance under the conditions of neutron radiation.

In this work the features of formation of brazed joints of molybdenum-stainless steel using brazing alloys with the structure of a solid solution based on the copper-manganese system, and the results of micro X-ray spectrum examinations of brazed joints and their strength characteristics are presented.

As the base metal, molybdenum, stainless steel 09Kh18N10T and brazing alloys based on cop-

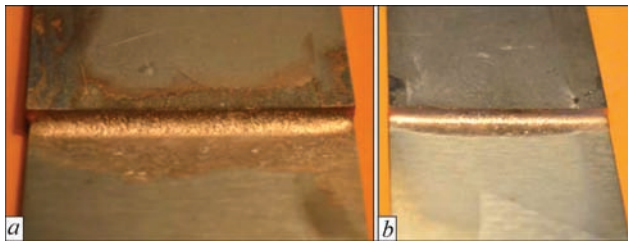


Figure 1. Appearance of brazed specimens of molybdenum-steel 09Kh18N10T: *a* — straight; *b* — reverse fillet

per-manganese system were applied. The brazing alloys were applied in the cast form and were produced by melting in the laboratory installation in the shielding atmosphere of argon. The produced ingots were overturned and remelted (up to 5 times) in order to average the chemical composition and provide a uniform distribution of elements. The solidus and liquidus temperatures of cast brazing alloys were determined using the installation of high-temperature differential analysis in the shielding atmosphere of helium at constant heating and cooling rate (40 °C/min).

For metallographic examinations the overlapped joints were brazed, the specimens were cut out perpendicular to the weld, the microsections were manufactured according to the standard procedure and examined using the scanning electron microscope TescanMira 3 LMU. The distribution of chemical elements was examined using the method of a local micro X-ray spectrum analysis applying the energy dispersion spectrometer Oxford Instruments X-max (80 mm²) under the control of the software package INCA. The locality of micro X-ray spectrum measurements did not exceed 1 μm, the filming of microstructures was carried out in back-scattered electrons

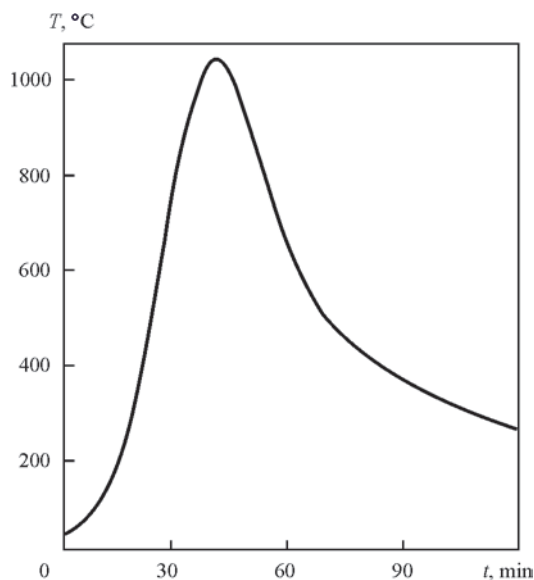


Figure 2. Thermogram of heating during brazing of molybdenum with stainless steel applying brazing alloy No. 1

Table 1. Applied brazing alloys and brazing modes

Number of brazing alloy	Basic alloying system of brazing alloy	Brazing temperature, °C/time, min
1	Cu–Mn–Ni–Fe–Si	1050/3
2	Cu–Mn–Ni–Si	1100/5
3	Cu–Mn–Ni	1084/3

(BSE), which allowed examining the microsections without chemical etching.

For mechanical tests the plane overlapped joints of the 100×30×3 mm size were brazed and tested using the installation MTS-810.

Among the peculiarities of molybdenum there is a low resistance to oxidation at high temperatures. Above 500 °C the sublimation of MoO₃ begins and at 600 °C it becomes more significant and at higher than 800 °C the MoO₃ is melting which leads to hyperactive oxidation in the air atmosphere [7]. Therefore, brazing of molybdenum was carried out in vacuum. During assembly of specimens for brazing the brazing alloy was placed near the brazing gap. During heating the brazing alloy was melted and due to capillary forces it flowed into the gap.

The visual inspection of appearance of brazed specimens showed that while using brazing alloys (Table 1) a smooth straight complete fillet (Figure 1, *a*) is formed. The inverse fillet differs from a straight one by a smaller size (Figure 1, *b*).

In brazing of dissimilar joints of stainless steel-molybdenum applying brazing alloy No.1 at the mode, shown in Figure 2, *a* wide brazed weld based on copper is formed (Figure 3, *a*).

In the central area of the brazed weld the solid solution based on copper (92.58 %) is crystallized which except of the constituent elements of brazing alloy contains also a small amount of iron, which is 2.87 %.

In some areas the brazing alloy penetrates into stainless steel to the maximum depth of 20 μm (Figure 3, *a*).

In the peripheral zone of brazed weld, which borders with molybdenum, two diffusion layers are observed, which are distinguished in the form of narrow solid bands along the brazed weld. One of them, based on molybdenum, (51.21 %) is enriched with iron (31.71 %), silicon (up to 5.88 %) and located closer to molybdenum (Figure 3, *b*). The second one is based on iron (68.02 %) and does not contain molybdenum but also enriched with silicon and borders with a solid solution based on copper. Their width is variable, but it does not exceed 5 μm for each one. The common feature for these layers is the presence of increased concentration of silicon from 4.83 to 5.88 % (Table 2).

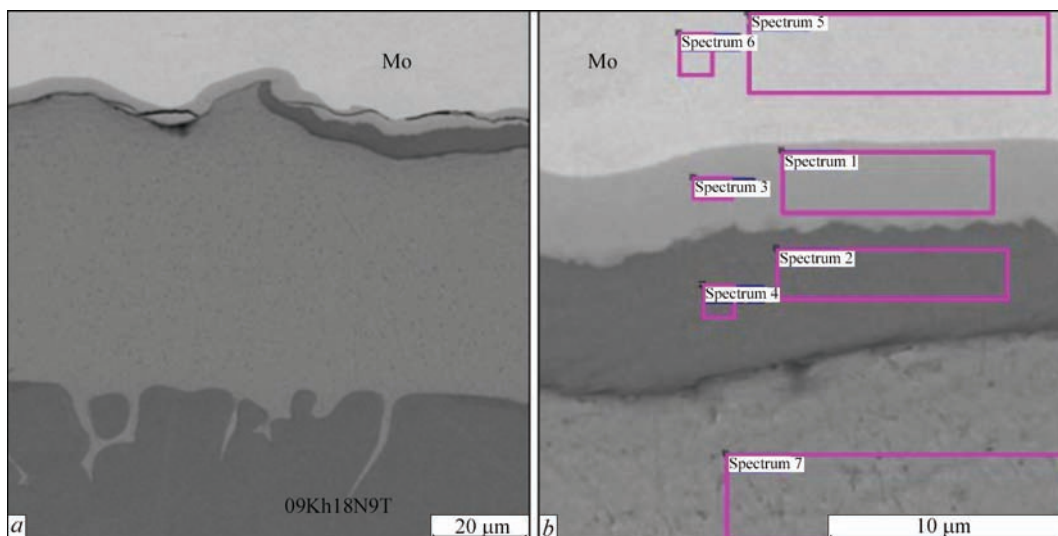


Figure 3. Microstructure (*a*) and examined regions of brazed joints (*b*), produced applying brazing alloy No.1

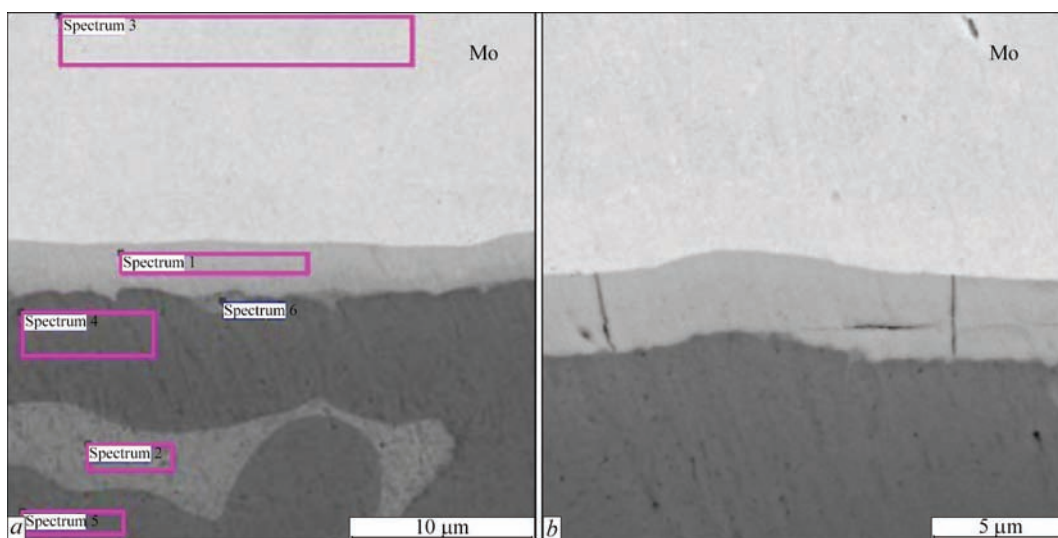


Figure 4. Examined regions of weld of brazed joint, produced applying brazing alloy No.2

It is obvious that during brazing the silicon interacts with iron and molybdenum, but during cooling of brazed joints under non-equilibrium conditions (at the drop of temperature and limited solubility of silicon) the phases are formed enriched with the latter.

The presence of gradient of concentration of chemical elements in these areas promotes the formation of longitudinal cracks (Figure 3, *a*) along the weld on the side of molybdenum over the diffusion layer based on molybdenum (51.21–52.59 %), enriched with iron

(31.71–32.07 %) (Table 2, spectrum 1, 3). Such a formation of brazed joints is caused by mutual diffusion processes, occurring at the brazing alloy-stainless steel interface.

In brazing applying the brazing alloy with a reduced (0.2 %) concentration of silicon (No.2) the formation of fillet areas does not differ externally from the previous specimen. The brazing alloy provides a good wetting of base metals, it also penetrates into the base metal (stainless steel) along the grain bound-

Table 2. Results of micro X-ray spectrum analysis of individual phases of brazed joint applying brazing alloy No.1

Number of spectrum	Chemical elements, wt.%							
	O	Si	Cr	Mn	Fe	Ni	Cu	Mo
1	–	5.88	7.08	0.77	31.71	2.54	0.81	51.21
2	–	4.83	16.79	2.23	68.02	4.46	3.67	–
3	–	5.65	6.56	0.86	32.07	2.27	0.00	52.59
4	–	4.92	16.50	2.48	66.79	4.63	4.68	–
5	1.74	–	–	–	–	–	–	98.26
6	1.85	–	–	–	–	–	–	98.15
7	–	–	0.30	3.04	2.87	1.21	92.58	–

Table 3. Chemical composition of investigated areas applying brazing alloy No.2

Number of spectrum	Chemical elements, wt. %							
	Si	Ti	Cr	Mn	Fe	Ni	Cu	Mo
1	0.92	0.00	8.41	0.69	23.55	2.52	0.49	63.41
2	0.09	0.00	0.98	4.93	4.65	2.22	87.13	0.00
3	0.08	0.11	0.00	0.00	0.17	0.00	0.00	99.65
4	0.69	0.00	13.66	2.92	61.36	9.84	5.66	5.87
5	0.61	0.00	15.52	2.55	64.90	8.75	6.12	1.55
6	1.11	0.00	11.55	1.97	36.83	3.43	4.27	40.84

aries. The examination of structure of brazed welds at high magnifications showed that between stainless steel and molybdenum a diffusion layer is observed in the form of a continuous band of 2.5 μm width based on molybdenum, which contains up to 23.55 % of iron but the concentration of silicon in it is lower and does not exceed 0.92 % (Figure 4, Table 3).

In accordance with the binary diagrams of metal systems there are significant regions of solubility in the molybdenum-iron system at high temperatures, but these regions are reduced rapidly at lower temperatures and at room temperature the mutual solubility is practically absent. Between the elements being considered there is a number of intermetallic phases, which can play a negative role, leading to the brittleness of a brazed joint [8].

The obtained results of investigations show that in some regions over the diffusion layer the microcracks are observed (Figure 4, *b*), they are located perpendicular to the plates being brazed, but they are absent in the brazed weld.

In order to eliminate the formation of cracks the brazing alloy No.3 was used in the brazed joints for brazing, which contains no silicon. The ternary alloys of Cu–Mn–Ni system are characterized by unlimited solubility in the liquid and solid state (Figure 5).

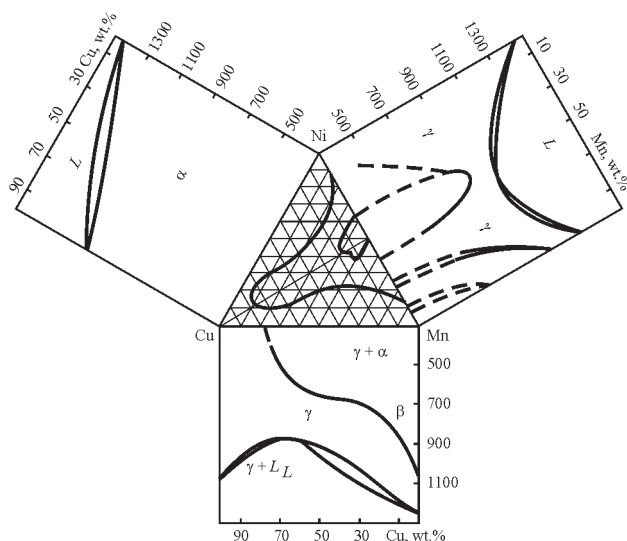


Figure 5. Ternary diagram of state Cu–Mn–Ni with adjacent binary systems [9]

In the system Mn–Ni the ordering of solid solution with the formation of phase Mn–Ni occurs at decrease in temperature [8].

The application of brazing alloys with the structure of solid solution during brazing of dissimilar joints with extended brazed welds allows reducing the influence of difference in thermal expansion coefficients. The brazing alloy acts as a soft interlayer, which provides relaxation of inner stresses occurring during heating and cooling.

The results of high-temperature differential thermal analysis are in good correlation with the diagrams of state of metal systems. At the thermal curve of heating a thermal effect was registered, which shows the melting range and corresponds to the solidus and liquidus temperature of the alloy (Figure 6).

The brazing mode applying the mentioned brazing alloy corresponded to the temperature of 1084 °C, however during investigation of brazed welds the cracks were not detected but the dense brazed joints are observed (Figure 7, *a*).

The use of a slight pressure during brazing has no effect on formation and chemical composition of diffusion layers, at the same time providing formation of dense brazed welds without cracks (Figure 7, *b*).

After metallographic and micro X-ray spectrum examinations the parameters of technological process of brazing were optimized and plane specimens of overlapped joints (three specimens for each brazing alloy) were manufactured for mechanical tensile tests at room temperature (Figure 8, *a, b*).

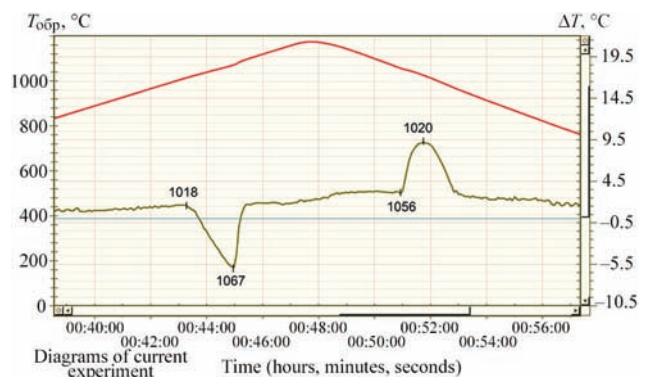


Figure 6. Temperature intervals of melting alloy of Cu–Mn–Ni system

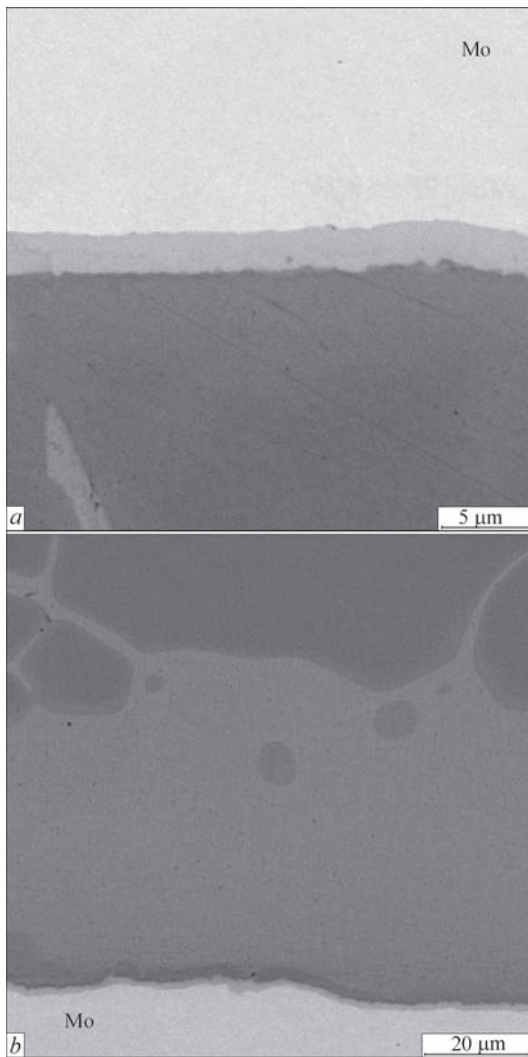


Figure 7. Microstructure of brazed joint, produced in brazing without (a) and with pressure (b) applying brazing alloy No.3

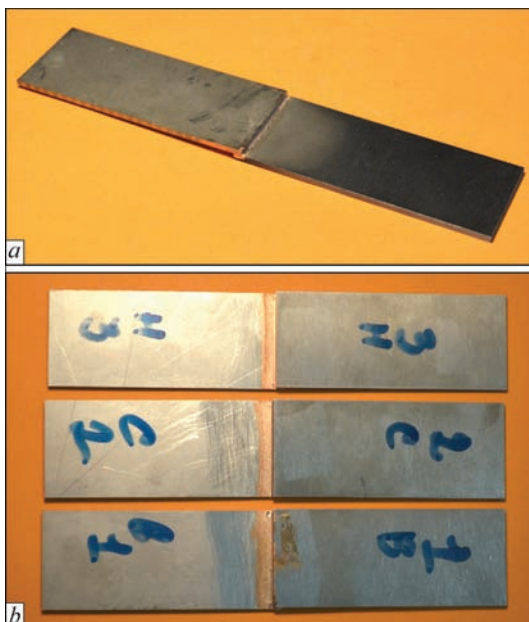


Figure 8. Appearance of specimens for mechanical tests

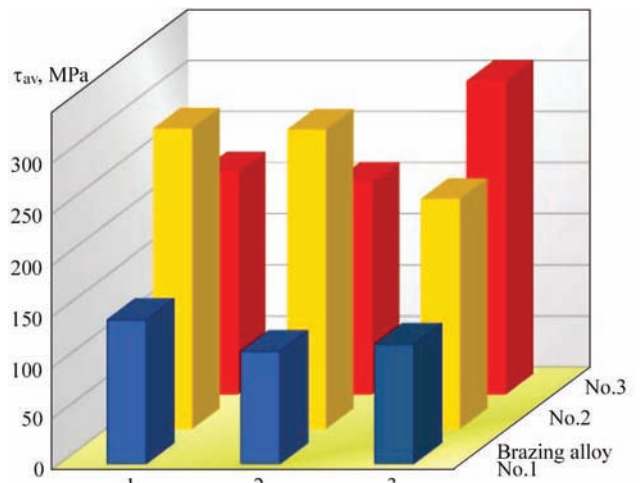


Figure 9. Shear strength of brazed joints of molybdenum-stainless steel

The carried out tests showed that the application of brazing alloy based on the system Cu–Mn–Ni, containing silicon (1 %), can not provide the shear strength higher than 110 MPa (Figure 9).

The reduction in concentration of silicon in the brazing alloy No.2 provided increase in shear strength. The application of brazing alloy based on the system Cu–Mn–Ni (No.3) with the structure of solid solution,

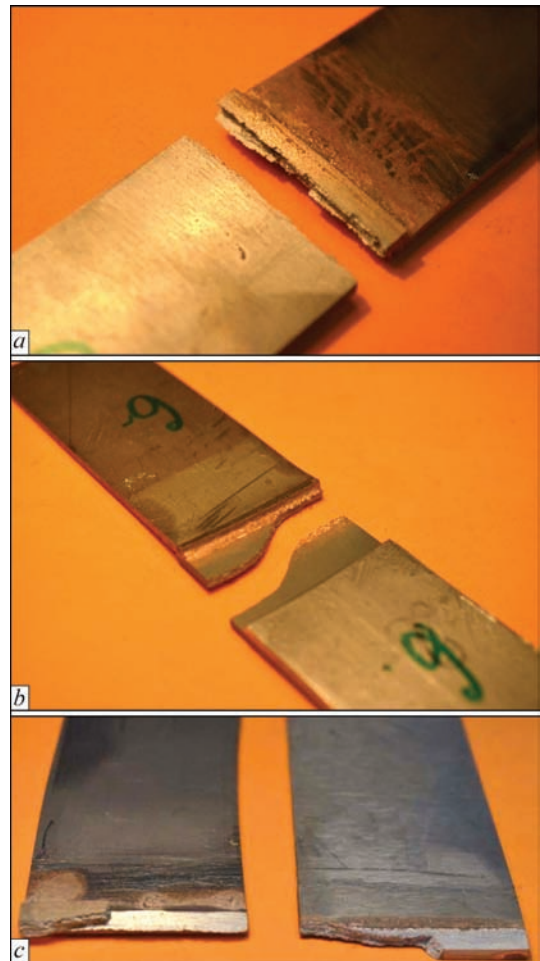


Figure 10. Brazed specimens after mechanical tests (description a–c see in the text)

containing no silicon, allowed increasing strength of the brazed joints up to 300 MPa (Figure 9).

It should be noted that during tests of brazed specimens produced applying the brazing alloy No.3 the fracture of specimens occurred along the brazed weld (Figure 10, *a*) and also along the base metal, i.e. molybdenum (Figure 10, *b*).

During fracture in weld the shear strength was at the level of 200–210 MPa (average value was 205). During fracture along molybdenum the maximum shear strength was 300 MPa. In some cases, a mixed character of fracture was observed: partially in weld and partially in base metal (see Figure 10, *c*).

Conclusions

Micro X-ray spectrum examinations revealed that in producing dissimilar joints of molybdenum-stainless steel using brazing alloys based on Cu–Mn–Ni–(Fe–Si) system, the central zone of a brazed weld is composed of a solid solution based on copper. The peripheral weld zone (on the side of molybdenum) is formed by diffusion phases based on iron and molybdenum, which are precipitated in the form of continuous bands along the brazed weld. At the 1 % concentration of silicon in the brazing alloy these areas are enriched by the latter, their composition and properties greatly differ from the chemical composition and properties of the brazed weld. Thus, the presence of a concen-

tration gradient at the interface results in formation of longitudinal cracks and low mechanical properties of brazed joints.

The carried out mechanical tests of brazed joints showed, that the application of brazing alloy based on Cu–Mn–Ni system with the structure of solid solution provides formation of dense brazed welds without cracks. The shear strength is at the level of 200–210 MPa during fracture along the brazed weld and 300 MPa during fracture along the base metal (molybdenum).

1. <http://stroirem.net/board/i-121776/svarka-svarivanie-raznorodnykh-tsvetnykhmetallov>
2. NEFT-GAZ. <http://www.tehn.oglib.ru/bgl/4010/577.html>
3. Metotekhnika. http://www.metotech.ru/art_molibden_1.htm
4. TK RZM-Metallurgiya. <http://uralferum.ru/molibden>
5. Palmer, A.J., Woolstenhulme, C.J. (2009) Brazing refractory metals used in high-temperature nuclear instrumentation. In: *Proc. of 1st Int. Conf. on Advancements in Nuclear Instrumentation Measurement Methods and their Applications — AN-IMMA* (7–10 June, 2009, Marseille, France). IEEE, 2009.
6. Lebedev, V.K. et al. (2006) *Machine building*: Encyclopedia. Ed. by B.E. Paton. Moscow: Mashinostroenie.
7. Tits, T., Wilson, J. (1968) *Refractory metals and alloys*. Moscow: Metallurgiya.
8. Drits, M.E., Bochvar, N.P., Guzej, L.S. et al. (1979) *Double and multicomponent copper-based systems*. Moscow: Nauka.
9. Chzan-Bao-Chan (1958) Examination of ternary copper alloys Cu–Ni–Mn. *Izvestiya Vuzov. Tsvetnaya Metallurgiya*, **5**, 107–115.

Received 24.10.2016

EFFECT OF WELDING MODES ON MECHANICAL PROPERTIES, STRUCTURE AND BRITTLE FRACTURE SUSCEPTIBILITY OF WELDED JOINTS OF STEEL 15Kh1M1FL MADE WITHOUT PREHEATING

N.G. EFIMENKO¹, S.V. ARTEMOVA² and S.N. BARTASH¹

¹NTU «Kharkov Polytechnic Institute»

21 Frunze Str., 61002, Kharkov, Ukraine. E-mail: svarka126@ukr.net

²PJSC «Turboatom»

199 Moskovsky Av., 61037, Kharkov, Ukraine

Structure and properties of metal of HAZ high-temperature area and weld were investigated in 15Kh1M1FL steel welding at higher modes using transverse hill method without preheating. Comparison of the received results with research data of welding process at moderate modes (160–170 A) determined that rise of current to 200–210 A results in increase of susceptibility to brittle fracture of HAZ high-temperature area and weld metal. The reason for this is high hardness caused by presence of martensite constituent in a bainite structure. 3 Ref., 1 Table, 5 Figures.

Keywords: steel, welding, preheating, bainite, martensite, brittleness, properties, structure

Formation of structure and properties in the different zones of welded joint is determined by thickness of welded metal being and its composition as well as parameters of technological process, i.e. effect of welding thermal cycle on metal [1].

Earlier carried investigations [2] showed that a method of transverse hill welding of steel 15Kh1M1FL at moderate modes without preheating and heat treatment provides for high indices of mechanical properties of the welded joints. At the same time from practical point of view it is reasonable to study an effect of higher modes on structure and mechanical properties, which is described in the paper.

The experiments were carried out on plates of 250×200×110 mm size, cast in a plant and subjected to heat treatment after casting. The latter includes homogenization at 1010–1030 °C; normalization at

970–1000 °C and high tempering at 720–740 °C temperature.

Sampling of metal, welded-up by transverse hill method using TML-3U electrodes of 4 mm diameter without preheating and concurrent heating at 200–210 A current, was mechanically carried out in the middle part of the plates in a section of 250 mm for performance of welds. No post weld heat treatment was applied.

The specimens for mechanical tests and structural examinations were made from the templates cut out in transverse direction in the upper, middle and bottom parts of the weld (Figure 1). Macro- and microstructure, and grain size, determined on GOST 5639–82 and on random linear intercept method [2], were examined. Hardness (*HV5*) was measured and characteristics of strength, ductility, impact toughness

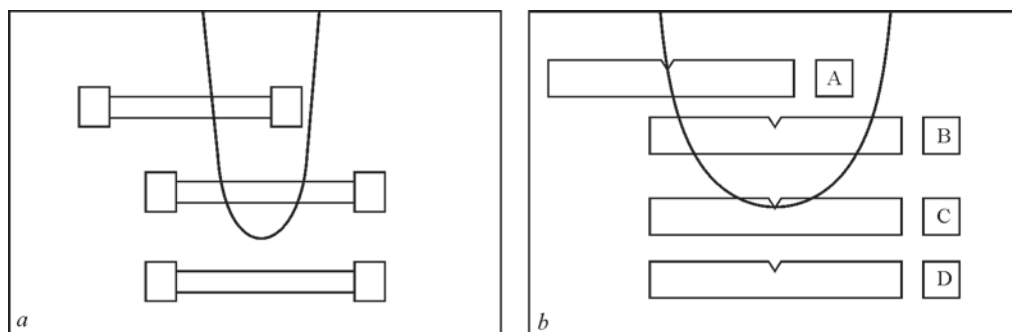


Figure 1. Scheme of specimen cut out from welded joint of steel 15Kh1M1FL: *a* — specimens for tensile testing; *b* — specimens for impact bending testing (A–D — illustration of cut place)

Indices of HV5 hardness of metal of HAZ high-temperature area of welded joint of steel 15Kh1M1FL in sections at different levels from weld surface

Variant number	Welding current <i>I</i> , A	Distance from weld surface, mm		
		10	25	40
		Hardness HV5		
1	160–170	277–278	276–278	281–287
2	200–210	360–368	388–405	365–366
3	In accordance with typical technology	–	355–358	–

KCV at –20; 0; 20 and 100 °C temperature were determined. Received test results were compared with the data of earlier investigations carried after welding on 160–170 A current [2].

Microanalysis determined that the weld height makes 65 mm, width is 55 mm and heat affected zone has 3–4 mm width. No macrodefects were found in the weld. Figure 2 shows a diagram of hardness change.

For comparison the Table provides for the hardness data in HAZ high-temperature area and weld metal in correlation with base metal after transverse hill welding (THW) at different current values as well as after welding using typical technology.

It should be noted that hardness in the near-weld zone and weld metal at all cross section levels of the joint made by welding at higher modes significantly exceeds that in these zones in the joints welded-up at moderate modes (Table, variant 1). At the same time, the levels of hardness of welded joints made by THW and typical technology are close (see Table).

Based on the results of tensile specimen testing it was determined that increase of the welding modes results in decrease of strength and ductility of HAZ

metal in relation to weld metal (Figure 3, *a*). At that strength of HAZ metal is somewhat higher and ductility is lower than that in the base metal. The weld metal is characterized by the highest indices of strength and ductility (Figure 3, *b, c*). If welding variants are compared then strength and ductility characteristics are higher for the second variant, however, level of full strength of the welded joint is lower. Strength and ductility of HAZ metal is somewhat lower for the second variant that can be referred to rise of hardness and structure inhomogeneity.

Metallographic examinations determined that structure of HAZ high-temperature area, i.e. overheated metal and partially melted grains, is inhomogeneous. The microstructure consists of bainite of different morphology. Together with upper bainite there are areas of lower bainite with sufficiently obvious orientation of carbide phase (Figure 4, *b*). These areas are located in a transfer area of base metal–weld fusion zone. The areas of high-temperature inhomogeneity

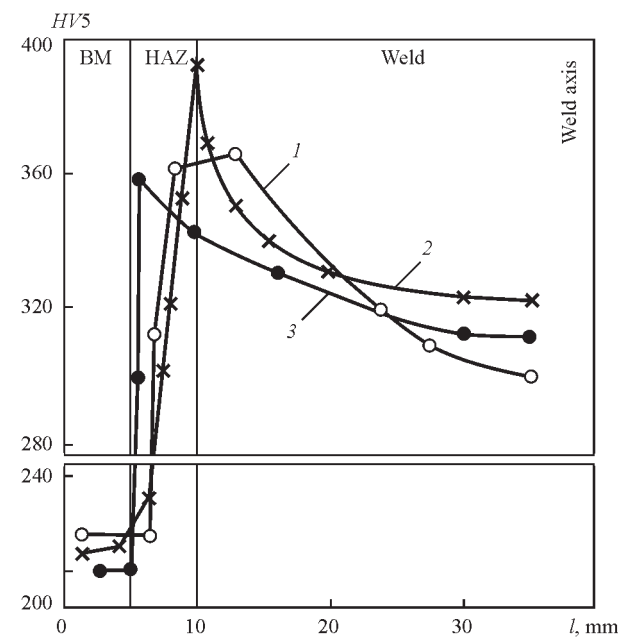


Figure 2. Variation of hardness of welded joint metal on steel 15Kh1M1FL made without preheating, at the following levels from weld axis: 1 — 10; 2 — 35; 3 — 40 mm. Welding current 200–210 A

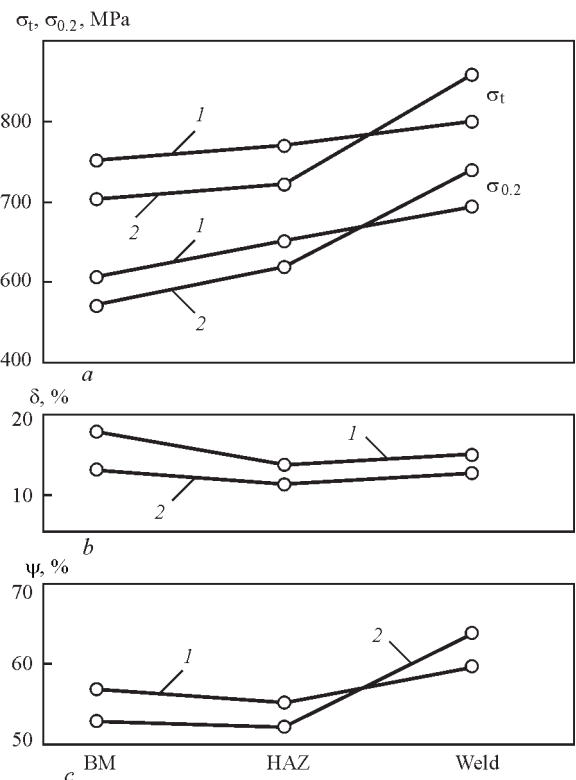


Figure 3. Mechanical properties of different zones of welded joint of steel 15Kh1M1FL: 1 — 160–170 A, 2 — 200–210 A

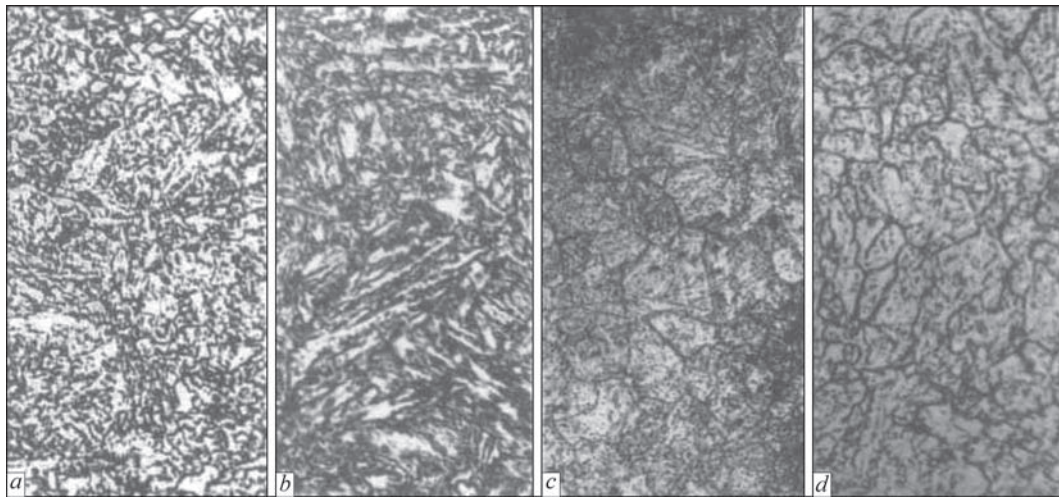


Figure 4. Microstructure of welded joint of steel 15Kh1M1FL made by THW at higher modes ($I_w = 200\text{--}210\text{ A}$): *a* — weld metal ($\times 500$); *b* — fusion boundary ($\times 500$); *c* — grain in HAZ metal in area of overheating ($\times 100$); *d* — grain in HAZ metal in a distance from overheating area ($\times 500$)

geneity have insignificant sizes and discrete location along conditional transition line.

The grains of granular bainite areas in HAZ metal and weld metal are fine (austenite grain $\check{D}_{\text{cond}} = 0.0138\text{--}0.0083\text{ mm}$, correspond to number 9–10 of GOST 5639–82 scale). At that it should be noted that a value of grain in such areas in welding at moderate modes corresponds to number 7–8 ($\check{D}_{\text{cond}} = 0.0192\text{ mm}$).

Austenite grain (Figure 4, *c*) in areas with acicular bainite is coarser ($\check{D}_{\text{cond}} = 0.053\text{ mm}$), however, lies in the ranges of acceptable norms and corresponds to number 9–10 of GOST 5639 scale.

Figure 5 shows the diagram of change of impact toughness in testing of sharp notch specimen (Charpy type), at which the results received in welding at higher modes are compared with the data of earlier carried out investigations (see Table, variant 1, moderate mode). As can be seen from the diagram, *KCV* of HAZ metal of the welded joints, made at higher modes, in testing at $-20\text{--}20\text{ }^\circ\text{C}$ temperature interval, is 30–50 J/cm^2 lower (Figure 5, curves 1 and 2).

Tendency to *KCV* decrease is observed in weld metal testing (Figure 5, curves 3 and 4). Increase of test temperature levels difference in the indices. No significant difference in *KCV* indices in upper, middle and bottom parts of the welded joint was found, including for the specimens with transverse orientation of fusion zone. Thus, it shows sufficient level of metal homogeneity in different places with various orientation of fusion zone.

The following conclusion can be done based on received experimental results. It is known [3] that homogenization of austenite before its transformation is not finished in HAZ during welding with high rates of heating and further cooling of steels containing active

carbide-forming elements (Cr, Mo, V etc.), which is typical for welding processes. The process of complete dissolution of carbides is not provided. Indicated factors decrease austenite stability properties. Under such conditions a transformation process is shifted in the bainite area. An important factor, effecting kinetics of homogenization process, is metal initial structural state.

Cast steel 15Kh1M1FL, used in given experiment, is characterized by coarse different-grain structure (see Figure 4, *c*) with significant dendrite and chemical inhomogeneity.

Welding of this steel with THW without preheating at moderate modes, as was set by us earlier [2], provides for formation of structure of upper bainite characterized by sufficiently high viscoplastic properties. Increase of welding modes (rise of heating rate) and cyclicity of heating (in multilayer weld deposi-

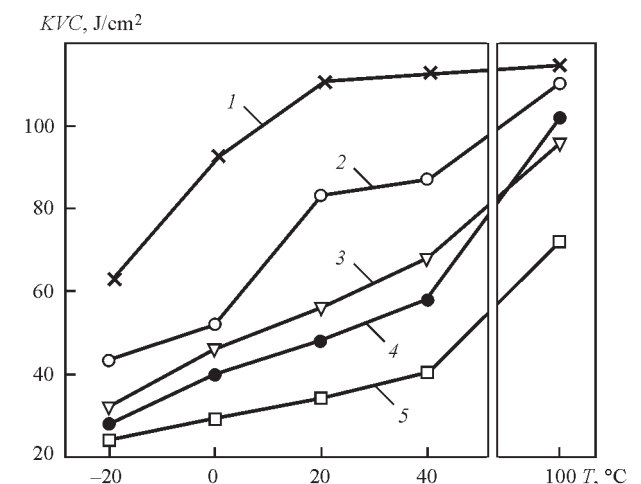


Figure 5. Impact toughness *KVC* of zones of welded joint of steel 15Kh1M1FL made by THW without current preheating: 1 — 160–180 A, HAZ (A, C); 2 — 200–210 A, HAZ (A, C); 3 — 160–180 A, weld (B); 4 — 200–210 A, weld (B); 5 — base metal (D) (see Figure 1)

tion) moves HAZ metal sections in the different time temperature conditions that results in formation of austenite with different level of homogeneity. As a result inhomogeneous structure is formed in cooling. Areas of acicular bainite (Figure 4, *b*) are formed together with granular bainite. Apparently, the transformation process in the grown austenite grain with higher homogenization completeness is shifted to the interval of lower temperatures, and formed acicular structure is a product of austenite decay in the area of «lower bainite–martensite» temperatures. At that, rise of hardness is observed in this zone (see Figure 2).

Thus, higher modes at THW without preheating of thick-walled cast structures of steel 15Kh1M1FL have negative effect on brittle fracture resistance of metal of HAZ high-temperature area. The main reason is, most probably, formation of inhomogeneous morphology of bainite, where acicular structure, being identified as lower bainite, is present together with upper bainite of granular shape. At that, metal of indicated zones have increased hardness typical for bainite-martensite structure.

Grains grown in HAZ are not a direct reason for embrittlement of this zone and influence indirectly. It is known fact [3] that grain growth in steels with the

active carbide-forming elements is a sign of increased homogenization level of austenite and, respectively, results in rise of its stability, and, hence, shift of transformation temperature to martensite area.

Conclusions

1. Bainite of different morphology, i.e. granular and acicular, is formed in welding of cast steel 15Kh1M1FL using transverse hill method without preheating at higher modes in high-temperature area of HAZ. The reason of formation of such structure is initial different-grain austenite with various level of homogenization and transformation resistance.

2. Welding at higher modes results in growth of hardness values in HAZ metal and reduction of impact toughness in -20 – 20 °C temperature interval that is a sign of increase of brittle fracture susceptibility.

1. Nazarchuk, A.T., Snisar, V.V., Demchenko, E.L. (2003) Producing welded joints equivalent in strength on quenching steels without preheating and heat treatment. *The Paton Welding J.*, **5**, 38–45.
2. Efimenko, N.G., Atozhenko, O.Yu., Vavilov, A.V. et al. (2014) Structure and properties of welded joints of 15Kh1M1FL steel at repair of casting defects by transverse hill method. *Ibid.*, **2**, 42–46.
3. Shorshorov, M.Kh., Belov, V.V. (1972) *Phase transformations and change of steel properties in welding*: Atlas. Kiev: Nauka.

Received 04.08.2016

INFLUENCE OF PARAMETERS OF ULTRASONIC MECHANICAL OSCILLATIONS ON THE STRUCTURE AND MECHANICAL PROPERTIES OF WELD METAL IN LASER WELDING OF FERRITIC STEELS

V.V. SOMONOV

Peter the Great St. Petersburg Polytechnic University
29 Politekhnikeskaya Str., 195251, St. Petersburg, Russian Federation. E-mail: ballak@inbox.ru

The problems of welding pool control in welding of ferrite stainless steels were considered. A comparative analysis of the works in the field of effect of ultrasonic and vibration oscillations on the weld was carried out. The results of preliminary experimental and metallographic examinations of specimens of joints produced by laser welding with additional ultrasonic effect on welding pool were reflected. The effect of positioning of clamps and the source of ultrasonic waves relative to the butt interface on the character of oscillations arising in it was studied. The most favorable frequencies and amplitudes of oscillations for generation of oscillations in the butt area were determined. The results on influence of the material thickness on the oscillations arising in it were obtained, which can exert an effect on stability and cooling rate of welding pool and, as a result, on the microstructure of weld metal. 11 Ref., 1 Table, 5 Figures.

Keywords: laser welding, ultrasonic waves, ferrite stainless steels, welding pool, microstructure

Ever often for welding of ferrite stainless steels the modern lasers, such as fiber or disc ones, are applied. This minimizes the thermal deformations of the structure at high welding speeds and subsequent treatment of welds, making stages of production shorter. However, in welding of these steels there are problems of increased tendency of welds to intercrystalline corrosion (ICC) and reduced mechanical properties (strength and hardness) as compared to the base metal. Traditionally, the following methods are used to prevent the problem of ICC: stabilization (Ti and Nb alloying), reduction of carbon content in steel to the value lower than 0.03 % or heat treatment. The technologies of stabilization and reduction of carbon content in steel are cost consuming, and the heat treatment is a power intensive and environmentally unfriendly process requiring large industrial areas. In this regard, the researchers attempted to create the more simple methods for solution of the problem. Among the methods the vibration or ultrasonic oscillations of welding pool during welding process may be used, however it is not completely clear what are the capabilities of application of this additional source for the control of weld properties.

The aim of the present investigations was the study of effect of positioning of the source of ultrasonic mechanical oscillations and clamping devices on formation of oscillations in the area of welded butt for the control of formation of the microstructure of weld metal in the laser welding of ferrite stainless steels, at

the same time improving its mechanical, metallurgical characteristics and reducing the tendency to ICC.

Analysis of investigation results from the materials of published works. In the investigations of effect of mechanical oscillations in the welding pool on reducing the tendency to ICC the scientists in Ufa were involved [1–3]. They came to the conclusions that the vibration and ultrasonic impact treatment in the process of welding allows increasing the resistance of the welded joint metal of austenitic stainless steel 12Kh18N10T to ICC. The ultrasonic impact treatment at the frequency in the range of 25–27 kHz increases the resistance to fatigue fracture by 24–26 % as compared to the vibration one. The latter allows decreasing the grain size, which contributes to the formation of a more uniform structure in the weld metal. In the works [4, 5] it was shown that the ultrasonic mechanical oscillations in laser welding of high carbon steels result in the displacement of different layers of metal in the welding pool. The molten metal is moved to the edge of the melt pool, which indicates about the elasticity of the pool. The effect of oscillations on the weld shape and distribution of elements in it was established. The forces acting on the molten metal during ultrasonic oscillations improve the contact between the melt pool and the solid substrate, which depends on the welding speed and acoustic power.

In the course of this effect the molten metal is located symmetrically around the vertical axis of the weld symmetry. From the center of welding pool it is forced out to the edges resulting in a deep pene-

tration and forming hemispherical areas with a slight inclination in the regions of a central hemisphere in the melt pool. The application of ultrasound improves mechanical properties of the weld metal during its crystallization due to refinement of structure and better removal of gases.

Typically the frequency range of 18–80 kHz is used. Such oscillations allow welding metals with an oxidized surface, covered with a layer of lacquer, etc., reducing or relieving residual stresses arising at that time. Applying ultrasound it is possible to stabilize the structural components of weld metal, eliminating the probability of spontaneous deformation of welded structures with time [6, 7]. At the Institute of Theoretical and Applied Mechanics of the Siberian Branch of the RAS the investigations of effect of ultrasound on improvement of plastic properties of the joints were performed. As a result of experiments the yield strength and ultimate rupture strength were not significantly changed, but the plasticity increased to more than 20 % [8]. From the literature sources it is known that it is possible to obtain longitudinal, transverse and torsional oscillations depending on design of the waveguide and fixation of the tool in the welding zone. Their amplitude is usually in the range of 10–30 μm [9, 10]. From the aforesaid it is seen that the ultrasonic mechanical oscillations have a strong influence on the properties of the weld being produced, but, unfortunately, the effect of positioning of the source and clamping devices relative to each other and the butt on the value, quality and depth of the effect created in the welding pool was not completely studied. Due to this there is no complete understanding of the processes occurring here.

Experimental investigations and analysis of the results. As experimental specimens the plates of the size of 100×100×2 mm of ferrite stainless steel of grade 1.4016 (Kh6Cr17) of the following chemical composition (mass.%): 0.08 C; 1.0 Si; 1.0 Mn; 0.04 P; 0.015 S; 16–18 Cr were used. According to

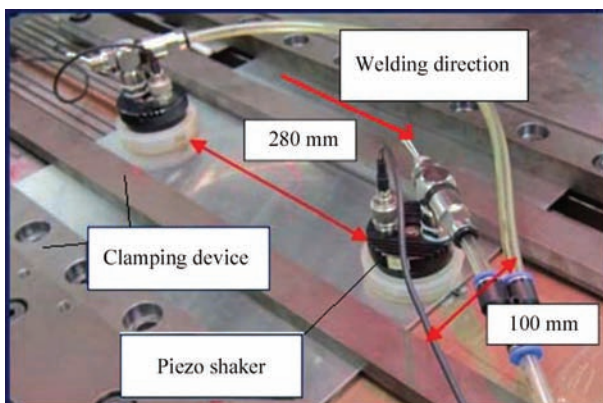


Figure 1. Appearance of specimens with fixed piezo shakers before laser welding

BS EN 10088-1:2005 [11] the chemical characteristics of this grade are the following: $\delta = 20\%$; $\sigma_{0.2} = 260\text{ MPa}$; $\sigma_t = 400\text{--}630\text{ MPa}$; $HV 126\text{--}197$.

To check the effect of oscillations on properties of metal of the produced weld, caused by ultrasound, the preliminary experiments on laser welding were carried out. The experimental stand, designed on the basis of the technological complex for laser welding of Reis Company, was applied. As a radiation source the ytterbium fiber laser of the model LS-10 was applied produced by the Company IPG Laser GmbH (Germany) with the maximum output radiation power of 10 kW, and for its supply to the surface of welded specimens the laser head of the model MWO 54 of the Company Laseroptik REIS Lasertec was used, equipped with the air cross jet for protection of the optics from vapors and metal spatters, with a focusing lens having a focal distance of 300 mm and a beam diameter in the focus df 0.4 mm. The movement of specimens relative to the laser beam was carried out by means of the four-axis manipulator of the Company Reis. To create oscillations two piezo shakers of the model PS-X03-6/500 of the Company Isi-sys GmbH (Germany) with the oscillation frequency F in the ranges of 0–30 kHz and the amplitude of oscillations controlled in the range of 0–5 V were used, fixed on the surface of specimens. The specimens themselves and two piezo shakers were fixed on the manipulator axis by means of the specially manufactured technological rigging. The welding was carried out along the straight trajectory with a pitch of 15 mm to the both sides from piezo shakers. At first the welds without oscillations and then with added oscillations were produced. The arrangement of piezo shakers on specimens during the experiments is illustrated in Figure 1.

As a result, several welded butts of joints with and without the effect of oscillations in the area of a butt were produced. At the same time the power of laser radiation P (kW), welding speed v (m/min), focus position relative to the surface of specimens being welded z_f (mm) were selected to provide a through penetration. From the produced welds the specimens were cut and metallographic sections were manufactured to study microstructure using the microscopes Leica Z16 APOA and Leitz Ergolux ($\times 1000$). Also the mechanical tensile tests in the stand of the model Z100 of the Company Zwick/Roell with the load of up to 10 kN were carried out and the microhardness of weld metal and the adjacent area were measured according to Vickers method at the load of 1000 N in the automatic durometer UT200 of the Company BAQ. The microstructure of the produced specimens is shown in Figure 2. The character of fracture of specimens

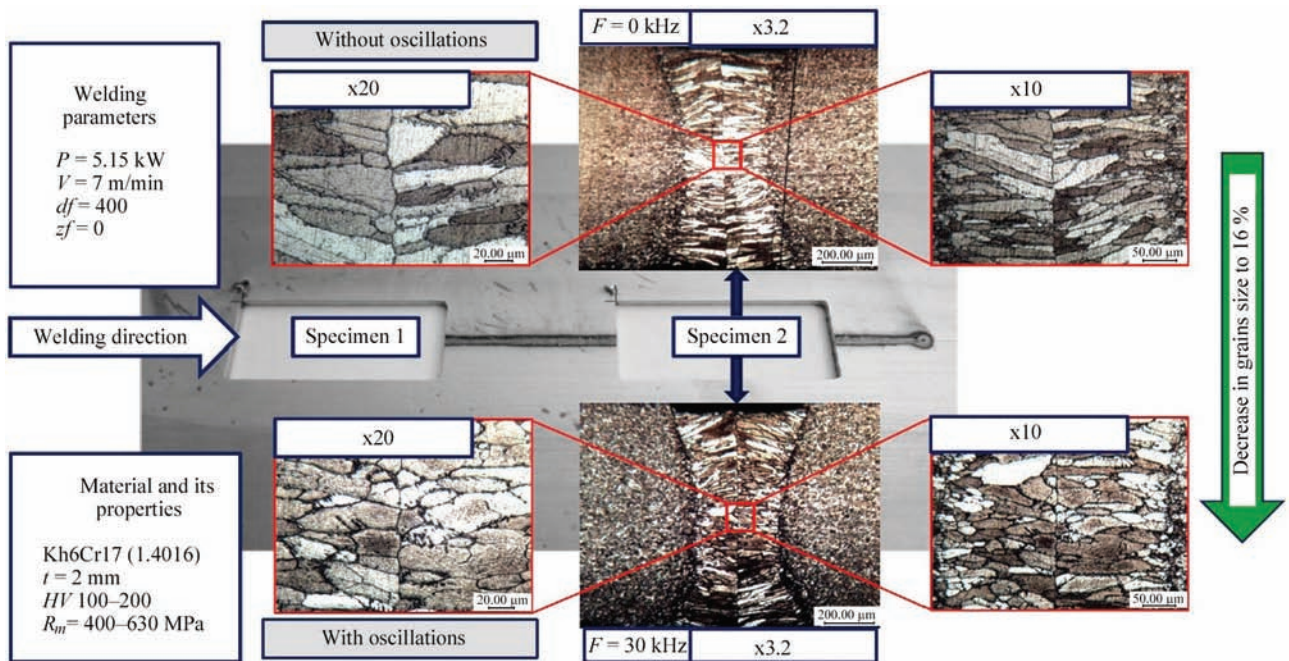


Figure 2. Microstructure of welds after laser welding without and with additional mechanical oscillations generated by piezo shaker

after tests and the results of measurement of microhardness are shown in Figure 3. In order to obtain a more detailed representation about the influence of oscillation parameters and intensification of the effect the investigations were carried out which allowed determining the optimum position for piezo shakers and clamps relative to the future welded butt. The experimental stand was designed consisting of the chamber for shearing speckle-interferometry (shearography), equipped with the system of diode laser illumination, piezo shaker of the model PS-X03-6/500, amplifier of piezo shaker signal of the Company Isi-sys GmbH and vacuum pump, which provides the fixation of piezo shaker at the surface of specimens.

In the course of these experiments the natural oscillations of the specimen surface, generated by piezo shaker, were registered. In order to develop the concept of the optimal position of piezo shakers the in-

fluence of the following factors on the formation of mechanical oscillations was studied: the parameters of the piezo shaker itself (amplitude of oscillations A (B), determined by the supplied voltage, the oscillation frequency f (kHz), generated by piezo shaker; position of piezo shaker relative to the butt (the distance between the edge of piezo shaker and the butt $\times 1$ (mm) and relative to the edge of the specimen $y1$ (mm), and the location on the facial or rear side of the specimen); thickness of the specimen h (mm), arrangement of clamps on the numbers 1–4 relative to the edges of specimen and future butt (Figure 4). During the experiments, the clamps 1 and 2 changed their position relative to the butt, it was determined by the distance between the clamp center and the butt interface $\times 2$ (mm). Before the beginning of experiments the surface of the specimen was coated with a thin layer of white paint, intended for shearography, which

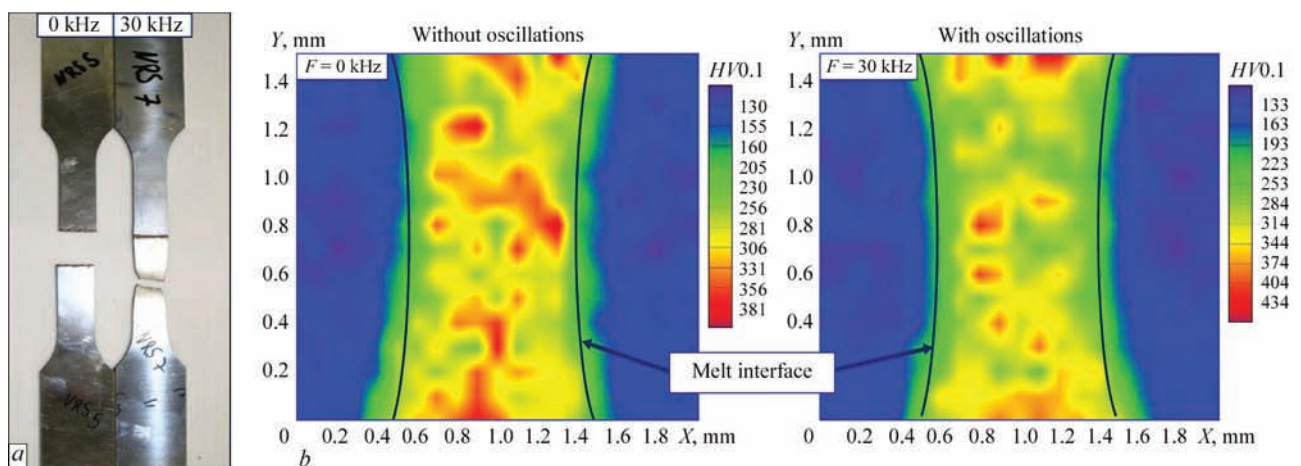


Figure 3. Results of mechanical tests: *a* — character of fracture of specimens during tensile tests; *b* — results of measurements of microhardness

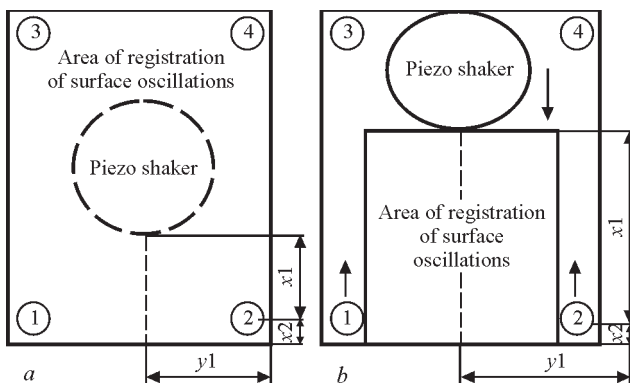


Figure 4. Scheme of arrangement of piezo shaker and clamps (1–4) relative to the specimen surface: *a* — from the rear side of the specimen without movement; *b* — from the facial side of the specimen with change of its position and also clamps 1 and 2

reduced reflection and enabled the receiving of a more distinct signal. The scheme of arrangement of a piezo shaker and clamps 1–4 is given in Figure 4. The arrows indicate the directions of change in the position of piezo shaker and clamps 1 and 2. The edge of the specimen closest to the observer was considered to be the interface of the future butt.

The results of measurements of ductility and microhardness of the weld metal of specimens (see Figure 2) obtained without the influence of oscillations: $\delta = 15\%$; *HV*0.1-205–381, after additional oscillations with a frequency of 30 kHz, $\delta = 40\%$; *HV*0.1-223–434.

The results (see Figure 3) indicate about the effect of mechanical oscillations, generated by means of ultrasound, on the properties of a weld (ductility and microhardness). Mainly microhardness of weld metal after the use of additional mechanical oscillations became more uniformly distributed within the limits of *HV* 284–314, whereas previously a large number of chaotically distributed areas with the increased microhardness of *HV* 331–381 was present.

The experiments on shearography were conducted in series changing one of the parameters. In the course of them the oscillation amplitude *A* (3, 5 V), the oscillation frequency *f* ranging from 10 to 30 kHz

with a pitch of 100 Hz was changed, the thickness of specimens was changed applied in the range from 2 to 8 mm by combining the plates of 2 mm thickness with each other using clamps, the arrangement of clamps and piezo shaker relative to the specimen surface and the surface itself, where it was located (facial or rear), were changed. The values of parameters of the experiments on shearography are given in the Table.

In welding of the considered steels the weld metal, as a rule, has a ferrite microstructure. This is caused by the lack of α - γ -transformations at 1000 °C, necessary for grain growth. In welding these steels are characterized by the formation of the coarse-grained structure in the fusion zone (see Figure 2, specimen 2, upper), which is impossible to prevent using conventional methods. Usually, after welding a decrease in impact toughness with increasing chromium content in the weld is observed. It results in increased tendency to ICC. As a result of investigations it was revealed that in laser welding of the given steel the ultrasonic waves affect the welding pool, contributing to refinement of the crystal structure of the weld (decrease in the grain size to 16 %) (see Figure 2, specimen 2, lower), resistance to deformations at a lower microhardness and its more uniform distribution in the volume of weld metal due to mixing the melt in the welding pool.

From these experiments it was found that the mechanical oscillations generated by piezo shaker in the specimen, located in the center of the rear side of the specimen, even at the adjusted non-maximal parameters, are distributed for the depth of more than 8 mm. The noticeable areas of oscillations were registered in the area of the future butt at the increase of the specimen thickness from 2 to 8 mm. This will allow applying this method of effect for welding of structures of plane sheets, as far as usually the thickness of sheet of the given steel does not exceed 8 mm. The most stable and strong oscillations in the area of a butt at the location of piezo shaker at the facial surface of specimen occur at the frequencies of 13.4; 18.6 and 24.7 kHz. The greatest effect on the interface of the

Parameters changed in the course of experiments on shearography of specimens produced applying ultrasonic oscillations

Number of series of experiments	Arrangement of piezo shaker relative to the specimen	Arrangement of piezo shaker on the specimen surface (<i>x</i> 1; <i>y</i> 1), mm	Thickness of specimen <i>h</i> , mm	<i>A</i> , V	Position of clamps 1 and 2 (<i>x</i> 2), mm
1	Rear side of specimen	In the specimen center	2	3	5
2			2 + 2	3	5
3			2 + 2 + 2	3	5
4			2 + 2 + 2	3	5
5	Facial side of specimen	5–45 (with a pitch of 10); 50	2	3; 5	5
6		15–45 (with a pitch of 10); 50	2	3; 5	10
7		15–45 (with a pitch of 10); 50	2	3; 5	15
8		15–45 (with a pitch of 10); 50	2	3; 5	30

Note. Frequency of ultrasonic oscillations *f* in all the experiments varied from 10 to 30 kHz (with a pitch of 100 Hz).

future butt is exerted by the frequency of 18.6 kHz. With increase in the oscillation amplitude from 3 to 5 V, the effect was increased slightly. When piezo shaker approaches the butt interface, the oscillations, arising in it, were disintegrated into pieces, but at the same time they were united from the separate zones into a new small one. The removal of clamps 1 and 2 from the butt interface leads to weakening of transfer of oscillations from piezo shaker and, consequently, weakening of the registered signal. As far as during welding the close arrangement of clamps and piezo shakers is not desirable to provide their preservation, the minimum possible distance for realization of their functions, namely 15 mm from edge of the butt, was selected.

To continue the further experiments on laser welding, as an optimal combination the following parameters, associated with mechanical oscillations, were selected: the oscillation frequency is 18.6 and 24.7 kHz; the oscillation amplitude is 5 V; the shaker position relative to the butt range from 15 to 25 mm; the positions of clamps relative to the butt are not more than 15 mm.

The example of registration of oscillations in combination of such parameters is shown in Figure 5.

In the Figure a change of color contrast of the occurred oscillation areas in the butt area as well as their packing are seen, which indicates about a large value of the influence exerted on the future welding pool by them.

In conclusion, the following should be noted. The experimental stand for laser butt welding with effect of ultrasound on the welding pool was designed. The investigations of vibration characteristics of ferrite stainless steel 1.4016 were carried out. The following optimal parameters for generation of maximum mechanical oscillations in the area of a butt were determined: the frequency is 18.6 kHz; the oscillations amplitude is 5 V; the position of piezoelectric shaker relative to the butt is 15 mm; the arrangement of clamps relative to the butt is 15 mm. It was found that in welding the use of oscillations of welding pool has a positive effect on the formation of fine-grained structure or decrease in the grain size, leading to increased resistance to deformations at a lower microhardness of weld metal. The effect of these oscillations on the degree of mixing the melt was noted, which is confirmed by obtaining a more uniform structure in the weld and a uniform distribution of microhardness in it.

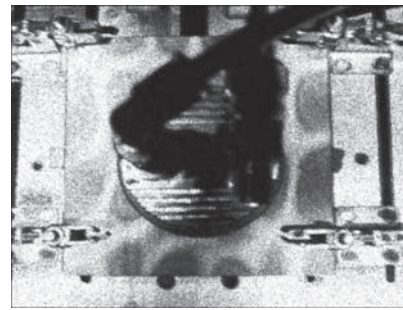


Figure 5. Registered oscillations of the specimen surface at the oscillation frequency of piezo shaker of 18.6 kHz and at the amplitude of 5 V, at the 15 mm distance between the interface of the future butt and piezo shaker, at the 15 mm distance between the interface of the future butt and the center position of the clamps

The results can be applied in the further investigations on laser welding of steels of a similar class, as well as transfer them for duplex stainless steels and fine-grained steels, or to take them into account for the joints of other type and thickness.

The work was performed at the financial support of the Education and Science Ministry of the Russian Federation within the frames of the Program «Mikhail Lomonosov» (2016–2017).

- Zaripov, M.Z. et al. (2010) Investigation of effect of vibration oscillations during welding on properties of 12Kh18N10T-steel welded joints of oil-and-gas equipment. *Neftegazovoe Delo*, **2**, 1–12.
- Karpov, A.L. et al. (2005) Increase in production quality of welded petrochemical apparatuses by vibration treatment during welding. *Bashkirsky Khimichesky Zh.*, **12**(1), 27–29.
- Karetnikov, D.V. et al. (2012) Manufacturing technology upgrading of welded sheets of vessels for oil and gas refining. *Oil and Gas Business*, **4**, 490–500.
- Henrike, A., Banasik, R., Henkel, K.-M. (2015) *Increase in viscosity of melt by vibration*: Report of DVS (Sci. Congress, Nuremberg).
- Watanabe, T. (2010) Improvement of mechanical properties of ferritic stainless steel weld metal by ultrasonic vibration. *J. of Materials Proc. Technology*, Issue 12, 1646–1651.
- Venkannah, S., Mazumder, J. (2009) Changes in laser weld bead geometry with the application of ultrasonic vibrations. In: *Proc. of the World Congress on Engineering* (July 1–3, 2009, London, U.K.), 2009, Vol. 2.
- Venkannah, S., Mazumder, J. (2011) Effects of ultrasound on the weld bead surface of high carbon steel sheets. *J. of Mechanics Engin. and Automation*, Issue 1, 87–99.
- Orishich, A.M. (2010) Laser conversion of welding. *Nauka iz Pervykh Ruk*, **32**(2), 18–19.
- Nikolaev, G.A. *Welding in machine building*: Refer. Book, Vol. 1, 375–376.
- Bannikov, E.A., Kovalev, N.A. (2009) *Welding works. Modern equipment and technology*. Moscow: Astrel.
- BS EN 10088-1:2005*: Stainless steels. Pt 1: List of stainless steels. Standards Policy and Strategy Committee.

Received 01.11.2016

FORMATION OF DIFFUSION ZONE IN WELDED JOINTS OF POROUS ALUMINIUM ALLOY WITH MONOLITHIC MAGNESIUM ALLOY AT CHEMICAL ACTIVATION BY GALLIUM

Yu.V. FALCHENKO, M.A. KHOKHLOV, Yu.A. KHOKHLOVA and V.S. SINYUK

E.O. Paton Electric Welding Institute, NASU

11 Kazimir Malevich Str., 03680, Kiev, Ukraine. E-mail: office@paton.kiev.ua

Comprehensive investigation of mechanical and physical properties of diffusion zone of the produced joints was performed as part of fulfillment of the technological task, namely producing superlight welded structures from porous aluminium alloys of Al–Mg–Zn system and monolithic magnesium alloys (ML4 standard alloy of Mg–Al–Zn system and experimental alloys of Mg–Ga system). The objective of the study was evaluation of the influence of heating cycle, characteristic for different welding processes, on the joints. Welding was performed by two methods with maximum heating temperature up to 300 °C: diffusion welding with long-term cycle of heating in vacuum, and welding with heating by passing current in air, which is characterized by short heating cycle. Gallium was used for forming a monolithic joint and diffusion activation. It is found that a diffusion zone about 10 µm wide forms on porous aluminium side, with slight lowering of micromechanical properties in pore walls, that is typical for aluminium alloys at contact with gallium. In magnesium alloys, an extended (60–100 µm) wavy intermetallic-strengthened diffusion zone forms along the joint line in both the welding processes, mostly of Mg₅Ga₂ composition with melting temperature of 456 °C that is higher than the welding temperature. Thus, the possibility of joining porous alloys to monolithic ones is shown at their slight heating and chemical activation of the joint zone by gallium. 11 Ref., 1 Table, 8 Figures.

Keywords: magnesium, porous aluminium, gallium, diffusion welding, welding with heating by passing current

Application of superlight porous alloys enables fabrication of structures with high specific strength, i.e. rational strength-to-weight ratio. Depending on density and type of porosity, such materials are 50 to 80 % lighter than monolithic ones [1]. Despite the diversity of commercially produced porous metals, their broad

application is still difficult for the reason of high cost and complexity of production, but it is quite justified for engineering solutions aimed at creation of housing or multilayer protective elements of aerospace microelectronics, where minimizing the structure mass is a priority [2]. Porous metals are in the top ten of «Materials of the Future» ranking, as are magnesium alloys, the mass of which is by 30 % less than that of the traditionally applied aluminium alloys.

New porous materials based on porous aluminium (PA) of «MetalFoam» Company (Germany) (Figure 1), available for experiment performance, as well as experience of producing welded joints at temperatures of about 300 °C [3–6], developed for manufacturing bimetal blocks for encapsulating microelectronics, allowed us actualizing and carrying on investigations, aimed at creation of superlight multilayer bimetal sandwich panels, using porous and monolithic alloys, in different sequences and combinations.

The objective of the study was producing bimetal joints of sandwich panels of PA with magnesium alloys based on mechano-chemical activation by gallium, limiting welding temperature to 300 °C, and application of two welding processes with different



Figure 1. Porous aluminium panels produced by MetalFoam Company with and without monolithic walls

rate and duration of heating. A comprehensive investigation of the features of formation of microstructure, chemical and phase composition, micromechanical properties of diffusion zone in the produced samples was performed for technological evaluation of optimality of application of short or prolonged heating.

Joined pairs of alloys were PA (Al–Mg–Zn system) with standard magnesium alloy ML4 (Mg–Al–Zn system) and PA with experimental doped alloy (Mg–Ga system).

PA contains a large number of gas-filled pores of 1–2 mm diameter with voids making about 80 % of total material volume. At deformation PA demonstrates non-linear behaviour, characteristic for porous structures so that the material has a high shock absorption coefficient (it is capable of adsorbing kinetic energy of the shock). PA is characterized by low hygroscopicity (1–3 %), is non-toxic, heat-resistant, and does not fail at exposure to fuels and lubricants, solvents, ultraviolet and radiation. When exposed to open flame, it gradually softens, if temperature in the heating zone reaches the melting temperature of 650 °C. Microhardness (Mayers) of PA pore walls is equal to 1.5 GPa, and Young's modulus of elasticity is 69 GPa.

Cast magnesium alloy ML4 is applied for manufacture of parts of engines and other units exposed to static and dynamic loads in service. Limit working temperature is 150 at long-term and 250 °C at short-term operation. Melting temperature is 720–750 °C. Mayers microhardness is 1.2 GPa and Young's modulus of elasticity is 43 GPa.

Experimental magnesium alloy of Mg–Ga system (64Mg + 32 Mg₅Ga₂ wt.%) based on standard ML4, alloyed with gallium and modified by fine particles of zirconia (of 20 nm diameter), was produced at induction remelting in argon [7] without subsequent treatment. Melting temperature was 750 °C. The alloy was dispersion strengthened by Mg₅Ga₂ intermetallics and modifiers, so that it has higher values of microhardness (Mayers) of 4–16 GPa, and Young's modulus of elasticity of 129–250 GPa.

Content of the main chemical elements in the joined materials is given in the Table.

Joints of 10 mm PA panels and 6 mm ML4 sheets (Figure 2) were produced by two different processes: diffusion welding for 3 h in vacuum and welding with heating by low-voltage passing current for 2 min in

Content of the main chemical elements of joined materials, wt. %

Material	Al	Mg	Zn	Ca
PA	83.2	6.7	5.9	–
ML4	5–7	88.4–92.9	2.0–3.5	–
ML4 + Ga	5	80	2.5	10

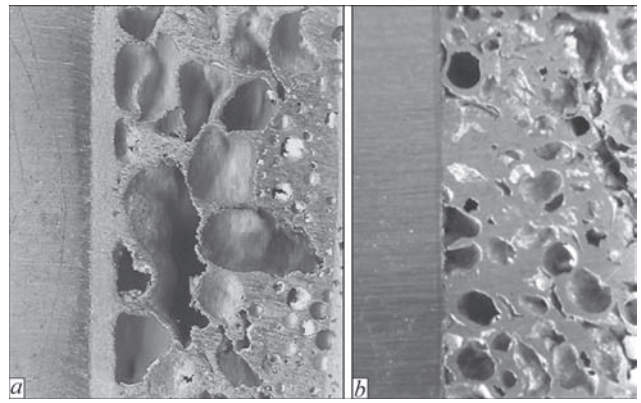


Figure 2. Welded joints of monolithic magnesium alloy ML4 with PA panels: with monolithic walls (a) and without them (b)

room environment. P-115 unit was used for diffusion welding (Figure 3, a) and laboratory unit was applied for welding by passing current (Figure 3, b).

Wetting of pre-ground surfaces to be joined by commercial gallium melted at 27.75 °C, was performed to remove oxide films and activate the surfaces being welded.

Microstructural studies of diffusion zone of samples and chemical element distribution were performed in scanning electron microscope JSM-35CF JEOL, fitted with INCA Energy-350 spectrometer of Oxford Instruments (SEM).

Coefficient of diffusion was assessed by simplified formula $D = x^2/T$, where x is the maximum depth of gallium penetration, T is the welding duration.

Gallium diffusion in PA is characterized by a depth range of about 10 μm and absence of a clear-cut zone, its concentration being 5–20 wt.%. Experimental coefficient of diffusion at prolonged heating (at the rate of 5 °C/min) in vacuum is $0.0092 \cdot 10^{-12}$ m²/s and at short heating (at the rate of 150 °C/min) by passing current it is $0.5555 \cdot 10^{-12}$ m²/s.

Wavy diffusion front on ML4 side was observed with both the welding processes (Figure 4). At prolonged heating a diffusion zone 85 to 100 μm wide

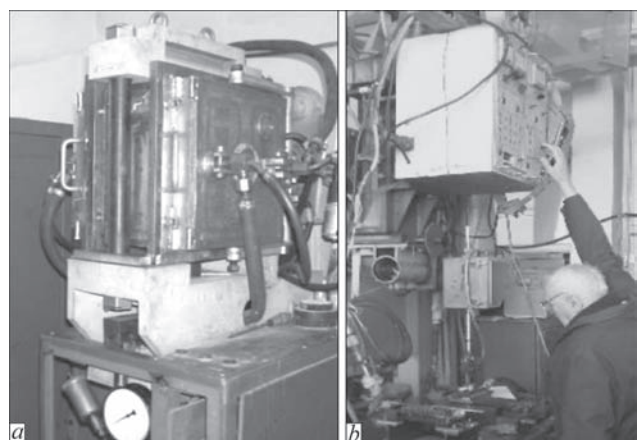


Figure 3. Equipment for welding with different heating rates: a — P-115 unit; b — laboratory unit

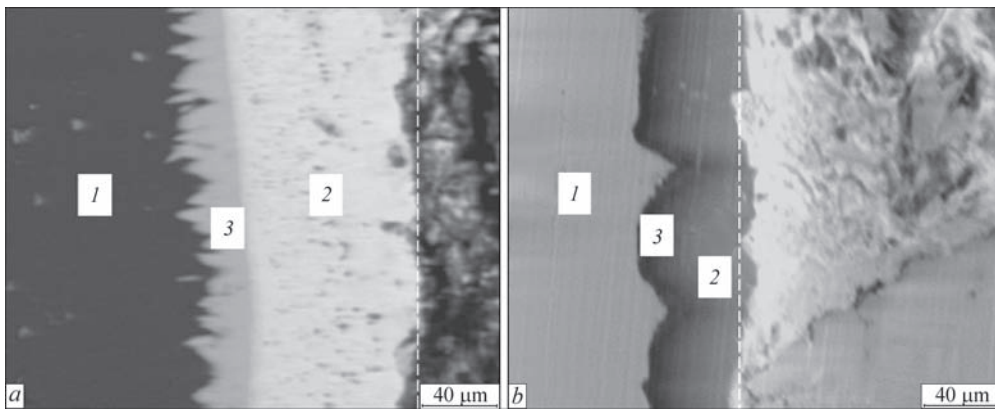


Figure 4. Microstructure of the joint zone produced at prolonged heating under VDW conditions (*a*) and short heating by passing current (*b*) (dashed line shows the limit of gallium application, PA is to the right of the line, and ML4 magnesium alloy is to the left; for designations 1–3 see the text)

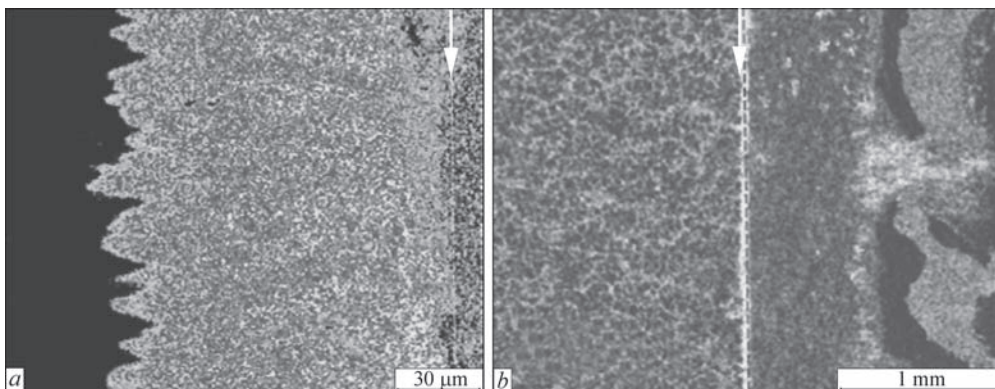


Figure 5. Element map of gallium distribution in ML4 base alloy (*a*) and in doped alloy (*b*). Dashed line shows the zone of gallium application, PA is to the right of the line, and magnesium alloys are to the left

is formed, and at short heating with current passage its width is up to 35–60 μm. Experimental coefficient of diffusion is equal to $0.92 \cdot 10^{-12}$ and $20 \cdot 10^{-12}$ m²/s, respectively.

Investigation of quantitative chemical composition of the diffusion zone from magnesium alloy side (Figure 4, zone 1 — base metal) showed the presence of two regions of excellent chemical composition. Zone 2 (closer to the point of activator application) contains, wt.%:

35Mg and 64Ga, zone 3 — 73Mg and 24Ga. Proceeding from simplified schematic of analysis of magnesium alloying at gallium diffusion into it [8] and according to binary diagram of this chemical system, MgGa, Mg₂Ga and Mg₃Ga₂ intermetallic compounds form, having melting temperature of 373–456 °C that is higher than the welding temperature.

In experimental magnesium alloy pre-alloyed with gallium, which is based on standard ML4, homoge-

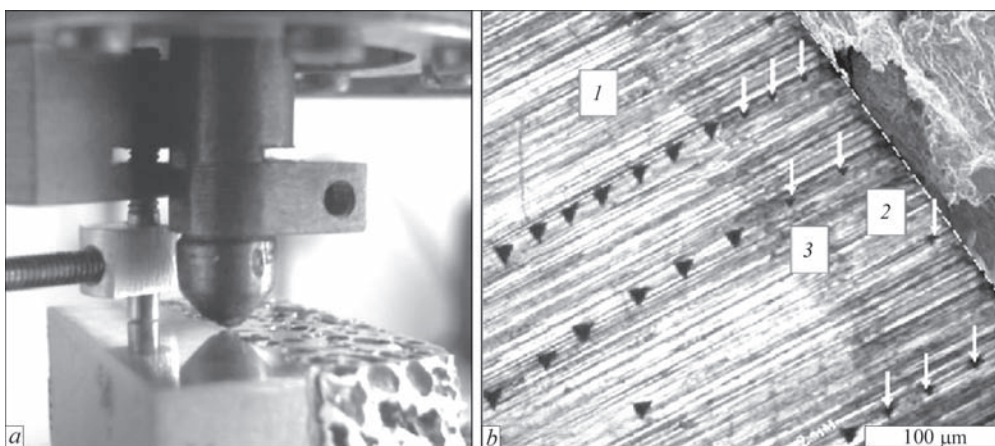


Figure 6. Micromechanical testing of ML4 + PA joint in Micron-gamma instrument (*a*) and indenter imprints in the diffusion zone on the side of magnesium alloy ML4 (*b*) (arrows show imprints of smaller area, characterizing strengthening; dashed line shows the zone of gallium application)

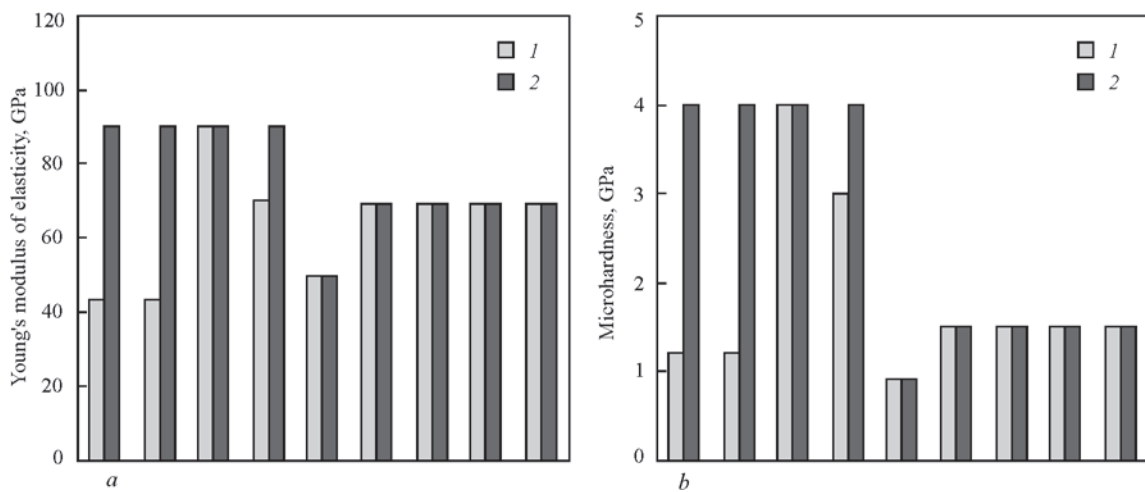


Figure 7. Diagram of tendencies of distribution of Young's modulus of elasticity (a) and hardness (b) across the diffusion zone of the joint of: 1 — ML4/PA; 2 — Mg + Ga/PA

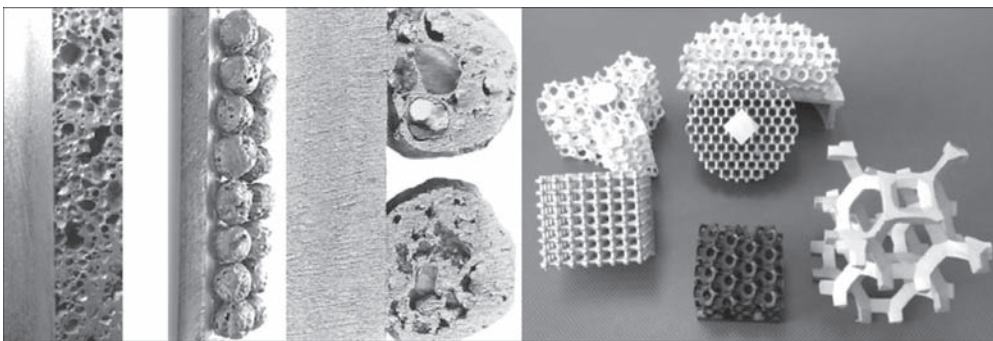


Figure 8. Fastening of diverse commercial cellular-porous materials to a monolithic base

nizing of chemical composition of near-contact zone and base material proceeds at joint activation by gallium (Figure 5). A clearly defined diffusion zone is absent.

Micromechanical testing of the diffusion zone of the joints was conducted by standard procedures [9, 10] according to ISO/FDIS 14577-1:2002 standard with Berkovich 3-face diamond pyramid [11] and application of Micron-gamma instrument. The instrument records Mayers microhardness and Young's modulus of elasticity at automatic recording of Berkovich indenter displacement, depending on the load applied to it. Maximum load was 500 g, load value error was 0.001; error of indenter penetration depth was 5 nm; maximum depth of indentation was 200 μm . Results are presented in the form of indentation diagrams at 20 g load with 50 μm increment. Preparation of samples for indentation was performed in keeping with the standard procedure of light alloy polishing to mirror surface and without etching.

From PA side, diffusion zone width is characterized by lowering of hardness from 1.5 to 1.0 GPa, of Young's modulus from 70 to 50 GPa. In the diffusion zone from ML4 alloy side (Figure 6), a considerable increase of Young's modulus from 42 to 73–110 GPa and of microhardness from 1.2 to 4.5 GPa is observed.

Magnesium alloy pre-alloying with gallium leads to a uniform level of Young's modulus and microhardness of base material and near-contact zone (Figure 7).

Welding with application of chemical activation by gallium enables fastening diverse commercial cellular-porous materials to a monolithic base (Figure 8).

Conclusions

1. Shown is the possibility of producing joints at 300 $^{\circ}\text{C}$ by two welding processes, differing essentially by heating duration and rates, for the case of manufacturing superlight multilayer bimetal sandwich panels, using porous and monolithic alloys based on aluminium and magnesium, in different sequence and combinations with application of chemical activation by gallium.

2. Investigation of microstructure and maps of chemical element distribution in the diffusion zone of the joint showed that the wavy front of gallium diffusion in monolithic magnesium alloy is typical as to its chemical composition for both the welding processes. Micromechanical studies of the joint diffusion zone showed a significant increase of microhardness and Young's modulus of elasticity from the side of monolithic magnesium alloy ML4, homogenizing of these

values in the diffusion zone and in the base metal in ML4 alloy alloyed with gallium, as well as a slight lowering of micromechanical properties in the walls of aluminium alloy pores. Thus, duration and rate of heating, depending on the applied welding technology and equipment, affects only the diffusion zone width.

Investigation results were obtained during performance of departmental program of the NAS of Ukraine «Investigation of structural transformations in welds and development of technologies of welding sheet hull and satellite structures from aluminium and dissimilar materials for fairings and adapters for rocket and space engineering» and Youth Basic Research Program of the NAS of Ukraine for young scientists «Optimization of the method of solid-phase joining of monolithic magnesium alloys to foamed aluminium».

1. (2002) *Handbook of cellular metals: Production, processing, applications*. Ed. by H.-P. Degischer, B. Kriszt. Wiley-VCH Verlag GmbH & Co.
2. Khokhlov, M.A., Ishchenko, D.A. (2015) Structural superlight porous metals (Review). *The Paton Welding J.*, **3/4**, 57–62.
3. Paton, B.E., Ishchenko, A.Ya., Ustinov, A.I. (2008) Application of nanotechnology of permanent joining of advanced light-weight metallic materials for aerospace engineering. *Ibid.*, **12**, 2–8.
4. Kharchenko, G.K., Falchenko, Yu.V., Fedorchuk, V.E. et al. (2012) Manufacture of stainless steel-aluminum transition pieces by vacuum pressure welding method. *Ibid.*, **1**, 26–28.
5. Khokhlov, M.A., Khokhlova, Yu.A. *Method of joining of bimetal bloc for thermal insulation of microelectronics elements*. Pat. 69145 UA, Int. Cl. B01B 1/00, B23K 1/00. Fill. 05.09.2011. Publ. 25.04.2012.
6. Khokhlova, J. (2013) Intergranular phase formation during reactive diffusion of gallium with Al alloy. *Materials Sci. Forum*, Vol. 768–769, 321–326.
7. Khokhlova, J., Khokhlov, M., Synyuk, V. (2016) Magnesium alloy AZ63A reinforcement by alloying with gallium and using high-disperse ZrO₂ particles. *J. of Magnesium and Alloy*, **4(Dec.)**, 265–269.
8. Khokhlov, M., Ishchenko, D., Khokhlova, J. (2016) Peculiarities of forming diffusion bimetallic joints of aluminum foam with a monolithic magnesium alloy. *Ibid.*, **4(Dec.)**, 326–329.
9. Kazuhisa Miyoshi. *Surface characterization techniques: An overview*, 12–22. <https://ntrs.nasa.gov/archive/nasa/casi.ntrs.nasa.gov/20020070606.pdf>
10. Oliver, W.C., Pharr G.M. (1992) An improved technique for determining the hardness and elastic modulus using load displacement sensing indentation experiments. *J. of Materials Research*, **7**, 1564–1583.
11. *Nano indenters from micro star technologies*. Revision 2.3 P.9. <http://www.microstartech.com/index/nanoindenters.pdf>

Received 21.12.2016

PECULIARITIES OF CONSTRUCTION AND SERVICE OF TANK RVS-200 FOR STORAGE OF DIESEL FUEL IN ANTARCTICA AT THE STATION «AKADEMIK VERNADSKY»

G.V. ZHUK¹, I.V. MOROZ², A.Yu. BARVINKO³, Yu.P. BARVINKO³ and Yu.N. POSYPAJKO³

¹SE «Experimental Design and Technological Bureau of the E.O. Paton Electric Welding Institute of the NASU»
15 Kazimir Malevich Str., 03150, Kiev, Ukraine. E-mail: oktbpaton@gmail.com

²National Antarctic Scientific Centre

16 Taras Shevchenko Ave., 01601, Kiev, Ukraine. E-mail: uac@uac.gov.ua

³E.O. Paton Electric Welding Institute, NASU

11 Kazimir Malevich Str., 03680, Kiev, Ukraine. E-mail: office@paton.kiev.ua

The analysis of materials of expert inspection of the welded tank RVS-200 for diesel fuel at the Ukrainian Antarctic Station «Akademik Vernadsky», made by the SE «Experimental Design and Technological Bureau of the E.O. Paton Electric Welding Institute of the NASU», is given. It was shown that according to the region of its location, the tank of only 200 m³ capacity is transferred to the highest criticality class CC3 with the fixed service life of not less than 40 years. Under these conditions the requirements to ecological purity of the object and the environment, at a complete isolation and limited capabilities of repair, predetermine the need in extraordinary constructive solutions on providing the maintenance-free service life. The specific technical solutions of the considered problem are given. 7 Ref., 5 Figures.

Keywords: welded tank, highest criticality class CC3, corrosion damages, austenitic stainless steel, corrosion protection

In 2007, at the Ukrainian Antarctic Station «Akademik Vernadsky» on Galindez Island in the archipelago of the Argentine Islands (Antarctica) the welded cylindrical tank RVS-200 for storage of diesel fuel was constructed (Figure 1). The project of the tank was developed by the OJSC «UkrNIIproektstalkonstruksiya», the metal structures were manufactured and assembled by the LLC «Kirovograd Plant of Technological Equipment». The natural conditions at the construction region are quite favorable for the vessel service. The climate is maritime, subantarctic, the minimum temperature over the years of observations has been not lower than -8 °C. However, the data about the minimum temperature of -47 °C in winter are available (the bulletin «Around the World», Ukraine, 2010, Issue 11). The wind is 30–35 m/s, the snow is 300 days in a year.

The requirement to the tank construction is contained in the memorandum of 20.07.1996 about the transfer of station «Faraday» by England to Ukraine, (at present, the station «Akademik Vernadsky»). Somewhat earlier, in 1992 Ukraine acceded to the Antarctic Treaty, which contains the specific requirements to preservation of the ecological environment in Antarctica. Until that time, at the station «Faraday» the English specialists constructed two vessels for

storage of liquid fuel. The main vessel is in the form of rectangle in design of about 6 m height. At the station «Akademik Vernadsky» the vessel has been successfully operated for over 20 years as well. The design of vessel is simple and the adopted simplicity guarantees its complete safety at the absence of repairs for more than 50 years. The spatial system with vertical and horizontal posts and cross-bars, lined with sheets of austenitic stainless steel class of 6 mm thick from inside, is assembled of steel girders on bolted joints. The sheets are fixed to the frame using bolts through sealing gaskets. In the wall and roof there are techno-



Figure 1. General view of the tank RVS-200 at the Antarctic station «Akademik Vernadsky»

logical branch pipes and hatches for pumping in and out the fuel and inspection of its structure. Let us note that for the period of designing the considered tank, in Ukraine there were no state regulations regarding the system of providing the reliability and safety of construction objects. In the first edition the listed regulations of Ukraine were adopted in 2009 [1].

The project of the newly constructed tank was fulfilled in accordance with the requirements of Ukrainian standards VBN V.2.2-58.2-94. These standards are applied to the tanks for storage of oil and oil products, which are constructed at the territory of Ukraine. The increased ecological safety of the tank is provided by applying the design of the «glass in glass» type. These are two welded steel tanks, where each has its wall, bottom and roof. The geometrical dimensions of the tank are the following: the inner (main) tank: the wall height is 5.96 m, the inner diameter is 6.63 m; the outer (protective) tank: the wall height is 6.58 m, the inner diameter is 6.96 m. The distance between the walls is 160 mm. The material of all the structures is steel VSt5ps. The thickness of wall and bottom of the main tank is 5 mm. The thickness of wall of the protective tank is 5 mm and 8 mm of the bottom. The inner tank is designed for permanent storage of diesel fuel. The outer tank is an emergency one. If the impermeability of the wall or bottom of the main tank is violated the outer tank should localize the spilling of diesel fuel within its range. After that, from the outer tank the fuel should be pumped over to the spare vessel, the entire tank should be transferred to the fire works with the possibility of human staying inside the vessel, detection of damages and their causes and performing the necessary repair. After the hydraulic test according to the established procedure, the double-walled tank is commissioned for the further storage of diesel fuel. The accepted scheme of restoration of working serviceability of the considered tank is based on the availability of the serviceable product pipeline for pumping over the diesel fuel



Figure 2. General view of basement arrangement of the tank RVS-200

into the spare tank. The corrosion protection is provided by thickening the bottom of the outer tank to 8 mm and applying the protective coating resistant to diesel fuel to the bottom and the lower girth of wall of the main tank. The applying of sand blasting to the surface of the wall and the bottom and deposition of more resistant coatings were not considered by the project. During construction of the tank the following deviations from the project were admitted: two man-hole-hatches of 500 mm diameter in the lower girth of wall were not assembled and the changes in the scheme of fuel supply to the vessel were introduced.

After 10 years of service, in accordance with the Ukrainian standard [2], in January-March, 2016 the SE «Experimental Design and Technological Bureau of the E.O. Paton Electric Welding Institute of the NASU» on a contract base with the National Antarctic Scientific Centre of Ukraine, carried out the full technical diagnostics of the considered tank RVS-200.

The aim of the work was:

- basing on the results obtained at the full inspection of the tank using instrumental and calculation means, to prepare the conclusions regarding the compliance of the structures and serviceability of the tank RVS-200 with the standards of Ukraine [3; 4];

- to develop the definite proposals on bringing the tank RVS-200 to state in compliance with the requirements of effective standards regarding reliability and structural security.

The results of technical diagnostics are described in detail in the report of the agreement [5], and in the publication [6].

Basement of the tank. The tank was constructed on the monolithic rocky foundation which represents a characteristic surface of Galindez Island. The basement of the tank was made as a two-tier system of girders (Figure 2). The lower tier is composed of seven parallel reinforced concrete girders of 650 mm height, 460 mm width in the lower and 330 mm in the upper part. The girders are fixed to the basement with anchors. The anchors are fixed in the boreholes drilled in the rock and welded-on to the girders reinforcement. The distance between the girders in the axes is 1.20 m. The upper tier of the girders is composed of 15 steel girders (double-T No.14), which are welded-on to the embedded parts on the upper surface of the lower girders. The distance between the girders in the axes is about 0.41 m. The bottom of the outer tank leans against the upper girders. According to the project, on the bottom of the outer tank the wooden girders are laid (the bars of 100×100 mm cross-section) at 300 mm pitch. The lower bottom at the top and the bottom as well as wooden and steel girders are not available for visual inspection and instrumen-

tal control. The bottom of the main tank lies on the wooden girders. The existing design of the tank base-ment virtually eliminates the subsidence of the outer and inner bottoms of the tank. According to the mea-surements, the maximum deviation of the outer and inner contour of the bottom is equal to 6 mm. There are remarks concerning small repair of the reinforced concrete girders and annual inspection and works on preventing corrosion of reinforcement of the lower girders, steel anchors and upper tier girders.

Technical state of the outer tank. *Wall of the out-er tank.* The wall is assembled of separate 3.0×1.5 m sheets of 5 mm thickness, previously rolled for the ra-dius of the tank, which corresponds to the project. The size of a sheet was in many respects dictated by the conditions of its transportation, especially from the ship to the berth of the base, unloading on the berth and assembly applying the available mechanisms. The deviation of the wall from the vertical amounts to +22 mm outside and -26 mm inside, which does not exceed the standard tolerances. All welded joints are produced outside without backup welding of weld root which is explained by the assembly of the outer wall after the assembly of the inner one. The inspec-tion and measurements of welded joints showed the good state of welds [5]. At the designed thickness of the wall being 5 mm and a three-fold safety margin, according to the calculated circumferential stresses, the one-sided welding provides a sufficient strength of vertical and horizontal welds. It is also important that the outer wall is loaded only in case of emergen-cy, when the integrity of the inner (main) tank is vi-olated. This eliminates its cyclic loading. The devia-tions from the standards existing in the welds, do not affect the serviceability of welded joints.

Bottom of the outer tank. The evaluation of the bottom was performed from the results of inspection and measurements of thickness of the projecting part of bottom (edges). The thickness of bottom is equal to 7.5–7.8 mm. To the bottom the branch pipe is weld-ed-in for draining the condensate from the space be-tween the walls. The branch pipe is brought outside the space between the reinforced concrete girders and ended with a valve. According to the data of the work [5] the lower bottom is serviceable.

The calculation for the static strength of wall of the outer tank showed that the estimated stresses in the first (at the bottom) and second girths amount to 45 and 35 MPa, which is 4–5 times lower than the allowable values for steel VSt5ps equal to 147 and 171 MPa [5]. The calculation confirms that the thick-nesses are accepted as-designed as the minimum ones acceptable according to the standards for the given vessel. Let us note that under the load the outer tank

can be only during its hydraulic testing and at the damage of the main (inner) tank with leakage of the stored diesel fuel from it. The state of the wall meets the project requirements.

Technical state of the inner (main) tank. The inner tank is intended for permanent storage of die-sel fuel. Accordingly, the pipeline for pumping out diesel fuel from the tank is welded-in to its wall and the breathing fitting-valves are mounted on the roof. The inner surface of the bottom and wall contact con-stantly the stored product. The hatches in the lower girth for access to the inside of the tank for inspection of structures by technical personnel are absent. The access to the tank is only possible through the upper sky-light and vertical step-ladder near the wall. Let us note that when there are no opened hatches the human staying in the tank is prohibited.

Wall of the inner tank. The wall is assembled of separate sheets previously rolled similarly to the out-er wall. The geometric shape of the wall meets the requirements of standards. On the surface the dents and convexities are absent. The deviation of genera-trixes from the vertical amounts to +38 and -31 mm, the difference of marks of the outer contour does not exceed 6 mm [5]. The vertical and horizontal welded joints are produced by two-sided butt welds with full penetration. The detected individual deviations in the shape of weld beads, undercuts and displacements of edges to 1 mm (Figure 3) do not affect the service-ability of welded joints. The 5 mm wall thickness is appointed from the condition of minimum normative admissible thickness for the given vessel, which is confirmed by calculations of the outer tank [5].

Bottom of the tank. The bottom of the inner tank is manufactured of separate sheets. At first the sheets



Figure 3. General view of vertical welds on inner wall surface of the main tank

were welded into five dimensional bands considering the tank diameter. After producing the transverse welds on the upper side, the bands were tilted and the welds were made on the rear side. At the 5 mm thickness of the bottom, the accepted technology provided impermeability of welds. Then, the dimensional bands were tightened on the bars with overlapping along the long sides and joined between each other by overlap welding. It can be assumed that according to this technology the lower bottom was manufactured as well. The performed visual inspection of the entire bottom surface and the vacuum control of all welded joints confirmed the impermeability of the bottom. In more detail, the technical state of bottom is described in [6]. At the bottom there is a branch pipe of the system for removal of under-product water and cleaning the tank. The branch pipe passes through two bottoms to the space between the reinforced concrete girders and ends with the valve.

Roof of the tank. Each tank (outer and inner) has its welded conical girder roof. Between the roofs the clearance is about 300 mm. Each roof was assembled of two shields on the ground. The flooring of each roof around the perimeter is welded-on by continuous weld to the fringing angle piece on the outer and inner wall. The flooring thickness is equal to 4 mm, which corresponds to the project. All branch pipes of hatches and valves pass through the flooring of both roofs being welded-on to them around the contour. The general view of the tank roof is shown in Figure 4. On the surface of roof there are no unacceptable defects in form of deflections and fractures under snow load. The surface of the existing separate dents, with the absence of paint layer on them, is exposed to shallow atmospheric corrosion of 0.2–0.3 mm depth. The state of the roof is serviceable.

Corrosion damages of the tank. At the general good technical state of metal structures of the considered tank (static strength and stability), the reliability of the tank is determined by the value of corrosion damages of main load-carrying structures. The per-



Figure 4. General view of roof of the tank RVS-200

formed diagnostics of the tank showed that the most affected by corrosion are the bottom of the inner tank and the lower inner surface of its wall to the height of up to 300 mm. This is the zone of accumulation of sludge water and different salt deposits: sulfides, chlorides, etc. The certain areas of the bottom, mostly those adjacent to the welds, have extended pit corrosion damages. The pit corrosion damages are concentrated as the regions of 10–20 cm² at the depth of 2.0 mm. A damage of the wall adjacent to bottom has a more uniform character with the depth of pits up to 1–1.5 mm. The available corrosion damages indicate that the surface state of the main bottom and lower part of the inner wall will determine the estimated service life of the tank. At the same time it should be taken into account that when there are corrosion damages at separate places going to the depth of 50 % from the thickness and more, the bottom is subjected to replacement [7].

Search for an optimal variant of corrosion protection of tank RVS-200 under the conditions of Antarctica. According to the classification of standards of Ukraine [1], the given tank RVS-200 with diesel fuel at its location in Antarctica, belongs to the criticality category CC3 as a biologically hazardous object. The service life of such tank should be at least 40 years. The accepted life in this case has also another justification. A very high cost for delivery of structures and manpower to the site area, the absence of any in-site repair facilities and requirements to trouble-free service of the tank dictate also the need in the maximum long-term service life. Under the normal conditions on the «mainland» this is achieved by application of epoxy based coatings, plasma spraying of zinc, basalt coating and a number of other. All the abovementioned coatings require cleaning of surface up to steel glittering by the class Sa 3 according to ISO 8501.

In view of small volumes of works, the delivery of equipment set, sand, coating components and workers to Antarctica and back will exceed the cost of the tank itself. As was repeatedly testified in Ukraine and in other countries, the actual service life of the mentioned coatings does not exceed 12 years (at the standard life of 10 years [4]).

In view of the already passed 10 years of the tank service, to achieve the life of 40 years, it would be necessary to renew the coating three times, performing its sand blasting each time. The logical conclusion follows, that under such conditions an extraordinary solution for increase in service life of the tank and a fundamentally different approach to guarantee the required life are needed.

As one of the variants, the arrangement of a new bottom with the wall of up to 400 mm height on the bottom of the inner tank is proposed (Figure 5). The bottom and wall should be made welded of sheets of austenitic stainless steel of 3 mm thickness. The sheets of optimal sizes should be stacked and welded on the existing bottom without any special cleaning. Then the assembly and welding of sheets of the wall are performed between each other and along the entire upper perimeter to the wall of the inner tank. All the works should be carried out according to the project. In fact, a full impermeable lining of the lower surface of the main tank will be performed, which is subjected to active corrosion. The proposed solution ensures maintenance-free period of serviceability of the bottom for at least 40 years.

Conclusions

1. The project of the tank RVS-200 and its construction were performed without full consideration of characteristics of location and long-term service of the tank at the station «Akademik Vernadsky». The implementation of conclusions and recommendations on the further service of the tank, stated in the report [5] and in the present publication, will provide the required reliability in its service.

2. The technical state of the tank RVS-200 at the time of inspection meets the requirements of the Ukrainian standards VBN V.2.2-58.2-94 regarding the static strength and stability, on the basis of which the project and construction were completed. The inner (main) tank has unacceptable corrosion damages of the bottom which requires the fulfillment of solutions on corrosion protection of the bottom and lower part of its wall within 2–3 years, taking into account the estimated service life equal to 40 years. We con-

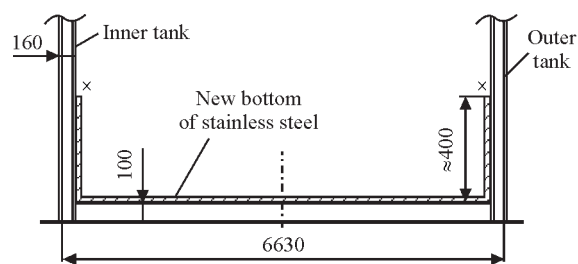


Figure 5. Scheme of constructive solution for protection of the inner bottom against corrosion

sider that one of such solutions, which are proposed in this publication, the arrangement of an additional protective bottom and a part of the wall of austenitic stainless steel can be.

3. The deviations from the project, made during the construction of the tank RVS-200, do not allow performing its maintenance in the period of the service keeping the accepted safety regulations. Over the next 2–3 years it is necessary to bring the tank in compliance with the requirements of the project.

1. *DBN V.1.2-14-2009*: General principles of reliability assurance and design safety of buildings, constructions, building structures and foundations. Kyiv: Minregionbud Ukrainy.
2. *DSTU-N B A.3-10:2008*: Guidelines for technical diagnostics of vertical steel tanks.
3. *VBN V.2.2-94*: Vertical steel tanks for storage of oil and oil products.
4. *DSTU B V.2.6-183:2011*: Vertical cylindrical steel tanks for oil and oil products.
5. (2016) *Technical report (expert opinion) on technical state of tank RVS-200 installed at Ukrainian antarctic Akademik Vernadsky station*. Kyiv: E.O. Paton SE EDTB.
6. Posypajko, Yu.M. (2016) Defectoscopy in the Antarctic: Technical diagnostics of tank RVS-200 at Ukrainian antarctic Akademik Vernadsky station. *Tekhn. Diagnostika i Nerazrush. Kontrol*, **4**, 46–51.
7. (1988) *Operating rules of tanks and instructions on their repair*. Moscow: Nedra.

Received 18.01.2017

EFFECT OF VIBROTREATMENT ON FATIGUE RESISTANCE AND DAMPING CAPACITY OF STRUCTURAL ELEMENTS WITH RESIDUAL STRESSES

V.A. DEGTYAREV

G.S. Pisarenko Institute for Problems of Strength, NASU
2 Timiryazevskaya Str., , 01014, Kiev, Ukraine. E-mail: ips@ipp.kiev.ua

A work, based on a complex diagram of cycle limit stresses, proposes a method for selection of vibrotreatment undamaging modes for the elements of metal structures in order to gain effective decrease of their residual stresses without a risk of fatigue damage during technological treatment. This method was approved by the example of testing of the structural elements of steel 20 and end pivot of steel 20GFL of span bolster of eight-axis rail tank car. Comparative fatigue tests showed 2.5 times increase of fatigue life of treated welded specimens and rise of their endurance limit by 40 %. In process of vibrotreatment of a circular element of steel St.3, decrease of residual stresses is accompanied by rise of its damping capacity. Growth of maximum cycle stresses promotes for increase of vibration decrement to larger value and its stabilizing in time matches with residual stress stabilizing. This allows assessing completion of a process of change and further stabilizing of the vibration decrement. Determined decrease of damping capability of the investigated sample after vibrotreatment indicates its strain aging, showing plastic strain during treatment. Rise of cycle stress amplitude reduces sample deformation after vibrotreatment at further aging to 1500 h and decrease of initial residual tensile stresses to 0.51 of yield limit of the material results in its geometry stability. 25 Ref., 2 Tables, 7 Figures.

Keywords: *vibrotreatment, welded joint, residual stresses, endurance limit, cycle stress amplitude, cyclic creep limit, vibration decrement*

Appropriateness and effectiveness of ecological and technological process of vibrotreatment (VT) of welded and cast parts having low consumption of energy and capable to reduce residual tensile stresses (RS) is proved by the world's and domestic experience [4, 5]. These stresses can reduce life of the part [1, 2] or change its shape [3]. Efficiency of the method (treatment time takes not more than 40 min) lies in the fact that cyclic loading of the structure in whole provokes RS decrease in all elements having different rigidity per one technological cycle.

However, a disadvantage of VT is that a value of fluctuating stresses, developed by mechanical vibrators, is selected experimentally. This can result in a stress amplitude, which is insufficient for necessary reduction of RS or such big that can lead to appearance of fatigue damages even at technological stage of treatment [6]. Alongside with indirect methods of VT control, in particular, on variation of current, consumed by vibrator [7, 8], and displacement of resonant peaks on frequency scale [9], there is a method of control on a change of amplitude-frequency characteristic (AFC) [10]. It lies in the fact that width of resonant peak reduces simultaneously with rise of vibration amplitude by VT end. This phenomenon indicates decrease of energy dissipated in the

part being treated. A proof is reference data [11] on vibrotreatment of 7000 kg halves of a welded frame of DC machine, which showed reduction of vibration decrement δ from 12.3 to 9 %.

The decrement was determined on width of resonant peaks, recorded before and after VT [12]. However, it is known fact that drop of RS in the metal structure takes place only as a result of plastic strain [13], presence of which should lead to rise of energy dissipated in the material [12]. Obvious contradiction in a direction of change of material vibration decrement to observed in practice vibration decrement of the part can be explained by the fact that located on the floor being treated parts together with energy dissipation in the material have also structural dissipation of energy, change of which is mainly reflected in AFC. This assumption is proved, first of all, by large absolute values of δ at VT of the specimen simulating structure of cast-iron frame of cutting machine (8.3 %) [14], and shells of titanium with welded stiffening ribs as well as steel shaft (4.0 and 3.5 %, respectively) [15]. Secondly, change of vibration decrement of the part in VT process, for example, in frame of DC machine by 3.3 % as well as in two welded bodies of coordinate measuring machines [11] by 4.2 and 2.8 %, respectively, somewhat exceeds absolute the value of the vibration decrement of material, which at stress, typical for VT and under room temperature conditions,

makes 0.2–1.0 % for carbon steels, 0.05–0.15 % for titanium alloys and 2–5 % for cast iron [16].

Thus, existing up to now contradiction on direction of change of the material vibration decrement to one observed under industrial conditions, first of all, indicates weakness of control of VT process on criterion, which is based on determination of integral characteristic of energy dissipation in the structure, change of which in the process of VT, firstly, is not related with change of residual stresses and, secondly, many times exceeds energy dissipation in the material. Since RS change takes place in the material of part being treated, then this process should be evaluated on variation of energy dissipation in the material.

In this connection, aim of the present paper lies in optimizing the VT method for the elements of metal structures and evaluation of its effect on their fatigue resistance and determination of interconnection of change of energy dissipation in the element being treated with residual stress kinetics.

Research objects, testing equipment. Research on VT method optimizing was carried out under laboratory conditions on specimens of steel 20 ($\sigma_t = 440$ MPa, $\sigma_y = 290$ MPa) of 100×400×420 mm size with a rib welded-up along the long side of the specimen as well as under industrial conditions. Welding-up of the rib by semi-automatic CO₂ welding with the specimen immersed to the middle in water allowed developing high residual tensile stresses. Their value and sign, matching with loading application direction, were determined by magnetic noise method, based on application of Barkhausen effect [17]. RS distribution diagram showed that they are maximum at weld to base metal interface and made on average 220 MPa, i.e. $0.76\sigma_y$ and at 12 mm distance they equal zero and then transform to compression ones. Value of the maximum residual tensile stress σ_{res}^i was further used in analysis of RS kinetics. Under industrial conditions VT was carried out for box-section bolsters (hereinafter bolsters) of 190×170×2000 mm size and zones of welding-up of end pivot to the elements of span bolster of eight-axis rail tank car of steel 09G2S. The pivots of complex configuration are made by electroslag casting of steel 20GFL ($\sigma_t = 740$ MPa, $\sigma_y = 590$ MPa) and bolsters were produced by welding of 20 mm thick sheet steel 20. Necessity of VT of the end pivot is explained by its frequent fatigue fracture in operation.

VT of the metal structures was carried out using electromechanic vibrator IV107 by means of development of fluctuating loads of resonant or near-resonant frequencies as well as applying pulsator TsDM-200pu in a forced vibration mode allowing tests at any cy-

cle asymmetry. Stress amplitude was measured by a strain-gage method.

Bending fatigue tests of the specimens were carried out on DSO-2 [18] machine at set coefficient of stress cycle asymmetry R under conditions of harmonic loading at 20 Hz frequency. Stress amplitude was measured by strain-gage method.

Investigation of change of energy dissipation in the material was performed using the specimens cut out from as-delivered St.3 steel pipe of 275 mm diameter and 8 mm thickness. Mechanical characteristics in tension of cylinder specimens, cut out from a pipe wall in tangential direction, made $\sigma_{0.2} = 235$ MPa, $\sigma_t = 450$ MPa. Circular specimen of 115 mm width with a cut was fixed in its upper part to vibration node by means of screw clamp, which in turn was stringed. Due to such scheme of fixing, there is no possibility of structural damping. A principle of resonant excitation of bending vibrations of the specimen is realized in the machine via electromagnets, fastened to its edges. Cyclic stresses were developed due to periodic approaching and removal of ends of the specimen and were calculated on deformation of strain gage, glued in the area of maximum bending moment effect. To develop RS on the outer surface, the specimen was deposited in the middle of circumference and its internal surface was cooled by running water. Evaluation of value and sign of RS in a near-weld zone, acting along the deposit, was carried out by magnetic noise method [17]. Values of σ_{res}^i at 2 mm distance from the deposit made on average 200 MPa, i.e. $0.85\sigma_{0.2}$, and at 8 mm distance it was 50 MPa. A vibration decrement was determined by recoding a vibrogram of free damped vibrations of the specimen [19] using for this indicated strain gage. Due to the fact that the deposit can damage a probe, determination of δ was duplicated applying one more method. Industrial TV unit PTU-61 was used to measure vibration span of the specimen. The TV camera in order to increase measurement accuracy was attached to MBS-1 microscope fixed on test machine body. A frequency meter was used for measurement of number of cycles of specimen vibration, corresponding to half damping of their span. The vibration decrement was determined at $\sigma_a = 7$ MPa cycle stress amplitude. The minimum σ_a in VT made 15 and maximum one was 60 MPa.

Analysis of research results. Optimizing of the VT method lied in selection of undamaging modes of loading of metal structures for reduction in them of RS without a risk of fatigue damage. It is based on application of complex diagram of cycle limit stresses (DCLS) (Smith diagram) (Figure 1). A line of limit stresses I was determined with respect to received endurance σ_R limits of the specimens with welded-up

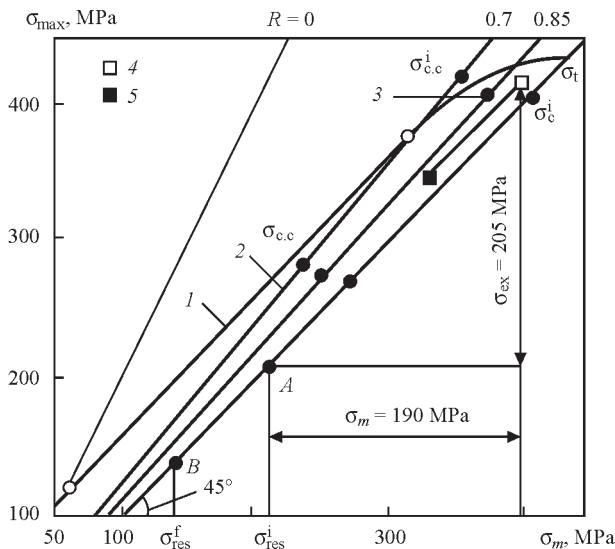


Figure 1. Diagram of limit stresses of steel 20 welded joint (1), lines of cyclic creep limits of material in tension (2) and bending (3), total stresses is in initial state (4) and after 10^5 cycles of loading (5)

rib of steel 20 on the basis of $2 \cdot 10^6$ cycles of loading at $R = 0$ and 0.7. It is limited by endurance limit at symmetric cycle of loading (not indicated in the Figure) and strength limit σ_t . Lines 2 and 3 correspond to experimentally determined limits of cyclic creep $\sigma_{c.c.R}$ [20] of steel 20 at tension and bend, obtained at $R = 0.7$ and 0.85, i.e. maximum stresses, under effect of which a set value of residual strain ϵ_{cr} is reached for given test basis in cyclic creep mode. In this case $\epsilon_{cr} = 0.2\%$. They are limited by creep limit at static loading (σ_y is allowed) and endurance limit, called the minimum cyclic creep limit $\sigma_{c.c}$. Since specimen tests were carried out at bending, then DCLS section received under the same conditions was used for setting the stresses from external loading σ_{ex} . Before VT, an initial maximum residual stress σ_{res}^i , varying in each

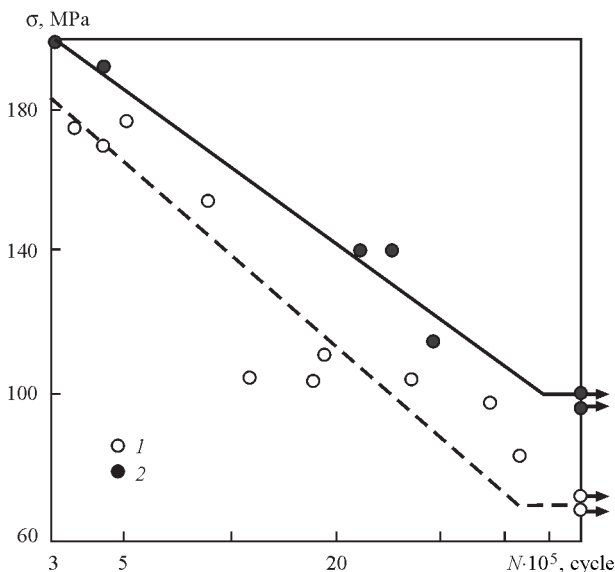


Figure 2. Fatigue curves of welded joint in initial state (1) and after VT (2) ($R = 0$)

specimen in 210–220 MPa range, was plotted on diagram (t. A). Stress from external load, which should be applied to the specimen, was determined following the condition

$$\sigma_{c.c.R} < \sigma_{ex} + \sigma_{res}^i < \sigma_R,$$

where σ_R , $\sigma_{c.c.R}$ are the stresses corresponding to intersection of effect of cyclic stresses with limit stresses lines 1 and 3, respectively. Condition $\sigma_{ex} + \sigma_{res}^i < \sigma_R$ provides for absence of fatigue damage after VT, and $\sigma_{c.c.R} < \sigma_{ex} + \sigma_{res}^i$ is the efficient reduction of RS. According to procedure, σ_{ex} is calculated in such a way that the maximum stresses locate below line 1, but above line 3, that guarantees absence of fatigue damages and effective decrease of RS. If σ_{res}^i was more than the average stress of respective $\sigma_{c.c}$, then application of symmetric cyclic load is enough for RS reduction. Since it absent in this case, then for RS decrease it is necessary to apply asymmetric loading, staying in a safe area of loading. $\sigma_{res}^i = 215$ MPa value was used for calculation of parameters of external load (their values are presented in Figure and in Table1). VT duration made 10^5 cycles of loading. The loading modes were kept stable during this time. It can be seen that VT provoked reduction for more than 40 % (darkened square in Figure) and it made on average $0.45\sigma_y$ of steel 20 (t. B). Comparative fatigue tests were carried out for evaluation of effect of low RS. Analysis of obtained results at zero loading cycle under room temperature conditions (Figure 2) indicates increase of endurance of the vibrotreated specimens in the whole range of applied stresses (curve 2). For comparison, the Figure shows fatigue curve 1 of the specimens with high RS, received in initial state. It can be seen that load fall provides for rise of their effect due to what fatigue curves separate. For example, endurance of the vibrotreated specimens increases from 1.5 to 2.7 times at decrease of stresses from 180 MPa to endurance limit stress level, equal 100 MPa. At that, endurance limit determined on the base of $5 \cdot 10^6$ cycles of loading grew by 40 %. VT of the bolsters and pivots was carried out by means of electromechanical vibrator IV107 at near-resonant frequency for around 20 min that corresponded to 10^5 cycles of loading. Decrease of residual stresses to σ_{res}^f was judged on measurement of current, used by vibrator. Stress amplitudes were determined based on condition mentioned above, and $\sigma_{c.c.R}$ value at $\epsilon_{cr} = 0.2\%$. The results of testing are given in Table 1. Analysis of the results showed that VT technology at maximum reached amplitude of stresses σ_a allowed decreasing initial RS by 20–22 %, which on average made $0.65\sigma_y$ of respective steel. In some bolsters RS were of such level that their reduction required a stress amplitude exceeding

Table 1. Results of reduction of maximum residual tensile stresses depending on type of equipment used in VT

Research objects	Equipment	Values of stresses at undamaging modes of vibrotreatment for RS decrease in welded structures, MPa							
		σ_{res}^i	σ_R	$\sigma_{c.c.R}$	σ_{ex}		σ_{max}	σ_{res}^f	$\sigma_{res}^f / \sigma_{res}^i, \%$
					Amplitude	Static			
Bolster	Vibrator	245	290	275	40	0	285	190	78
		230	330	265	20	70	320	155	67
	Pulsator	230	330	265	22	70	322	150	65
		200	320	265	28	88	316	145	72
		175	315	265	24	109	308	120	69
Pivot	Vibrator	480	530	515	35	0	515	385	80
Specimen	DSO-2	215	430	405	15	190	420	125	58
Bolster	Heat treatment	240	–	–	–	–	–	100	42
Pivot	Same	480	–	–	–	–	–	210	44

line 1 (see Figure 1). In this cases TsDM-200pu pulsator was used for asymmetric cyclic loading in a mode of forced vibrations of 10 Hz frequency. Asymmetric loading allows significant expansion of VT capability due to increase of stresses from external load, values of which are given in Table 1, keeping them in the safe area. It can be seen that in this case vibrotreatment decreased initial RS on average by 32 %, which made $0.5\sigma_y$. For comparison, let's note that RS values in the bolsters and pivots after heat treatment made on average $0.35\sigma_y$.

Thus, carried tests showed that VT can compete with annealing in increase of endurance and fatigue resistance of non-critical structures, in particular, if consider high cost and duration of annealing technological cycle.

Effect of amplitude of cycle stresses and time of RS change in the circular specimens and their vibration decrement was also investigated at VT. Design of the specimen and scheme of its loading allowed de-

termining variation of vibration decrement in the material as well as its geometry stability. The diagrams of RS distribution on the specimen width at different number of loading cycles showed that the maximum RS have the most intensive reduction, and at 6 mm distance from the weld, where initial RS equal approximately $0.5\sigma_{0.2}$, their change was not observed. The results of relative change of decrement and maximum RS are given in Figure 3, where the δ^i and δ_{res}^i are vibration decrement and residual stress in initial state, and δ , σ_{res} are their current values in process of VT. Table 2 shows values of δ^i at $\sigma_a = 7$ MPa and σ_{res}^i for each tested specimen.

Obtained results indicate that cyclic loading of the specimens promotes simultaneous decrease of RS and rise of vibration decrement that can be a consequence of material plastic strain [12]. Plastic strain in the specimens is proved by the data on relative change of vibration decrement δ/δ^i in course of time after VT of the specimens at different maximum cycle stresses

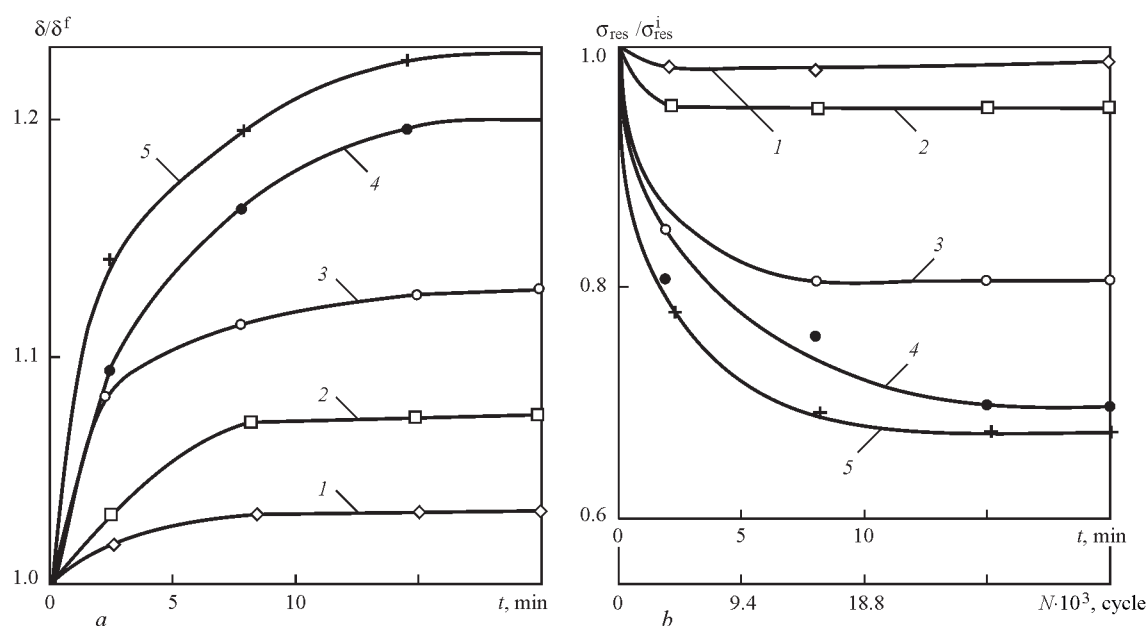


Figure 3. Dependence of relative change of vibration decrement (a) and maximum residual stress (b) on VT time at different maximum cycle stresses σ_{max} : 1 — 185 MPa ($\sigma_a = 15$ MPa); 2 — 205 MPa (15 MPa); 3 — 230 MPa (50 MPa); 4 — 235 MPa (30 MPa); 5 — 265 MPa (60 MPa)

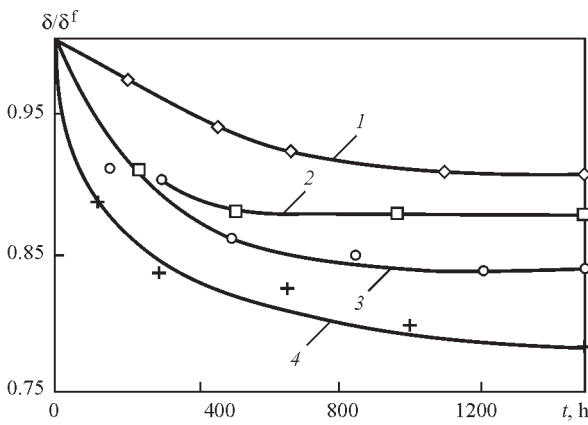


Figure 4. Relative change of vibration decrement in course of time after VT of specimens at different maximum cycle stresses σ_{max} : 1 — 185 MPa ($\sigma_a = 15$ MPa); 2 — 205 MPa (15 MPa); 3 — 230 MPa (50 MPa); 4 — 265 MPa (60 MPa)

(Figure 4), where δ is the current decrement value, δ^f is the final value of decrement after VT end (determined using the curves given in Figure 3). Presented graphs (Figure 4) show that the vibration decrement drops in all specimens in course of time, that indicates passing of process of strain aging in the material of specimens after VT. It appears only as a result of plastic strain of material [21]. The larger value of decrement at VT, the lower is its decrease in time. In 1000–1500 h its value was virtually stabilized depending on maximum cycle stresses.

Effect of static stresses on vibration decrement of the specimens [16] is known. Similar effect of residual stresses can be expected. Reference data [22] were used for evaluation of decrement change only due to residual stress decrease. It is shown that change of static constituent from 150 to 100 MPa at amplitude of bending stresses 60 MPa in the specimens of low-carbon steel results in a relative rise of vibration decrement approximately by 3 %. The results of test-

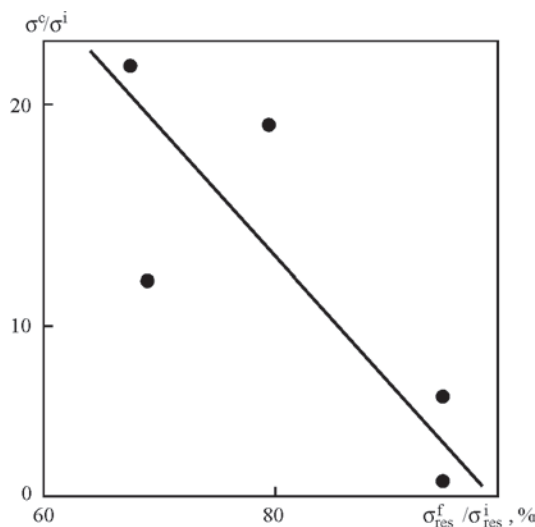


Figure 5. Dependence of relative change of vibration decrement δ^f on relative change of residual stress σ^f_{res} determined at the end of VT at different modes of cyclic load

Table 2. Initial values of vibration decrement of material and maximum residual tensile stress

Specimen number	σ^i_{res} , MPa	δ^f , %
1	170	0.107
2	180	0.112
3	190	0.12
4	205	0.111
5	205	0.13

ing of the specimens of steel 45 [23] at all did not show decrement change in reduction of static stress from 250 to 150 MPa. Relative increase of δ of circular specimen at the same stress amplitude at the end of VT made 1.22, i.e. 22 % (see Figure 3). It is obvious that the main reason of change of vibration decrement of the circular specimens material was their plastic strain at cyclic loading. Measurements of RS in the specimens at different intervals of time after VT did not show their changing. Increase of maximum cycle stresses, equal $\sigma_{max} = \sigma^i_{res} + \sigma_a$, promotes the highest rise of the vibration decrement and decrease of RS (see Figure 3). The most intensive decrease of RS and increase of δ is observed in course of 5–10 min, that corresponds to $(9.4-18.8) \cdot 10^3$ cycles of loading. Moreover, the lower the maximum stress, the smaller is the time of stabilization processes in the specimen. Further rise of VT time has virtually no effect on RS and δ . Analysis of the reference data [24] also verifies obtained result on effect of number of loading cycles on RS decrease at VT. It is also necessary to take into attention that stabilizing of the vibration decrement and RS on number of cycles virtually matches. Therefore, change and further stabilizing of δ can be used for judging the process of reduction and further stabilizing of RS in the part being treated, and, respectively, time necessary for its VT. Since, according to data of the Figure, stress amplitudes from 15 MPa and more provokes change and further stabilizing of the processes taking place in the specimen material, then, apparently, only nature of δ change without its numerical value can not be used for evaluation of VT efficiency from point of view of quantitative reduction of residual stresses.

Quantitative relationship of relative change of the vibration decrement and RS, determined in 20 minutes of VT of the specimens with different stress amplitude is given in Figure 5, where the final values of vibration decrement and RS are determined on data of Figure 3. Reduction of RS was observed, regardless the fact that maximum cycle stresses at VT of the most specimens were lower than the yield limit. VT at the most intensive in the experiment mode of loading ($\sigma_a = 60$ MPa) resulted in relative increase of the

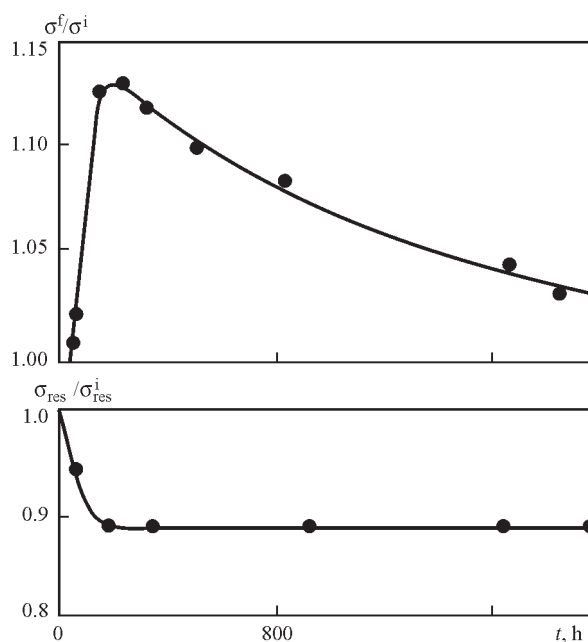


Figure 6. Dependence of relative change of vibration decrement and maximum RS on time in specimen without VT

vibration decrement by 22 % and reduced initial RS (205 MPa) by 32 %. In an absolute value, rise of the vibration decrement of the material $\Delta\delta = \delta^f - \delta^i$ only for 0.024 % corresponds to decrease of initial RS by 65 MPa. Such a graph can be useful for determination of the optimum mode of VT. Obtained experimental results showed that evaluation of efficiency of VT on criteria of total energy dissipation in the structure at such a small value of vibration decrement of the material and, its far lower change in process of RS reduction in the material, is impossible without consideration of structural energy dissipation.

In order to evaluation VT efficiency the observations were directed on relative change of the vibration decrement and RS in the specimen in a different time periods after making a longitudinal deposit under condition that the specimen was not subjected to VT. Analysis of the results, given in Figure 6, showed that δ rises and RS decrease up to 150 h similar to the specimens subjected to VT. Moreover, stabilizing moment of the studied characteristics matches in time. Then as a result of strain aging the vibration decrement drops virtually to initial value, and RS remain unchanged. Decrease of δ indicates that even in absence of VT an effect of high RS provokes plastic strain in the specimen, that results in reduction of initial RS. Comparing the experimental data in Figures 3 and 6 it can be noted that stabilizing process at natural aging takes place after a longer period of time (in this case in 150 h), regardless the similar nature of change of the vibration decrement and RS. It can be practically concluded that VT significantly accelerates (450 times) the pro-

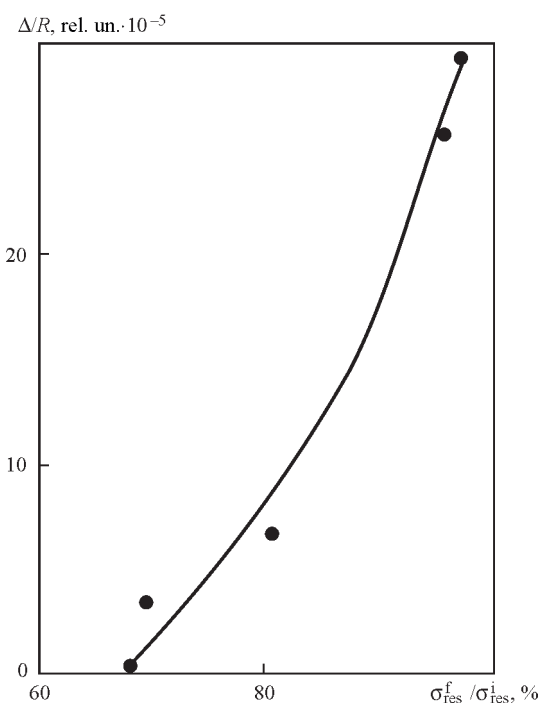


Figure 7. Dependence of change of relative gap in circular specimens on relative change of RS determined in 1500 h of aging after vibrotreatment at different amplitude of cycle stress ($\sigma_a = 15, 15, 30, 50, 60$ MPa). R — circular element radius

cess of RS decrease in the welded structures. Therefore, in earlier works [25] term «vibrotreatment» was used as «vibroaging».

One of the VT tasks includes also prevention of buckling of structure elements in storage and operation, therefore this work also studies effect of stress amplitude on change of a linear size of the circular specimens, which was expressed in a change of gap Δ between its free ends during VT as well as after it. Received results showed that gap decrease mainly takes place in course of $7.5 \cdot 10^3$ cycles of loading and after $15 \cdot 10^3$ cycles of loading it does not change independent on σ_a value (not indicated in Figure). Also it can be noted that increase of applied amplitude σ_a provides for reduction of the value of further after VT buckling of the specimen and at $\sigma_a = 60$ MPa change of the gap in process of specimen aging in course of 1500 h was not observed. A dependence, presented in Figure 7, gives an evaluation of change of the relative gap in the circular specimens due to relative change of RS, determined in 1500 h after VT. Smaller change of the gap after VT corresponds to larger value of residual stress decrease. It is determined that decrease of initial RS by 32 % that corresponds to $0.51 \sigma_{0.2}$ of the investigated material did not provoke change of the specimen gap. The results of testing showed an appropriate level of RS reduction in this case in order to reach geometry stability of the investigated element.

Conclusions

1. The method for selection of the undamaging modes of vibrotreatment of the welded elements of metal structures was developed and experimentally tested based on a complex diagram of cycle limit stresses. They provide for efficient decrease of residual stresses and increase of endurance limits.

2. It is determined that reduction of residual stresses in vibrotreatment results in increase of damping capability of the part material. Growth of the maximum cycle stresses provokes increase of vibration decrement on larger value, and its stabilizing and stabilizing of residual stress match in time. This allows making a conclusion about process end on beginning of vibration decrement stabilizing.

3. Decrease of vibration decrement after VT indicates the process of strain aging pointing plastic strain of the specimens in vibrotreatment. This results in decrease of residual stresses.

4. Vibrotreatment can also provide geometry stability of the welded elements. It is determined that decrease of initial maximum residual tensile stresses to 0.51 of material yield limit results in geometry stability of the circular specimen.

1. Asnis, A.E., Ivashchenko, G.A. (1978) *Increase of strength of welded structures*. Kiev: Naukova Dumka.
2. Kudryavtsev, I.V., Naumchenkov, N.E. (1976) *Fatigue of welded structures*. Moscow: Mashinostroenie.
3. Shpeer, F.Z., Panov, V.I. (1983) Vibration treatment of large-sized welded structures for decrease deformation and crack susceptibility. *Svarochn. Proizvodstvo*, **5**, 13–15.
4. Nedoseka, A.Ya. et al. (1974) Efficiency of methods of residual welding stress relaxation. *Avtomatich. Svarka*, **3**, 66–69.
5. Dreger, D.R. (1978) Good vibes reduce stresses in metal parts. *Machine Design*, 50(13), 100–103.
6. Zimnitsky, Yu.A., Khvalynsky, V.N. (2004) Experimental validation of low-frequency vibrotreatment effect on service reliability of hull structures. *Sudostroenie*, **1**, 50–52.
7. Sutyryn, G.V. (1983) Decrease of residual stresses in welded joints by low-frequency vibrotreatment. *Svarochn. Proizvodstvo*, **2**, 22–23.
8. Zubchenko, O.I., Gruzd, A.A., Orekhov, G.T. (1974) Application of vibration loading for relaxation of residual stresses in welded frames. *Avtomatich. Svarka*, **9**, 64–66.
9. Galyash, A.A., Kozin, M.Yu., Kolomeets, N.P. (1992) Application of low-frequency vibrotreatment for stabilization of sizes of welded and cast products of machine building. *Tyazh. Mashinostroenie*, **8**, 30–32.
10. Thompson, L. *Method and device for stress relaxation in parts by vibration*. Pat. 3622404 USA. Publ. 23.11.1971.
11. Dryga, A.I. (1992) Vibrostabilizing treatment of large-sized body parts of electric machines and hydrogenerators. *Tyazh. Mashinostroenie*, **8**, 23–25.
12. Pisarenko, G.S., Yakovlev, A.P., Matveev, V.V. (1971) *Vibro-absorbing properties of structural materials*. Kiev: Naukova Dumka.
13. Ryakhin, V.A., Moshkarev, G.N. (1984) *Service life and stability of welded structures of building and road-making machines*. Moscow: Mashinostroenie.
14. Adoyan, G.A., Aldoshin, Yu.S., Gerchikov, A.M. (1979) Vibro-ageing of cast iron parts of metal-cutting machines. *Litejnoe Proizvodstvo*, **11**, 24–25.
15. Galyash, A.A., Vasilchenko, K.I., Chernetsov, G.P. (1992) Determination of loading frequency in low-frequency vibrotreatment of welded structures. *Svarochn. Proizvodstvo*, **8**, 35–36.
16. Matveev, V.V. (1985) *Vibration damping of deformable bodies*. Kiev: Naukova Dumka.
17. Grishakov, S.V., Kovalev, A.I. (1988) *Application of Barkhausen effect for evaluation of stresses and damages in ferromagnetic materials*. Kiev: IPS.
18. Degtyarev, V.A. (1982) Machines of DSO type for fatigue tests under impact reloading with different cycle asymmetry. *Problemy Prochnosti*, **10**, 110–113.
19. Yakovlev, A.P. (1985) *Dissipative properties of inhomogeneous materials and systems*. Kiev: Naukova Dumka.
20. Degtyarev, V.A. (1991) Influence of stress cycle asymmetry coefficient on fatigue and cyclic creep of low-alloy steels. Rep. 2. *Problemy Prochnosti*, **2**, 27–31.
21. Astafiev, A.A. et al. (1977) Influence of strengthening and embrittlement on energy dissipation in deformation ageing of reactor vessel steels for NPP. *Ibid.*, **10**, 94–102.
22. Pisarenko, G.S., Khilchevsky, V.V., Goncharov, T.I. (1968) Study of energy dissipation in material at bending vibrations in field of static normal stresses. In: *Energy dissipation at vibrations of elastic systems*. Kiev: Naukova Dumka.
23. Pisarenko, G.S. (1962) *Energy dissipation under mechanical vibrations*. Kiev: AN Ukr.SSR.
24. Olenin, E.P. et al. (1983) Relaxation of residual stresses in welded components using vibrotreatment. *Svarochn. Proizvodstvo*, **5**, 11–13.
25. Ragulskis, K.M., Stulpinas, B.B., Tolutis, K.B. (1987) *Vibration ageing*. Ser.: Vibration equipment, Issue 9. Leningrad: Mashinostroenie.

Received 07.12.2016

MOBILE PROTECTIVE SCREEN FOR NONSTATIONARY WORKPLACES FOR MANUAL ARC WELDING

O.G. LEVCHENKO and A. Yu. KHARLAMOV

NTUU «Igor Sikorsky Kiev Polytechnic Institute»

115 Borshchagovskaya Str., 03056, Kiev, Ukraine. E-mail: levchenko.opch@ukr.net

Results of analysis of workers protection from ultraviolet radiation generated by welding arc are given. It is shown that intensity of ultraviolet radiation in coated electrode manual arc welding and mechanized gas-shielded welding can many times exceed the admissible norms at the distance of several tens of meters from the welding site. Thus, hazardous radiation can affect the support personnel who are in the area, and, usually, have no individual protection means, other workers, as well as random people who happened to be (pass by) at an unsafe distance from nonstationary workplaces for arc welding. Proceeding from the obtained results, a pilot sample of a mobile protective screen for nonstationary workplaces of welders has been developed and produced. Results of development and testing of the proposed mobile protective screen are given. 6 Ref., 1 Table, 7 Figures.

Keywords: arc welding, ultraviolet radiation, nonstationary workplaces, mobile protective screen

In keeping with safety requirements, the welder uses the following individual protection means (IPM) at application of all kinds of electric arc welding: the eyes are protected by a filter, which is selected taking into account the brightness and spectral composition of optical radiation (OR); helmet, overalls and goggles do not leave any exposed skin. Thus, OR harmful effect can be neglected, if the welder observes the safety requirements. However, both foreign [1–4] and our own research results [5] show that the levels of intensity of ultraviolet radiation (UVR) exceed the maximum permissible level (MPL) at the distance of several tens of meters from the welding site. Thus, hazardous radiation can affect support personnel who are in the area and, usually, have no individual protection means, other workers, as well as random people who happened to be (pass by) at unsafe distance from nonstationary workplaces for arc welding.

The most common nonstationary workplaces for manual arc welding, where work is performed in open air and near which unprotected people can happen to be, are as follows: construction, emergency and repair operation sites, large-sized metal structure fabrication yards and home welding areas. The problem of protection from light radiation of the welding arc is also highly urgent during performance of welding operations in ship-repair and ship-building shops, car building and repair, as well as machine shops, where a large number of welders and workers of other professions and engineering-technical personnel are employed simultaneously, who often cannot avoid expo-

sure to this hazardous factor that may result in them developing vision diseases.

Thus, the considered problem has always been urgent, and up to now it did not have any specific solution in the case of welding in nonstationary workplaces. Therefore, based on analysis of published and own data, as well as considering numerous comments of the workers and welding operation supervisors, the authors of this work came to the conclusion that it is necessary to create special means for protection from optical radiation of workers of different professions, being at a relatively short distance (up to 65 m) [5] from the welding site.

The main processes of welding in such places are coated electrode electric arc welding and mechanized gas-shielded metal-arc welding. Modern welding equipment, which is used in such processes, is characterized by relatively compact size and high mobility that allows welding operations to be performed in sites (territories) not prepared for it. Unpredictable conditions of welding in such cases do not allow developing versatile measures of UVR protection.

Time protection cannot be used, as in keeping with acting normative document [6], irradiation of exposed skin is not permitted at all.

Distance protection is complicated by exceeding normative UVR values within the radius of tens of meters that under the conditions of nonstationary welding sites makes it impossible to observe a safe distance for support personnel and environment, for instance, in dense urban developments.

Lowering of UVR intensity in its generation source also has a low efficiency, because even with the most optimum welding parameters (selection of welding



Figure 1. Welding cabins

consumable type, mode, current, etc.), at which minimum UVR level is observed, its effective values still are much higher than the requirements specified in normative documents.

Lowering UVR intensity in its propagation path, i.e. shielding, remains the only effective method of protection.

Welding cabins (Figure 1) are used in stationary workplaces, the walls of which should be painted in light colours with addition of zinc oxide or titanium white to paint for UVR absorption.

Cabin height is 1.8–2.0 m, the walls should not touch the floor by 25 to 30 cm to improve cabin ventilation. Use of such cabins in nonstationary workplaces nullifies the speed and mobility of performance of single welding operations. As transportation and mounting a cumbersome cabin or its assembly in structure welding site takes a lot of time, the cost of welding operations rises, particularly, in case of emergency welding operations. Moreover, welding conditions can be incompatible with welding cabin dimensions or position.

In petrochemical industry welding tents (Figure 2) are widely used during performance of welding operations on pipelines.

Welding tents offer a number of advantages: they provide protection from unfavourable meteorological conditions (rain, snow, low temperatures), are resistant to wind gusts, unlike curtains or enclosures, and



Figure 2. Welding tents

make effective UVR shield. However, welding tents also have a number of significant disadvantages:

- need for compulsory application of ventilation — in an almost closed space natural removal of welding fumes at their significant evolution becomes impossible. It is necessary to use supply-and-exhaust ventilation, which increases the time to prepare the workplace, makes additional requirements to power supply and increases the work cost;

- possible lack of natural light — the tent material cannot be totally transparent, as a green house effect is created, so that during daylight hours the tent should be lighted by an artificial light source;

- absence of versatility — during pipeline laying the tent encloses the pipe and can move along it to the next welding site. Thus, there is no need to spend time and resources on assembly-disassembly of the tent. Under other conditions such an advantage turns into a disadvantage that in combination with mounting of ventilation and lighting systems makes application of welding tents in nonstationary workplaces not cost effective.

Curtains or mobile welding screens are devoid of all the above disadvantages: they have relatively small weight, are convenient in transportation, and are easy to mount in any sites. Curtain posts can be additionally fitted with rollers for ease of movement over flat hard surface, and can be of sliding or hinged design that allows changing curtain height or profile. Used as the screen can be polished aluminium, which effectively absorbs UVR, or less expensive fireproof canvas. Polyvinylchloride (PVC) films have been developed recently, which have multiple advantages over traditional screen materials.

The objective of this work is a comprehensive study of requirements to mobile devices for UVR shielding and development of a mobile protective screen (MPS) on their base.

Conditions of welding in nonstationary workplaces are characterized by their unpredictability. Therefore, a number of factors should be taken into account in MPS development:



Figure 3. Hazard warning signs «Caution. Non-ionizing radiation» (a) and «Caution. Welding» (b)

Structure stability. Unevenness of the surface, on which MPS is placed, should be taken into account, as well as this surface hardness. During welding operations, which are performed outside, it is necessary to envisage resistance against wind gusts;

Height adjustment. In stationary welding stations the parts being welded are placed on work tables, and the welder is working while sitting that enables calculation of the height of enclosure and height of the space between the floor and screen lower edge. Under the conditions of nonstationary workplaces the parts can be on floor (ground) level or, contrarily, at a certain height. It is necessary to envisage such MPS position as to ensure free access of air at the bottom of the screen for ventilation, and, at the same time, effective UVR shielding;

Easy access to the workplace. In welding cabins the workplace can be accessible from one side through a door or canvas curtain. When mounting MPS it is necessary to envisage the possibility of free sliding of the screens both for outside access to surfaces to be welded from the required side, and for leaving the welding zone to the safe side after work completion;

Durability and wear resistance of the structure. MPS design should take into account a large number of assembly-disassembly cycles for transportation and displacement and it should be easy to clean from contamination. The screen should be fireproof and resistant to the impact of spatter and drops of molten metal;

Characteristics of ScreenFlex protective film

Parameter (properties)	Parameter value	Norm (Standard)	Description
Fire resistance	–	EN 1958	Standard classification of refractory properties and fire resistance of material
Light transmission, %	0.01–13	–	Quantity of visible light passing through the material
Sound insulation, dB	>35	DIN 52210	Averaged level of sound pressure (frequency of 0.1–3.2 kHz) that is reduced by a curtain of 1.76 m ² area and 5 mm thickness
Thermal conductivity, W/(m·K)	0.16	ASTM C177	The smaller this value, the more insulating the material
Application temperature, °C	–15–50	EN 1876	Temperature range, in which material preserves its mechanical properties (flexibility)
Surface resistance, Ohm·cm	4·10 ¹³	IEC 60093	Electrical resistance of material surface, measured at 500 V voltage
Water absorption, %	–0.2	EN ISO 62	Change of material mass after staying under special conditions (evolution)
Density, g/cm ³	1.2–1.3	ASTMD 792	Mass per unit of volume

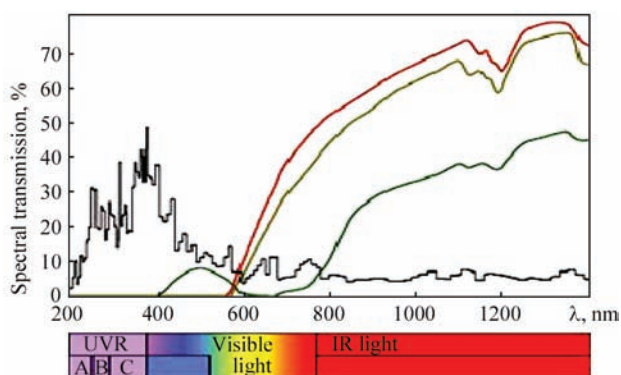


Figure 4. Dependence of screen material spectral transmission on wave length

Placing safety signs. MPS not only has a protective function, but also gives a warning about unsafe work performance and presence of hazardous factors. Therefore, it is recommended to place hazard warning signs according to DSTU ISO 17846:2013 (Figure 3).

Considering the features of working conditions during welding operations performance, and, primarily, the need for effective UVR shielding, it is proposed to use Screenflex PVC film as a protective screen. Screenflex protective film has the properties of ultraviolet/infrared radiation filter, which effectively filters welding arc radiation. This allows application of the material as a protective screen, in keeping with EN 1598. Characteristics of EN Screenflex film are given in the Table.

The above-mentioned characteristics lead to the conclusion that the film meets all the main requirements for protective screen material, namely:

- provides effective UVR shielding in keeping with EN 1598;
- transmits light in the visible range;
- has acoustic insulation properties;
- has dense, tear-resistant design that promotes long-term application;
- is fireproof and resistant to molten metal drops and sparks;
- does not conduct electric current;

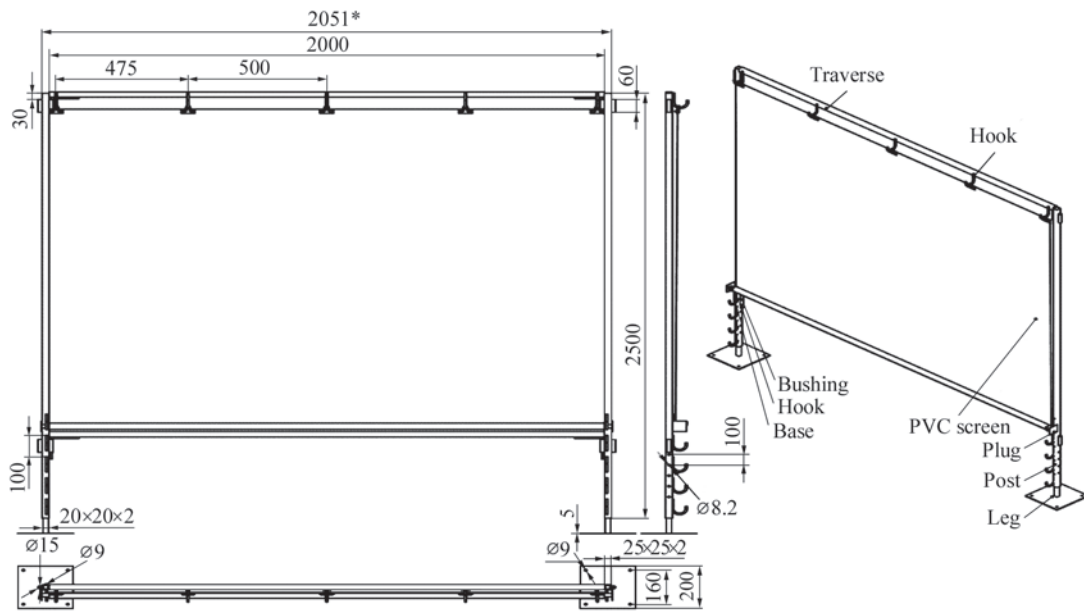


Figure 5. MPS assembly drawing

- does not absorb moisture and is easy to clean.

Note the combination of absolute opacity of screen material for UVR and light transmission in the visible range. Graphs of dependence of spectral transmission on wave length are shown in Figure 4.

It is recommended to use red-coloured PVC film as MPS material. Firstly, the red colour is a signal of possible hazard. Secondly, this is exactly the material that better transmits light in the visible range in its warm portion that allows safely observing performance of welding operations and monitoring compliance with safety requirements and progress of the process.

It is also important to note that the screen almost does not delay infrared radiation and, thus, greenhouse effect is eliminated that provides comfortable working conditions.

A pilot sample of the respective MPS was designed and manufactured, taking into account all the above requirements and recommendations (Figure 5).

The screen consists of two sliding posts, adjustable by height using bushings and traverse with hooks, to which the PVC screen, which is rolled around a metal rod, is fastened.

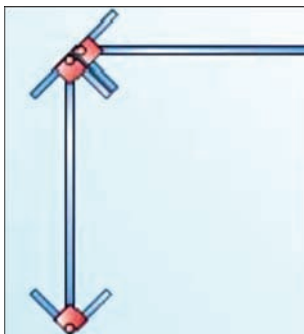


Figure 6. Example of MPS positioning at 90 degr. angle

The post lower part has four hooks, that enables moving the coil with PVC screen by height from 0.1 to 0.4 m for ventilation, depending on the features of the welding site. Bushings enable reliable fixing of the coil rod to the hooks that gives additional rigidity to the entire structure.

Moreover, different legs can be fastened to the posts, if required. Leg fastening by «arrow» type enables placing several MPS at 90 degr. angle (Figure 6) that provides a tight enclosure of welding operations site.

Pilot sample of MPS (Figure 7) was manufactured and tested in June, 2016 in the plant of OJSC «Pivnichni-Ukrainiskij budivelnij alians». Welding of metal structures was performed by Fronius TransPocket 2500 welding unit in unprepared workplaces, using Monolith RTs 46 electrodes of 4 mm diameter during daylight hours in an open area at moderate wind. MPS

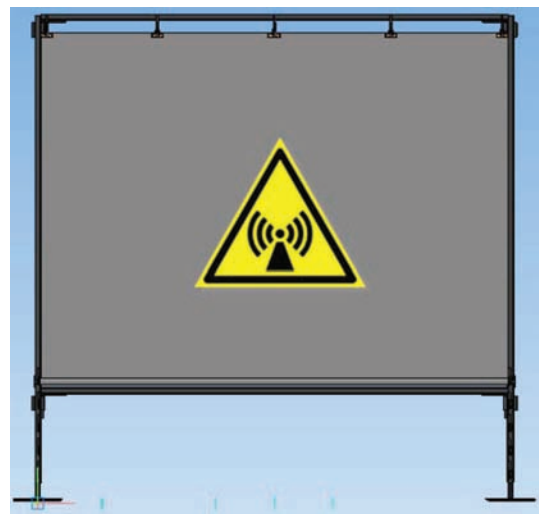


Figure 7. Pilot sample of a mobile protective Screen (MPS)

structure was placed on an uneven surface directly on the ground. MPS stability was ensured by driving four metal rods into the ground through holes in post bases. Handling operations were performed at 15 to 20 m from the welding site, and builders cabin, path for passage of people and site of concreting works were in the line-of-sight zone. MPS was located at 1.5 m distance from the welding site, so as to block direct visibility of the welding arc from all the places of possible stay of workers. Under these conditions of operation performance, application of one MPS was enough. It was noted that such MPS positioning does not interfere with welder's work, protects nearby workers from UVR adverse impact, warns about possible hazard of staying near the work performance site, and still enables monitoring the welding operations.

Testing in production premises allowed determination of the following advantages of MPS: com-

compactness, easy mounting, convenience of movement, availability of adjustments for surface unevenness and ability of safe outside observation. Placing hazard signs on the surface of screen protective film can be also regarded as a positive new feature.

1. Okuno, T., Ojima, J., Sayto, H. (2001) Ultraviolet radiation emitted by CO₂ arc welding. *The Annals of Occupational Hygiene*, 45(7), 597–601.
2. Terry L. Lyons (2002) Knowing the dangers of actinic ultraviolet emissions. *AWS Welding J.*, 12, 28–30.
3. Dixon, J., Dixon, B.F. (2004) Ultraviolet radiation from welding and possible risk of skin and ocular malignancy. *The Medical J. of Australia*, 181(3), 155–157.
4. Schwass, D. et al. (2011) Emission of UV radiation during arc welding. In: IFA Information, 1–12. www.dguv.de/ifa
5. Levchenko, O.G., Malakhov, A.T., Arlamov, A.Yu. (2014) Ultraviolet radiation in manual arc welding using covered electrodes. *The Paton Welding J.*, 6/7, 151–154.
6. DNAOP 0.03-3.17-88/SN 4557–88: Sanitary norms of ultraviolet radiation in production premises. Introd. 1988-02-23.

Received 07.11.2016

SEMINAR «WELDING MATERIALS»

On January 24, 2017 the seminar «Welding Materials», devoted to the 90th birthday anniversary of academician Pokhodnya Igor Konstantinovich (1927–2015), was held at the E.O. Paton Electric Welding Institute (PWI) in Kiev. The scientists and specialists of the PWI, a number of enterprises-manufacturers of welding consumables (LLC «Sumy-Elektrod», PJSC «PlazmaTek», LLC «VitaPolis», LLC «VELMA», «TM.VELTEK», Pilot Plant of Welding Materials of the E.O. Paton Electric Welding Institute), teachers of NTUU «I. Sikorsky Kiev Polytechnic Institute», directors of some Institutes of Department of Physical-Technical Problems of Materials Science of the NAS of Ukraine. Above 80 participants took part in the Seminar.

Academician *L.M. Lobanov*, the Deputy Director of the E.O. Paton Electric Welding Institute, made an opening address to the participants. He described a great contribution of I.K. Pokhodnya, a well-known scientist and a prominent organizer of science, to the development of fundamentals of metallurgy and technology of metals, materials science and electric welding. His name is associated with fundamental studies of physical-chemical processes of arc welding, new high-efficient processes of manufacture of materials, establishment of a scientific school in the field of metallurgy and technology of arc welding, development of science-intensive technologies and advanced welding materials, organizing of their production. He prepared above 50 Doctors and Candidates of Technical Sciences, above 900 papers, and published tens of monographs. I.K. Pokhodnya was a Vice-President, Chief

Scientific Secretary of the NAS of Ukraine and then headed the Department of Physical-Chemical Problems of Materials Science in the Academy for 27 years.

His pupil, *V.V. Golovko*, the Chief of Department of the PWI, told about creative developments of I.K. Pokhodnya. He and the next speakers *I.R. Yavdoshchin* and *A.S. Kotelchuk* told about the creative atmosphere of the PWI Department, established and headed by I.K. Pokhodnya, promoting the development of low-toxic welding materials and technology of their industrial production, creation of powerful specialized shops on manufacture of coated electrodes, reconstruction of a number of existing electrode enterprises. Due to joint efforts of scientists-welders and metallurgists, designers and manufacturers it was managed to solve an important national economic problem: to provide the manufacture of national high-efficient low-toxic electrodes on a short time. Investigations, carried out under the supervision of I.K. Pokhodnya, gave an opportunity to develop a number of different-purpose flux-cored wires and to offer unique designs of their sheath. This became a significant progress in technique and technology of the mechanized welding in site and under the field conditions.

Paper of *S.V. Pustovojt* (PWI) was devoted to the topic «State-of-the art and tendencies of development of market of welding materials». The important conclusion of this information is the fact that it was managed by the efforts of scientists of Ukraine and specialists of enterprises-manufacturers of welding materials to prevent greatly the expansion of foreign



Presentation of Yu.N. Omelchuk, the commercial director of corporation «PlazmaTek»



Near the stand of the Pilot Plant of Welding materials (Prof. I.V. Krivtsun, Deputy Director of the PWI, Dr. V.N. Shlepakov and P.A. Kosenko, director of this plant)

suppliers of electrodes and flux-cored wires to the market of Ukraine. Moreover, in the recent years the tendency of increasing the export of welding materials from Ukraine is observed.

N.A. Protsenko (PWI) told about algorithm and required activities of companies of Ukraine concerning the documentation and support of system of plant industrial control to assure the conformity of products, manufactured for the market, to International and European standards, regulating the working characteristics of materials. At present four Ukrainian manufacturers of welding materials received the right of marking their products by sign CE: LLC «VitaPolis», Boyarka town, Kiev region; LLC «Metiz», Brovary town, Kiev region, corporation «PlazmaTek», Vinnitsa city, LLC «Sumy-Elektrod», Sumy city.

Yu.N. Omelchuk, the representative of the corporation «PlazmaTek», dwelled on organizing the production distribution in his speech. Today, the corporation occupies the first place at the post-Soviet territory by volumes of manufacturing and selling of electrodes. In 2016 its volume of production reached 30 thous. tons. The main products (80 %) are electrodes on base of ANO-36 grade with high welding-technological properties.

They successfully compete with electrodes of corporation ESAB (Sweden) and Turkish manufacturers. Corporation «PlazmaTek» established logistic centers in Russia (2), Belarus (2) and Kazakhstan (1). It is planning to organize these centers in Romania, Moldova, Poland and Uzbekistan. The corporation is planning the increase in volume of production of copper-plated welding wire, mastering the production of stainless welding wires.

V.N. Lipodaev (PWI) told about the information support of specialists, working in the field of development, mastering of production and consuming of welding materials. In this aspect the leading role of the



Near the stand of LLC «Sumy-Elektrod» (Prof. L.M. Lobanov, Deputy Director of the PWI and P.N. Pogrebnoj, director of this plant)

journal «Avtomaticeskaya Svarka» was noted. For the seminar the January issue of journal, devoted to the topic «Welding materials» was published and distributed among the participants. Many times the journal was issued as Proceedings of International Conferences, held at the E.O. Paton Electric Welding Institute. The activity of association «Elektrod» is also efficient in a regular organizing of conferences on welding consumables and publishing of appropriate Proceedings.

At the seminar the pupils of I.K. Pokhodnya, becoming the heads of enterprises made a speech: *A.A. Golyakevich*, Director, LLC «TM.VELTEK», *M.F. Gnatenko*, Director, LLC «VELMA». They expressed sincere thanks to I.K. Pokhodnya for help in their formation as specialists, capable to apply effectively the experience acquired at the PWI.

Directors of Institutes of the NAS of Ukraine also shared their memories. They noted a valuable contribution of I.K. Pokhodnya to scientific-organizational activity of Department of Physical-Technical Problems of Materials Science, demonstrating the effective activity in the system of the NAS of Ukraine. The seminar was continued by inviting the participants to the blitz exhibition of manufacturers of welding materials, organized at the demonstration hall of the PWI. Stands of corporation «PlazmaTek», LLC «Sumy-Elektrod», LLC «TM.VELTEK», SE «Pilot Plant of Welding Materials of PWI», LLC «VitaPolis», LLC «SteelWork» were presented, attracting a keen interest of the specialists.

At the business lunch, organized in conclusion, the seminar participants could discuss the different aspects of such not simple production as manufacturing welding materials in informal atmosphere and recollect once again the beloved expression of Igor Pokhodnya: «**I see, young men, that You relaxed. . . .**» as an address and appeal to the effective work.

V.N. Lipodaev, A.T. Zelnichenko, PWI

PATON PUBLISHING HOUSE

www.patonpublishinghouse.com

SUBSCRIPTION

The Paton
WELDING JOURNAL

АВТОМАТИЧЕСКАЯ
СВАРКА

«The Paton Welding Journal» is Published Monthly Since 2000 in English, ISSN 0957-798X.

«Avtomaticheskaya Svarka» Journal (Automatic Welding) is Published Monthly Since 1948 in Russian, ISSN 005-111X.

«The Paton Welding Journal» is Cover-to-Cover Translation of Avtomaticheskaya Svarka» Journal into English.

If You are interested in making subscription directly via Editorial Board, fill, please, the coupon and send application by Fax or E-mail.

The cost of annual subscription via Editorial Board is \$348 for «The Paton Welding Journal» and \$180 for «Avtomaticheskaya Svarka» Journal.

«The Paton Welding Journal» can be also subscribed worldwide from catalogues subscription agency EBSO.

SUBSCRIPTION COUPON

Address for journal delivery _____

Term of subscription since _____

20

till

20

Name, initials _____

Affiliation _____

Position _____

Tel., Fax, E-mail _____

We offer the subscription all issues of the Journal in pdf format, starting from 2009.

The archives for 2009–2014 are free of charge on www.patonpublishinghouse.com site.



ADVERTISEMENT

in «Avtomaticheskaya Svarka» and «The Paton Welding Journal»

External cover, fully-colored:

First page of cover
(190×190 mm) — \$700
Second page of cover
(200×290 mm) — \$550
Third page of cover
(200×290 mm) — \$500
Fourth page of cover
(200×290 mm) — \$600

Internal cover, fully-colored:

First/second/third/fourth page
of cover (200×290 mm) — \$400

Internal insert:

Fully-colored (200×290 mm) —
\$340
Fully-colored (double page A3)
(400×290 mm) — \$500

- Article in the form of advertising is 50 % of the cost of advertising area
- When the sum of advertising contracts exceeds \$1001, a flexible system of discounts is envisaged

**Size of journal after cutting is
200×290 mm**

Editorial Board of Journal «Avtomaticheskaya Svarka» and «The Paton Welding Journal»

E.O. Paton Electric Welding Institute of the NAS of Ukraine

International Association «Welding»

11 Kazimir Malevich Str. (former Bozhenko Str.), 03680, Kiev, Ukraine

Tel.: (38044) 200 60 16, 200 82 77; Fax: (38044) 200 82 77, 200 81 45

E-mail: journal@paton.kiev.ua; www.patonpublishinghouse.com